REPORT DOCUMENTATION PAGE

Form Approved
OMB No. 0704-0188

1. REPORT DATE *(DD-MM-YYYY)*	2. REPORT TYPE	3. DATES COVERED *(From - To)*
June 30, 2005	Quarterly Report	1 Apr. to 30 Jun. 2005

4. TITLE AND SUBTITLE
Advanced Wireless Integrated Navy Network (AWINN)

5a. CONTRACT NUMBER
N00014-05-1-0179

5b. GRANT NUMBER
N00014-05-1-0179

5c. PROGRAM ELEMENT NUMBER

6. AUTHOR(S)
Warren Stutzman and Rick Habayeb

5d. PROJECT NUMBER

5e. TASK NUMBER

5f. WORK UNIT NUMBER

7. PERFORMING ORGANIZATION NAME(S) AND ADDRESS(ES)
Virginia Polytechnic Institute and State University
Electrical and Computer Engineering Department
302 Whittemore Hall (0111)
Blacksburg, VA 24061

8. PERFORMING ORGANIZATION REPORT NUMBER
2

9. SPONSORING/MONITORING AGENCY NAME(S) AND ADDRESS(ES)
Office of Naval Research
ONR 313
875 N. Randolph St.
Arlington, VA 22203-1995

10. SPONSOR/MONITOR'S ACRONYM(S)

11. SPONSOR/MONITOR'S REPORT NUMBER(S)

12. DISTRIBUTION/AVAILABILITY STATEMENT
Approved for public release; distribution unlimited.

13. SUPPLEMENTARY NOTES
The views, opinions and/or findings contained in this report are those of the author(s) and should not be constructed as an official Department of the Navy position, policy or decision, unless so designated by other documentation.

14. ABSTRACT
Quarterly progress report No. 2 on AWINN hardware and software configurations of smart, wideband, multi-function antennas, secure configurable platform, close-in command and control for Sea Basing visualization of wireless technologies, Ad Hoc networks, network protocols, real-time resource allocation, Ultra Wideband (UWB) communications network and ranging sensors, cross layer optimization and network interoperability.

15. SUBJECT TERMS

16. SECURITY CLASSIFICATION OF:			17. LIMITATION OF ABSTRACT	18. NUMBER OF PAGES	19a. NAME OF RESPONSIBLE PERSON
a. REPORT	b. ABSTRACT	c. THIS PAGE			Rick Habayeb
U	U	U	UL		19b. TELEPHONE NUMBER *(Include area code)* 540-231-4353

Advanced Wireless Integrated Navy Network -

AWINN

2nd Quarterly Report

Virginia Tech

April 1, 2005 – June 30, 2005

TABLE OF CONTENTS

Executive Summary **1**
1. TASK 1 Advanced Wireless Technologies **2**
1.1 Task 1.1 Advanced Antennas 2
1.2 Task 1.2 Advanced Software Radio 16
1.3 Task 1.3 Collaborative and Secure Wireless Communications 32
2. TASK 2 Secure and Robust Networks **37**
2.1 Task 2.1 Ad Hoc Networks 37
2.2 Task 2.2 Real-Time Resource Management, Communications, and Middleware 44
2.3 Task 2.3 Network Interoperability and Quality of Service 58
2.4 Task 2.4 Cross-Layer Optimization 59
3. TASK 3 Visualization of Wireless Technology and Ad Hoc Networks **72**
3.1 Overview 72
3.2 Task Activities for the period 72
3.3 Importance/Relevance 77
3.4 Productivity 77
4. TASK 4 Testing and Demonstrations **80**
4.1 TIP#1: Distributed MIMO UWB Sensor Networks Incorporating Software Radio 80
4.2 TIP#2: Close-in UWB Wireless Application to Sea Basing 86
4.3 TIP #3: Secure Ad Hoc Networks 92
4.4 *TIP #4:* Integration of Close-in UWB wireless with ESM crane for Sea Basing applications 96
5. FINANCIAL REPORT **97**

Executive Summary

This second quarterly report provides summaries on the activities and accomplishments of the AWINN team at Virginia Tech. The report covers the following thrust areas:

Advanced Wireless Technology
Secure and Robust networks
Visualization of Wireless Technology and Ad Hoc Networks
Technology Integration projects

Also, it includes Quad charts and Timelines of scheduled events, which will be used as a road map for future activities.

The antenna group is making great strides in supporting the antenna needs of the AWINN team of Tasks 1.2, 1.3, 3, 4.1, and 4.2. During this reporting period, the SDR group focused on the development of prototype receivers and algorithms to support UWB communications, position location and ranging. The group concentrated on Rake receivers for efficient narrow pulse detection and collection of multi-path returns to optimize the range of UWB communications. The SDR group is supporting the Smart Antenna API (SA-API) working group of the SDR Forum. The collaborative and secure wireless communications team is developing a multi-transceiver for inter and intra communications between network nodes. The cross-layer optimization effort is focused on cross-layer design of UWB for position location networks PoLoNet and collaborative radio networks. The networking group is evaluating the metrics and the integration of mobile ad hoc networks. The group is investigating various protocols for QoS, security, mobile routing, and cross-layer optimization. The real time system team is concentrating on the standard for the distributed real-time specification of Java (DRTSJ), and the time utility function. The video communications effort is focusing on battery life issues and protocols of video networks of distributed sensors. The visualization of wireless technology team has been collecting data on cargo transfer, and preparing several UWB ranging experiments during the following quarter. The technology integration projects (TIP) are progressing with integration of hardware and software.

1. TASK 1 Advanced Wireless Technologies

1.1 Task 1.1 Advanced Antennas

1.1.1 Overview

Task Goal: This task investigates new antenna technologies that may be applicable to Navy missions and provides hardware for AWINN integration projects.

Organization: This task is managed by the Director of Virginia Tech Antenna Group (VTAG) using the following personnel:

Bill Davis, Director
Warren Stutzman, Faculty
Randall Nealy, Engineer
Taeyoung Yang, GRA

Summary: This quarter, progress continued in the development of antennas in support of other tasks that use UWB and small antennas. Identification of specific requirements for antennas to support the AWINN demonstrations has been completed.

A review of the antenna specification requests from the software defined radio task (Task 1.2) follows.

Directional Antenna for SDR Receiver

Size	Not a major constraint, but we would like it to be able to fit in a 6" x 6" x 6" cube.
Transmitted Pulse Width	Given a 500 ps pulse input, the transmitted pulse width should be 1000-1500 ps, with minimal pulse dispersion or ringing.
Gain	Not a major constraint, but 5-10 dBi Gain would be nice.
Weight	Not a concern
Absolute Frequency Range	Whatever is required to achieve the above pulse width
Date Required	Early to mid Fall 2005 (September/October). Will be used in Demo 2 (Currently scheduled for November 2005).

Comments:

- 6" gives a maximum wavelength of 30 cm for a peak frequency of 0.98 GHz.
- Expected pulse width of 1 ns. To reduce the ringing, a tapered antenna structure is needed. If the gain is desired, either a tapered slot or TEM horn will be required. The major problem with the tapered slot or a TEM horn is that they tend to be long (much greater than 6"). Although the bandwidth will be reduced somewhat, a 6" length will be used.

Omnidirectional Antenna for SDR Receiver

Size	Small form factor, similar to a monopole whip antenna.
Transmitted Pulse Width	Given a 500 ps pulse input, the transmitted pulse width should be 1-3 ns, with minimal pulse dispersion or ringing.
Gain	Not a major constraint, but 3-5 dBi Gain would be nice.
Weight	Probably less than 1 lb.

Absolute Frequency Range	Whatever is required to achieve the above pulse width
Date Required	Mid Spring semester 2006 (February/March). Will be used in Demo 3 (Currently scheduled for May 2006).

Comments:

- Expected pulse width is directly related to the size. However, the 1-3 ns would again suggest dimension on the order of 6 in or less. To reduce the ringing, a tapered structure is needed. For the omni-directional nature, a biconical antenna is a good choice. If gain is desired, either a tapered slot or TEM horn will be required, or a flattened bicone.

Directional Antenna for Imaging

Size	Very small, able to fit in a 2" x 2" x 2" cube.
Absolute Frequency Range	About 100 MHz up to >10 GHz.
Transmitted Pulse Width	Given a 100 ps input pulse, the transmitted pulse width should be no more than 200 ps.
Gain/Efficiency	Not a constraint. The maximum range of the imaging system is probably 6"-12", so we could even tolerate some loss.
Weight	Not a constraint.
Date Required	Early 2006 (January/February). Will be used for experiments and evaluation between Demos 2 and 3. (Changed to September 2005 to meet the sea-basing test simulations)

Comments:

- If a very small (=> 2") is used, there is a minimum frequency of 3 GHz. This definitely is in conflict with the 100 MHz expectation. The problem then becomes one of transmission efficiency with the major problem being antenna mismatch at the lower frequencies.
- Expected pulse width is directly related to the size. The 2" size would suggest an expected pulse width of about 0.3 ns. Gain is not a constraint, so the half-disk and bicone are good candidates.
- The imaging system is for the ship container project task that requires a system to measure the distance of a container above the ground and possibly other objects. At this stage, only the ground will be considered. Antennas are needed at the four upper corners of the container to provide a pulse to be measured and used for predition of the distance to the ground. For the scaled version, antennas that have a response from about 10 GHz to 20 GHz are needed. Because reflections from the simulation room ceiling must be avoided, the directional tapered slot antenna in a small size is a likely candidate. A suggestion has been made to consider multiple polarizations, but this would require additional receiver channels and possible transmit channels, which is beyond the scope of this project and not expected to provide substantial benefit. A discussion of the antenna concepts and types is provided in the next section.

A key problem with the frequency response desired is often an impedance mismatch at the lower frequencies and a resultant efficiency issue. One has to be careful since the peak amplitude is the major need, not the energy.

Review of Various Antenna Types

Theoretical concepts:

The basic response of a typical link is given in Fig. 1.1-1.

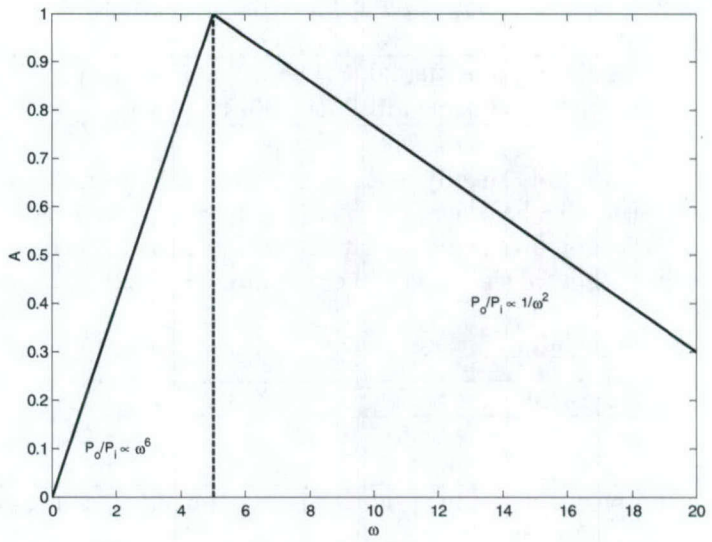

Figure 1.1-1 Typical line-of-sight response expected from identical antennas.

The link response can be separated into the antenna realized effective lengths and the time derivative. It should be noted that the realized effective length includes the effective length and the mismatch loss of the antenna. The mismatch dominates the low frequency portion of the response. The peak response generally occurs when the maximum dimension is approximately a half-wavelength. This frequency also dominates the ringing that is typical of the transient response. As seen in the sample plot of Fig. 1.1-2, the width of the response is approximately 0.6 ns that approximates the period of the 2.5 GHz peak.

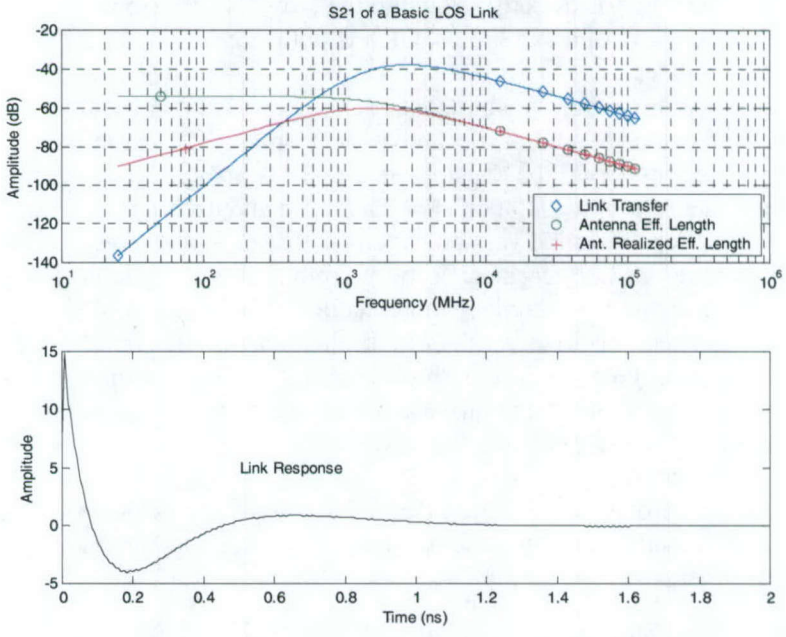

Figure 1.1-2 Typical link response amplitude in frequency and time.

If we consider a response that is dominated by a stronger low frequency response, we find a response with a bit more ringing as shown in Fig. 1.1-3.

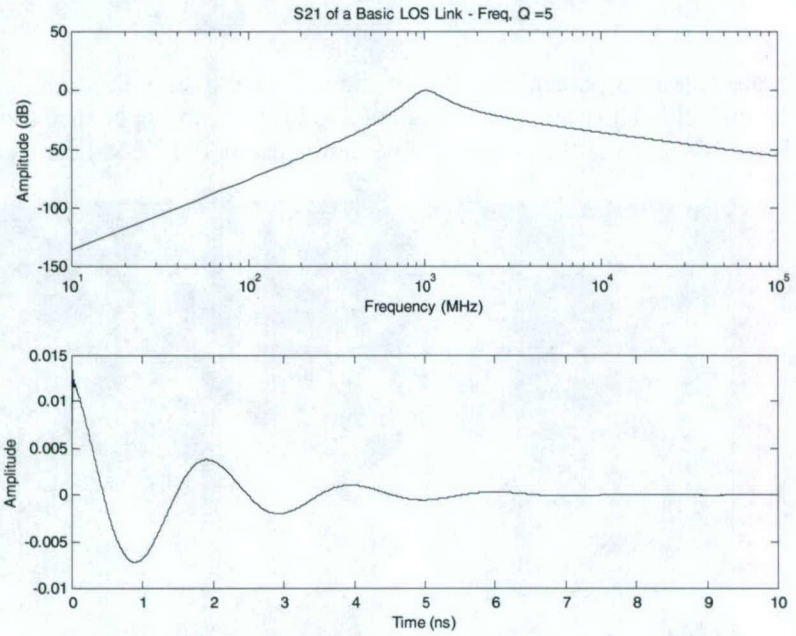

Figure 1.1-3 Link response for resonant antenna elements.

These responses assume a linear phase response. If the phase response becomes non-linear, we have phase dispersion and the response is typically represented by a chirp.

The design goals of the antenna for pulsed UWB are as follows:

1. Small Size. The maximum dimension for the lowest frequency sets the basic width of the pulse.
2. Linear phase response. This generally requires that the antenna have a taper, such as a horn, so that the energy can travel from the antenna while maintaining a continuous frequency response to prevent dispersion.
3. Directional radiation pattern. Directional properties are accomplished by tapering the antenna in the desired direction of peak radiation.

Candidate antennas:

1. Bicone or Discone: These provide an omni-directional pulsed response. The top of the element is often loaded with a cylinder to absorb the current flow at the cone edge.
2. TEM Horn: A directional version of the Bicone. The major problem is the balun feed structure.
3. Tapered slot (or Vivaldi): Retains the directional relationship of the TEM horn in the plane of the slot, but has more of a dipole pattern in the plane perpendicular to the slot.
4. Half-disk and variations
5. Fat dipole, Vee dipole, or sleeve dipole

6. BowTie
7. Ridged TEM horn

All of the candidate antennas (except the simple dipole) have a smooth transition from the feed point to the radiation field. The transition is designed to provide an impedance transform from the feed to space. The TEM horn is the simplest. The hardware model TEM horn is depicted in Fig. 1.1-4.

Figure 1.1-4 TEM horn over a ground plane.

If we consider a uniform linear taper TEM horn, the ***E*** and ***H*** field at the end of the horn are approximately orthogonal and related by $\eta = 377\ \Omega$. The voltage and current that would exist in this TEM type of transmission line are approximately

$$I \approx wH$$

$$V \approx hE$$

or

$$Z = \frac{V}{I} \approx \frac{hE}{wH} = 377\frac{h}{w}$$

For a 50 Ω input, $w/h = 7.54$ (width/height), which is a relatively flat structure. Due to reflections at the end, it is common to roll the ends a bit to minimize reflections. The lowest operating frequency occurs when $h \approx \lambda/2$. Thus a lowest operating frequency of 1 GHz, requires a h=15 cm height. The unit will still operate below this frequency, but with degrading performance until the length is approximately $\lambda/4$. In this lower region there will also be some resonance phenomena because the unit acts like a Vee dipole with the transmission line effect of the structure providing the tuning.

If the plates of the TEM horn are bent upward to form a flat plane with a slot, it forms a tapered slot structure. The classic tapered slot antenna has an exponential taper shape as shown in Fig. 1.1-5.

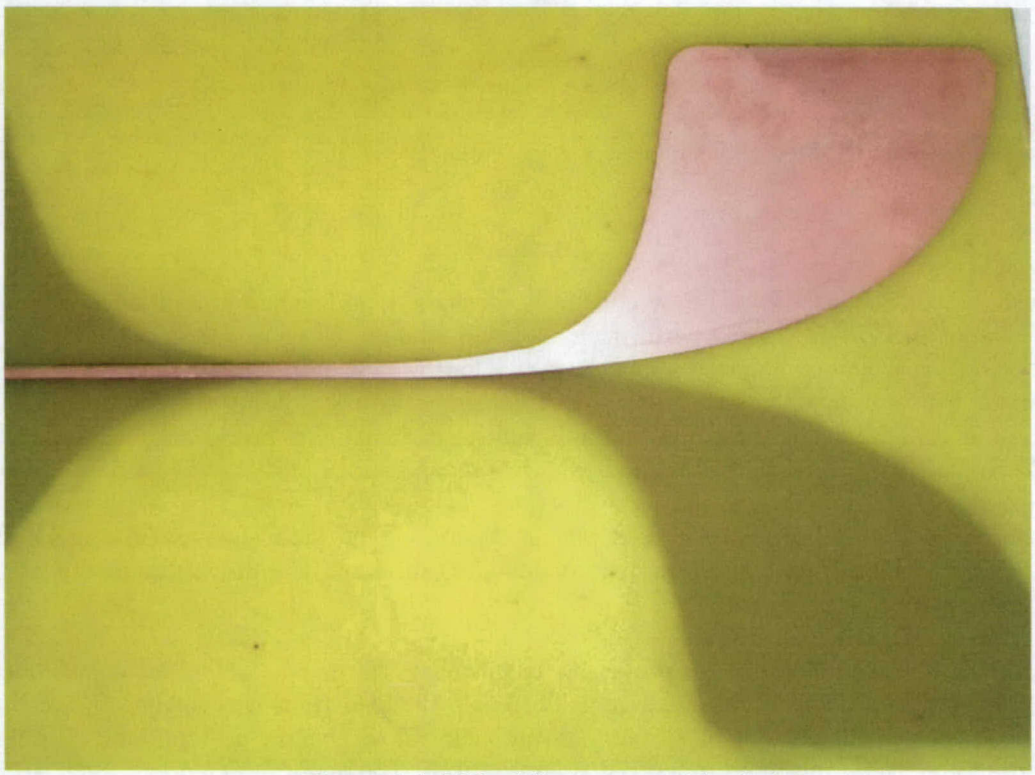

Figure 1.1-5 Vivaldi structure with a balun.

A true Vivaldi has a slot in a single plane; such an antenna was used by Northrop Grumman for the Predator UAV. The double sided structure used in Fig. 1.1-5 created a few problems in performance with an apparent slight tilt in polarization at higher frequencies. In addition, the balun structure radiated. Alternate baluns should be considered.

The ridged horn shown in Figure 1.1-6 is actually a form of tapered slot with a shield. This antenna is fed with a small cavity at the back of the unit as is often done with other tapered slot structures. The performance is uniform down to about 500 MHz.

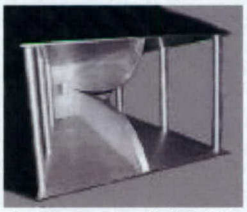

Figure 1.1-6 A Commercial Ridged TEM horn.

The bicone Fig. 1.1-7 and its discone variation provide an omni-directional pattern similar to the TEM horn shown in.

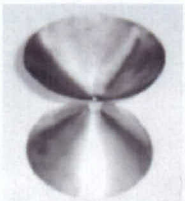

Figure 1.1-7 Bicone without cylindrical termination.

The input impedance of the bicone antenna is approximately

$$Z \approx \eta \frac{\pi - 2\theta}{2\pi \sin\theta} \Rightarrow \theta \approx 67^\circ \text{ for } 50\ \Omega \text{ input}$$

To absorb the current at the ends of the cone, it is common to add a short cylindrical section that further extends the low-frequency performance a small amount. The low-frequency boundary of the bicone occurs when the height is approximately a half wavelength. The discone is a monopole variation of the bicone with the upper cone replaced by a disk ground plane. Both antennas provide omni directional coverage in azimuth and a sector pattern in elevation. The antenna typically has relatively constant pattern and gain over its operating band.

The bowtie antenna of Figure 1.1-8 is a planar version of the biconal antenna. The bowtie generally does not have an extremely wide bandwidth, although it is useful for television and related applications.

The fat dipole and related structures provide a reasonable performance for pulsed UWB, but are not extremely wideband. The response generally has a damped ringing related to the resonant nature of the structure. The fat or sleeve variations extend the bandwidth and smooth out the resonances to be useful in some limited UWB applications. The major deficiency in such cases is a reduced efficiency manifested by reduced signal amplitude.

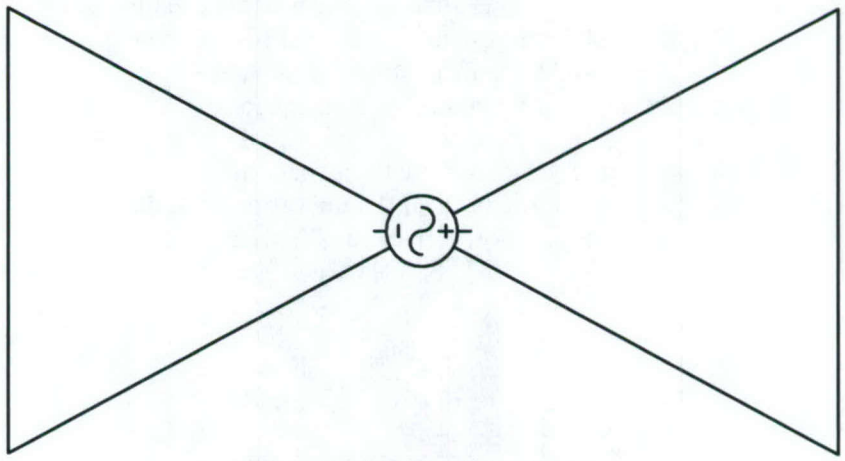

Figure 1.1-8 Bowtie antenna.

A small, but effective antenna is the half-disk structure. It is a variation on the spherical monopole that is a sphere mounted over a ground plane. The spherical structure provides a form of tapered cone equivalent. Cutting the top of the sphere off causes only minor differences in the response with a reduction by a factor of two in the height. The half-disk is a planar version of the spherical monopole, with the addition of a typical planar feeding structure that eliminates the ground plane. This arrangement is shown in Fig. 1.1-9. The response of half-disk antenna is

surprisingly good, as shown in Fig. 1.1-10. There is a slight ringing due to the dipole nature of the antenna, but it is minimal and the damping is acceptable for most applications.

For the sea-basing experiment a small tapered slot is currently planned with a range of 10-20 GHz. The tapered slot will be used due to the directional nature that is considered to be important to avoid reflections from undesired directions. The 10 GHz minimum frequency is desired to be compatible with the short pulse length of about 100 ns or less that will be required in the prototype. The operational system would require a larger antenna going to about 1 GHz.

Figure 1.1-9 Half-disk antenna.

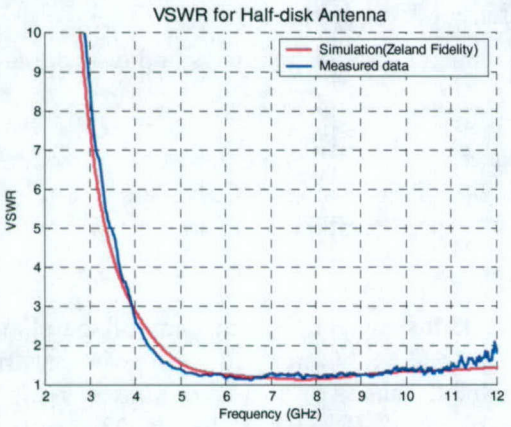

(a)

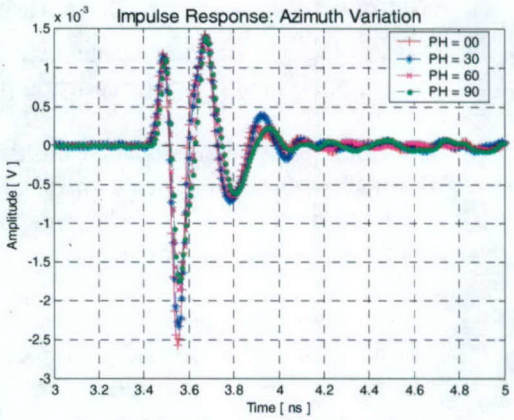

(b)

Figure 1.1-10 Response of the half-disk antenna of Fig. 1.1-9: a) VSWR and b) link time-domain response.

The half-disk structure is currently planned for the software-designed-radio to provide a small and yet wideband antenna structure for UWB applications. The same antenna can be used for the robotic task to provide a small antenna that easily mounts on the desired systems.

1.1.2 Task Activities for the Period

Task objective: Investigate new antenna technologies applicable to Navy missions and provide hardware for AWINN integration projects.
Accomplishments during reporting period: Additional progress on compact planar UWB antennas and determination of the basic specifications for the antenna requirements in other AWINN tasks.
Links to other tasks: Tasks 1.2, 1.3, 3, and 4

Subtask 1.1a Investigation of compact antennas for handheld and mobile terminals

Task objective: Design compact planar UWB antennas for various applications and systems.
Accomplishments during reporting period:

1. The work continues on the new top-loaded ultra-wideband antenna covering both a 2.4 – 10.6 GHz impedance bandwidth (VSWR < 2.5) and the 2.05 – 11.6 GHz UWB band with nearly constant radiated power. The antenna is a good candidate for the software defined radio (SDR) task in the 2.4 GHz ISM band and for the indoor/outdoor ultra-wideband frequency range of 3.1 – 10.6 GHz. It has demonstrated excellent performance for impulse UWB use and is thus also an excellent candidate for multi-band OFDM. A major contribution of the unit is the size of the planar structure with an approximately 1 inch square area.

2. The folded-notch creates a frequency notch with a resultant dual band structure for the 2.4-2.5 and 3.1-10.6 GHz bands. The notch is adjustable with parametric changes in the antenna and notch selections. The antenna maintained a low VSWR over the entire dual band range. The results were presented at the 2005 APS-URSI Conference

Links to other tasks: This task supports Tasks 1.2 and 4
Schedule: Antenna development continues through the December 2005.
Personnel: Taeyoung Yang, GRA

Subtask 1.1b Antenna Characterization – transient & wideband

Task objective: Provide antenna characterization methods in both frequency and time domain
Accomplishments during reporting period:

Continued characterization of the designed compact planar UWB antennas with top-loading and frequency notch were performed in both frequency (radiation patterns, EIRP, and return loss) and time domain (link impulse response). The measured response demonstrated the desired notch/dual-band performance.

As reported last quarter, the relative permittivity and loss tangent for the camouflage cloth were estimated using microwave measurements with a TRL calibration and the two-microstrip-line method. The results showed that camouflage cloth has $\varepsilon_r \sim 1.5$ and $tan\delta \sim 0.02$. The characterized information was used for the wearable UWB antenna design. The pattern and transient performance of the antenna were measured.

The results of this task were presented at the 2005 APS-URSI Conference.

Links to other tasks: This task supports Tasks 1.1a, b, c, and e.
Schedule: This continues through the first year.
Personnel: Taeyoung Yang, GRA

Subtask 1.1c UWB antenna design (support of AWINN demonstrations)

Task objective: Design various UWB and other antennas needed for AWINN demonstrations
Accomplishments during reporting period:

Revised the specifications for the required UWB antennas of other tasks.

Reviewed the candidate antennas that can be used and evaluated the pros and cons of the antennas for specific needs. Feasibility has been a major concern in the evaluation of the specifications for the actual design.

The application of the fundamental limit theory to the design process for new antennas was evaluated on a limited basis. These considerations are directly related to the antenna selection for the AWINN demonstrations.

Links to other tasks: This task supports the Tasks 1.2 and 4
Schedule: Initial design and fabrication will be done in next 6 months and performance improvement and optimization continues up to end of the year. The antenna needed for the sea-based simulator is to be completed by September 2005. The UWB system support antennas are to be completed by November 2005. Antennas in support of the robotic tasks will be developed in the Fall 2005 in parallel with the UWB system support design.

Personnel: Taeyoung Yang (GRA), Randall Nealy (Engineer), and W. Davis (PI)

Subtask 1.1d Antennas providing polarization, spatial, and pattern diversity – Evaluation of antennas in a MIMO environment

Task objective: Base station/access point antennas providing polarization, spatial and pattern diversity useful in supporting MIMO and space-time coding processing. Evaluation of antennas in a MIMO environment.
Accomplishments during reporting period: Related dissertation work has been performed by a group graduate student. This work uses UWB modeling to predict the interaction of radiated energy with canonical objects. At present, measurements have been made for a sphere, the complex resonances determined with the associated amplitudes, and the results compared to the theoretical poles (resonances). The comparison was excellent, though several poles were not found. Evaluation of the theoretical amplitudes has not yet been completed that will likely explain the absence of some poles in the measured data. The purpose of this work is to predict the interaction of radiation with basic canonical objects in a statistical manner and then apply the principles to the prediction of propagation in a multipath environment, particularly and indoor environment. Such information would be applicable to propagation within a ship cavity or on the cluttered deck of a ship, in time or frequency based systems.
Links to other tasks: This topic may impact on the frequency selection and interaction of the measurements used for the Sea-Based cargo systems being considered in Task 3.
Schedule: The majority of the work on this task will follow the development of the antennas and is projected for Spring 2006.

Personnel: Garauv Joshi, GRA (Ph.D.)

Subtask 1.1e Support physics/engineering-based models for Digital Ships

Task objective: Support of Task 3 to develop physics/engineering–based templates for Digital Ships for radar simulation, including EW techniques.
Accomplishments during reporting period: None to date
Links to other tasks: In support of Task 3 on Digital Ships
Schedule: As requested by the personnel of Task 3 – Expected during Fall 2005

Subtask 1.1f Wideband balanced antenna/array feed networks

Task objective: Development of array feed networks for wideband balanced antenna systems such as the Fourpoint antenna investigated in the NAVCIITI program

Accomplishments during reporting period: None to date
Links to other tasks: This is related to potential directional needs of other tasks, but has no direct link at present
Schedule: Begin Fall 2005

1.1.3 Importance/Relevance

The compact planar UWB antennas can accommodate the current needs for the handheld and mobile terminals. The designed frequency notch UWB antennas might provide a solution to reduce the inference to the other existing narrow band applications.

Specific requirements have been identified to set the antenna specifications for the software defined radio and sea-based tasks. This has been described in the task summary for this quarter.

The pole-residue modeling of radiation scatterers is expected to offer a significant step toward the design of effective multipath propagation environments, such as the selection of specific object sizes to reduce interaction at particular frequencies and the addition of other scatterers to enhance the radiation characteristics in specific cases – such a hallway corners and coupling into room doors. The models may have a significant impact for communication link simulation.

Contact: The information of desktop antenna and propagation prediction is an item of critical interest in the design of topside platform configurations. This work is currently being performed by the J-50, EMC team at the Naval Systems Warfare Center – Dahlgren Division. I am coordinating contact with Mike Hatfield of that section.

1.1.4 Productivity

Conference publications

1. Taeyoung Yang, William A. Davis, and Warren L. Stutzman, "Folded-Notch Dual Band Ultra-Wideband Antennas," IEEE AP-S International Symposium (Washington, DC), July 3-8, 2005 - Presented.
2. Taeyoung Yang, William A. Davis, and Warren L. Stutzman, "Small, Planar, Ultra-Wideband Antennas with Top-Loading," IEEE AP-S International Symposium (Washington, DC), July 3-8, 2005 - Presented.
3. Taeyoung Yang, William A. Davis, and Warren L. Stutzman, "Wearable Ultra-Wideband Half-Disk Antennas," IEEE AP-S International Symposium (Washington, DC), July 3-8, 2005 - Presented.
4. William A. Davis, "Development of New Antennas and Applications: UWB Antenna Modeling and Aspects of Smart Antennas," Institute for Defense & Government Advancement (IDGA) Military Antennas Conference in Crystal City, September 19-21, 2005 – to be presented
5. Warren L. Stutzman, William A. Davis, and Taeyoung Yang, "Fundamental Limits on Antenna Size and Performance," Antenna Systems Conference (Santa Clara, CA), Sep. 22-23, 2005 – To be presented
6. Taeyoung Yang and William A. Davis, "The Planar UWB Antenna Response and UWB performance issues," General Assembly of International Union of Radio Science (New Delhi, India), Oct. 23-29, 2005 – to be presented

Books and Book Chapters

1. W. A. Davis, "Antennas", *An Introduction to Ultra Wideband Communication Systems*, ed. J. H. Reed, Ch. 4, Prentice Hall, 2005, New York
2. W.L. Stutzman & W.A. Davis, "Antenna Theory," *RF Encyclopedia*, Wiley, 2005, New York.

Honors and Recognitions

1. W. A. Davis, Vice-Chair of the IEEE AP-S Symposium and USNC/URSI National Radio Science Meeting, 3-8 July 2005, Washington, DC

Students supported

Taeyoung Yang, Jan. 15, 2005 – May 15, 2005 (on summer internship)

Faculty supported

Dr. William A. Davis, VTAG Director, Jan. 15, 2005 – present
Dr. Warren L. Stutzman, Faculty, Jan. 15, 2005 – present

Staff and other personnel supported

Mr. Randall Nealy, VTAG Engineer, Jan. 15, 2005 - present

1.1.5 Summary Quad Chart

AWINN Task 1.1 – Advanced Antennas

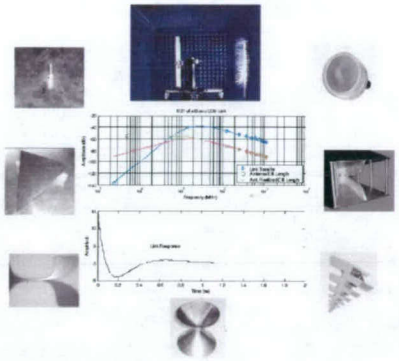

Technical Significance

- To support the design and implementation of a flexible, reconfigurable wireless network with multiple frequency requirements, including the capabilities of ultra-wideband (UWB) radio technology and indoor/topside propagation
- The modeling and design techniques will improve the time to production of antennas to meet the Navy mission for a multitude of needs

Major Performers

Virginia Polytechnic Inst. and St. U.,
Dr. William Davis
Dr. Warren Stutzman

TASK 1 Advanced Wireless Technologies

New antenna technologies applicable to Navy missions & hardware for AWINN integration projects.

Task 1.1 Advanced Antennas

- Investigation of compact antennas for handheld and mobile terminals
- Antenna Characterization – transient & wideband
- UWB antenna design (support of AWINN demonstrations)
- Antennas providing polarization, spatial, and pattern diversity – Evaluation of antennas in a MIMO environment
- Support physics/engineering-based models for Digital Ships
- Wideband balanced antenna/array feed networks

Impact

- Potential new techniques for design of antennas and propagation channels to more effectively used the mission environment, particularly for applications requiring small antennas if frequency flexibility. The techniques also offer the potential of simplifying the topside design of the electromagnetic environment.

1.1.6 Timeline Chart

Task 1.1 Advanced Antennas

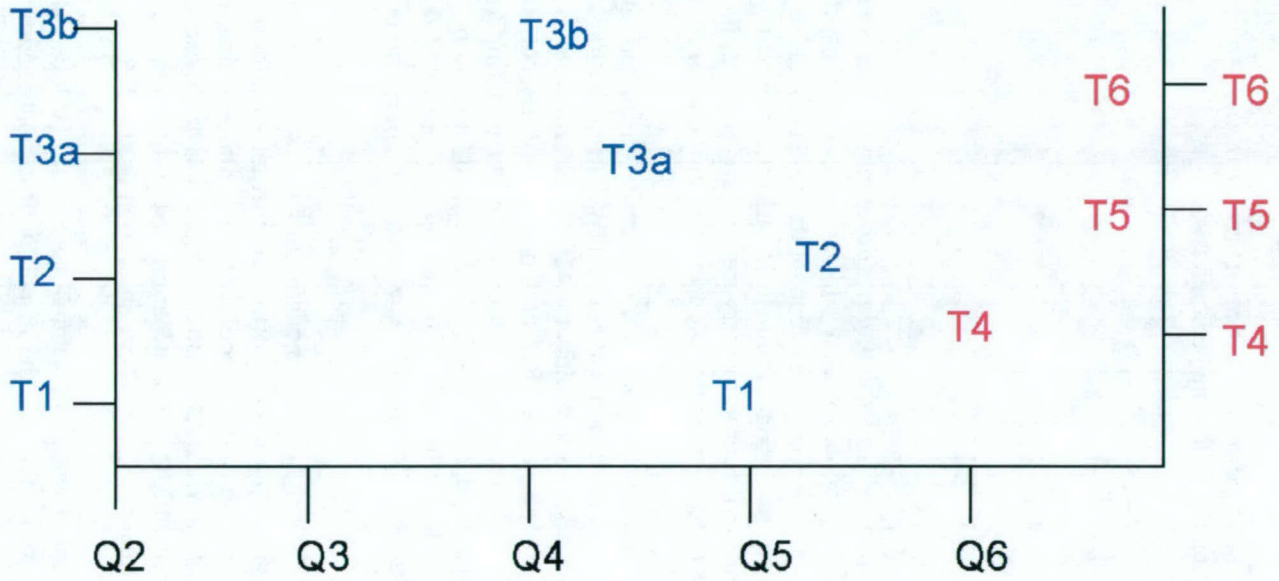

T1: Mobile Design T2: Characterization T3a: SDR Antennas T3b: Sea-Base Antennas

T4: Diversity T5: Physics Models T6: Wideband Array Feeds

1.2 Task 1.2 Advanced Software Radio

1.2.1 Overview

Task Goal: This task investigates an advanced Software Defined Radio (SDR) which can take advantage of the unique properties of Ultra Wideband communication for Navy applications such as precision position location, ranging, and low probability of intercept.

Organization: This task is managed by the Deputy Director of the Mobile and Portable Radio Research Group (MPRG) using the following personnel:

Jeffrey H. Reed, Deputy Director
R. Michael Buehrer, faculty
William H. Tranter, faculty
Chris R. Anderson, GRA
Swaroop Venkatesh, GRA
Jihad Ibrahim, GRA
Maruf Mohammad, GRA

Summary: This quarter we focused on finalizing the development of a prototype version of the SDR receiver. Board layout and signal integrity simulations indicate that the system will run at the desired sampling rate of 2 GHz. The capability to synchronize receivers has been incorporated into the board so that we can evaluate D-MIMO algorithms. Additionally, a data capture mode will allow us to perform rudimentary ranging and position location measurements. We expect the prototype boards to be operational during the third quarter of this year.

SDR algorithm development during the past quarter focused on increasing the performance of signal acquisition, as well as data demodulation for UWB transmissions. UWB propagation environments are very rich in resolvable multipath, which makes a simple correlator matched to the transmit pulse shape highly inefficient. Research has mainly concentrated on Rake receivers as candidates for efficient UWB detectors, because of the inherent fine time resolution of the UWB pulse. We are investigating the use of pilot-based data demodulation, where pilot symbols are generated from both dedicated pilot pulses as well as data pulses. Incorporating both pilot and data pulses into the matched filter template waveform reduces training overhead and can improve system performance.

Recent developments in light-weight multi-mode/multi-band software radios can leverage a multi-band communication capability and network-wide position location information to achieve the same benefits offered by space-time coding (STC) and multiple-input-multiple-output (MIMO) communication systems without the use of antenna arrays. In particular, we are working on adapting such a distributed MIMO communication system to operate using UWB signals to improve the range and performance of UWB communication links.

For ranging and position location, initial algorithms have been developed and tested in a simple proof-of-concept laboratory environment. The results indicate that ranging accuracy should be within a few inches, and that position location via evaluation of the multipath delay profile is possible. These algorithms are currently being updated to provide full 3-D ranging and positioning information, as well as incorporate the use of the SDR receiver.

1.2.2 Task Activities for the Period

Subtask 1.2a Develop flexible software radio platforms that includes cross-layer optimization with capabilities for UWB and ad hoc networking

Task objective: The overall goal of this subtask is to design an advanced software-defined/reconfigurable radio that is optimized for ultra wideband communication and then to implement the system using off-the-shelf components. The software-defined radio implementation to provide tremendous flexibility compared to a single hardware implementation—for example, providing the capability to utilize one of several different popular UWB modulation or multiple access schemes, to operate in one of several modes (communication, ranging, or data capture), as well as to utilize more traditional broadband communication schemes.

Accomplishments during reporting period: In any high-speed digital system, prototyping is the key to ensuring the final system is fully functional and operational. Prototyping provides a means to discover and correct potential problems and to measure any unknown quantities, as well as an opportunity to fine-tune the software algorithms. As a result of a series of design reviews by both academia and industry, it was decided to create a scaled down prototype receiver to demonstrate that the TI-Sampling receiver concept could indeed work both at the system level and at the PCB level.

Additionally, the performance of a TI-Sampling architecture is highly dependant on matching the individual ADC gains, offsets, and timing delays. Mismatches can result in a significant distortion of the received signal, which can be thought of as noise added to the ideal received signal by the TI-Sampling process. Mismatches can be caused by minor physical differences between ADC components (due to variations in the semiconductor fabrication process), as well as fluctuations due to noise and environmental variations (temperature, vibration, etc.). Many researchers have investigated the SNR degradation of a TI-Sampling array for CW inputs; however, no one has investigated the performance of such an array for a UWB or other pulse-based signal.

To quantify how tightly the ADC parameters must be controlled, a series of simulations were performed using three different pulse widths: 1.0 nanosecond monocycle, a 1.5 nanosecond monocycle, and a 2.0 nanosecond monocycle. For each pulse width, four separate simulations were performed: Gain Mismatch, Offset Mismatch, Timing Mismatch, and Total Combined Mismatch. For each simulation, the received signal was modeled as a simple Gaussian Monocycle. Quantization effects of the ADCs were included in the simulation, and pulses had an amplitude equal to the full-scale ADC input voltage. The pulse rate was set at 100 Mpulses/sec, the effective sampling rate set at 8 GHz and 8 bits of quantization, which lead to 80 ADC samples per received signal pulse. Simulation results are shown in Figure 1.2-1. From the figure, we note that a 6 dB degradation in the receiver SNR means that we can tolerate a maximum mismatch of ± 10%. A worst-case ±100% mismatch reduces the receiver SNR to only 10 dB.

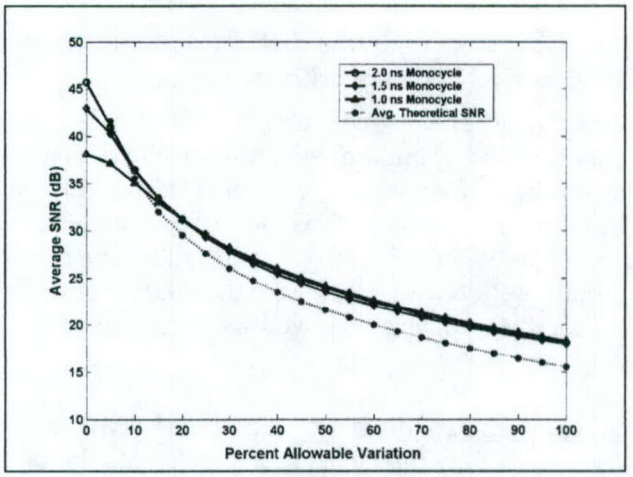

(a)

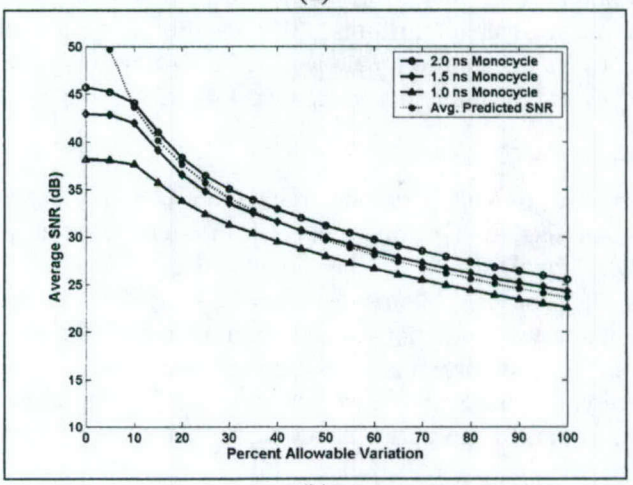

(b)

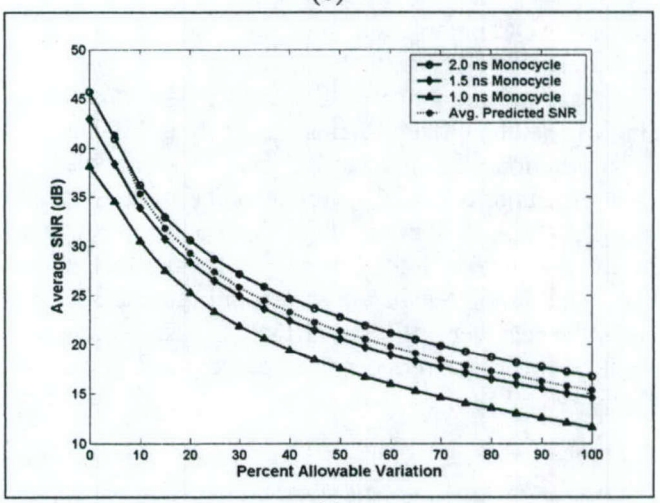

(c)

Figure 1.2-1 Performance evaluation of an 8-ADC TI-sampling system for total combined mismatches for 100% allowable variation is a gain mismatch of ±50%, an offset mismatch of ±5.5 least significant bits, and a timing mismatch of ±125 ps. (a) Gain mismatch. (b) Offset mismatch. (c) Timing mismatch.

Schedule:

- January – July 2005
  - Develop 2-ADC Prototype Receiver
- August-September 2005
  - Fabricate Receiver
    - Update Transmitter Design
    - Evaluate Prototype Receiver Hardware and FPGA Code
- October-December 2005
  - Develop 8-ADC Full Receiver
    - Upgrade UWB Transmitter
    - Begin Integration of Receiver with Other AWINN Activities
- 1st Quarter 2006
  - Fabricate 8-ADC Full Receiver
    - Verify Operation of Receiver Hardware and FPGA Code
- 2nd Quarter 2006
  - Demonstrate Transceiver Operation
    - Integrate Transceiver with Other AWINN Activities

Personnel:

Chris R. Anderson – Transmitter and Receiver Hardware Development
Deepak Agarwal – Receiver FPGA Code Development

Subtask 1.2b Software radio research applied to UWB, including design parameter space exploration.

Task objective: The objective of this task is to investigate innovative SDR architectures and algorithms for both traditional broadband and UWB communications. These algorithms will be implemented on the advanced SDR receiver developed in Subtask 1.2a.

Indoor UWB systems have to contend with extremely frequency-selective communication channels. The received signal is very rich in resolvable multipath, which makes a simple correlator matched to the transmit pulse shape highly inefficient. Research has mainly concentrated on Rake receivers as candidates for efficient UWB detectors, because of the inherent fine time resolution of the UWB pulse. However, it has been shown that the Rake energy capture is relatively low for a moderate number of fingers, making its implementation impractical for UWB systems. The pilot-assisted receiver is another widely studied type of receiver which aims at gathering all the signal energy by using the received pulse shape itself as a correlation template. Pilot-assisted receivers suffer from a "noise-cross-noise" term, caused by the use of a noisy signal as a correlation or matched filter template. Consequently, a prohibitively large number of pilots are required to overcome this limitation. The training overhead can be reduced by using a data-aided pilot-assisted scheme, where channel information is jointly extracted from the training and data signals. However, performance is still limited by the low SNR operating levels of traditional UWB systems. A potential solution is to add a strong error correcting code. Error correction coding is especially attractive for systems employing low-duty cycle pulses, since coding can be added while maintaining the data rate by reducing the symbol repetition time.

Accomplishments during reporting period:

Receiver Design

We propose a novel approach to UWB signal detection, based on sequence optimization for the multipath transmission channel. The transmit waveform is made up of a train of delayed and scaled pulses, the amplitudes of which can be represented by a real-valued sequence. The correlator template at the receiver is formed of another real-valued sequence. Both sequences are jointly optimized such that the correlation of the received signal with the correlation template is maximized. This results in coherent combining of a substantial number of the multipath components at the receiver, leading to very high energy capture with the use of a simple receiver. Simulation results based on measured channel profiles show that the proposed scheme offers substantial improvements over a Rake receiver using a large number of fingers and maximum ratio combining. Also, the proposed scheme gives improved performance over a pilot-assisted template receiver with a heavy training overload.

The performance of the proposed scheme is compared to other signal detection methods in Figure 1.2-2. The training overhead (for channel estimation) is equal to 250 pilots for the proposed method. First, note that the simple matched filter employing the transmit UWB pulse shape as a correlation template leads to poor performance, since only the energy in the first arriving path is captured. Using a non-optimized, random sequence also leads to similar performance, because the multipath energy adds noncoherently, thus leading to a very low energy capture. A Rake receiver using maximum ratio combining with 10 fingers (where it is assumed that the energy in the strongest 10 paths is perfectly captured) gathers only a fraction of the total received energy, and yields a performance that is about 4.5 dB worse than the perfect Rake case (Rake receiver with an infinite number of fingers with perfect channel estimation). A pilot-based receiver with 250 pilots only achieves performance that is within 2 dB of the perfect Rake. The proposed receiver based on the optimal sequence out performs the perfect Rake by about 2 dB. Also, using 250 pilots results in negligible performance loss compared to the perfect channel knowledge case.

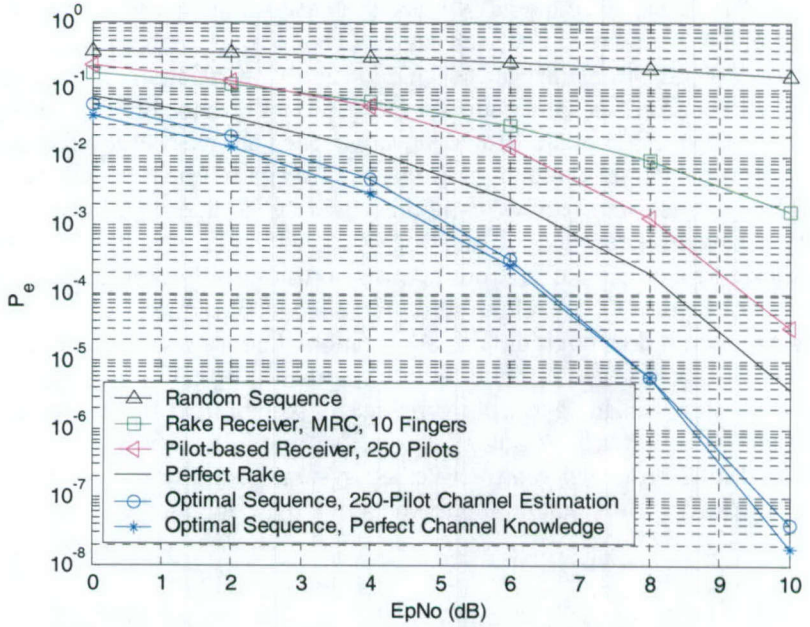

Figure 1.2-2 Simulation results for the performance of sequence optimization receiver.

Acquisition

Acquisition of Impulse Radio Ultra Wideband (UWB) signals is a challenging problem because narrow, pulses along with relatively low duty cycles, result in an extremely large search space (i.e. uncertainty region). With traditional search techniques, the large search space results in prohibitively long acquisition times. Additionally, in dense multipath environments (e.g., indoors), unlike traditional spread spectrum, there exists a larger number of cells within the uncertainty region that can lead to false or suboptimal acquisition lock. However, for many applications not all of these lock positions are equally desirable since locking to an arbitrary multipath component results in either range error (positioning applications) or reduced energy capture (communications applications). In this work, we present a modified framework for the analysis of UWB acquisition that accommodates multiple lock cells. Further, the framework divides the acquisition process into two distinct phases. The two phases, which are termed "coarse" and "fine" acquisition, are analogous (but not identical) to the acquisition and tracking processes in traditional synchronization. We also propose and analyze specific algorithms for each phase. The first acquisition phase, called jump-phase search, is a fast implementation of traditional serial search which takes advantage of the large number of cells which can terminate the search process. The second phase exploits statistics derived from the first phase and the clustered nature of multipath arrivals to determine the earliest arriving path, even when it is severely attenuated. Analysis and simulation results are presented for each phase. We show that the first phase provides a substantial improvement in mean acquisition time compared to traditional serial search and that the second phase provides improved performance for both ranging and communications applications.

As an example, the application of two-stage acquisition to ranging is illustrated in Figure 1.2-3. The acquisition time error τ is mapped into a ranging error d by $= c\tau$, where c is the speed of light. Notice that the two-stage acquisition approach acquisition results in significant reduction in ranging error compare to traditional acquisition (serial or linear search).

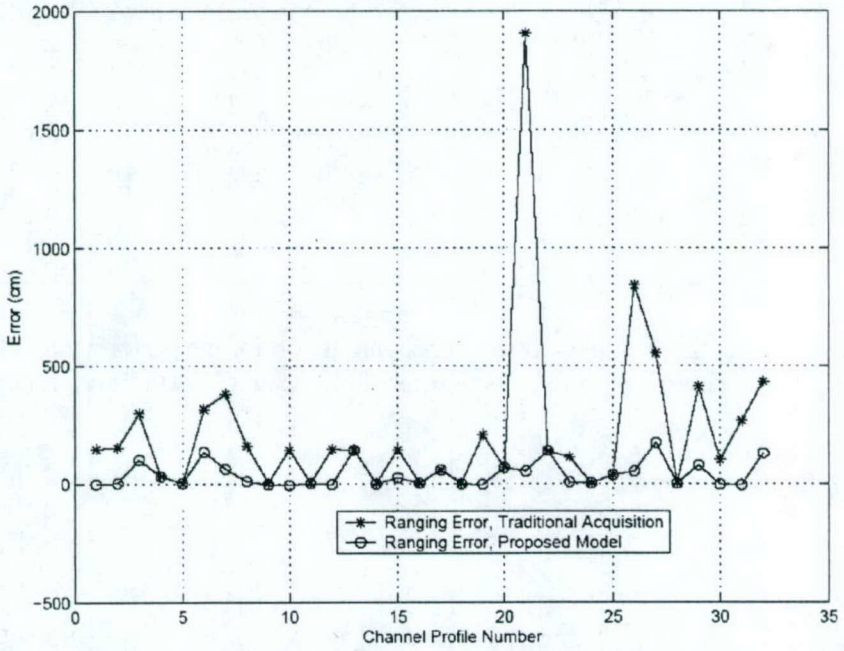

Figure 1.2-3 Simulation results for the performance of fine acquisition in ranging. SNR = 15 dB for a spreading code length = 64, showing range error in cm versus channel profile number.

Interference Mitigation

A narrow band interference (NBI) mitigation scheme for ultra-wide bandwidth (UWB) signals using multiple receive antennas is examined. The low spatial fading of UWB signals compared to NBI signals is exploited to provide "interference diversity". Whereas classical diversity techniques are designed to increase the desired received signal power, the aim of interference diversity is to minimize the effective NBI power. Selection diversity (SD), equal gain combining (EGC) and maximal ratio combining (MRC) methods are investigated. It is shown that SD and ECG result in a 3-dB performance improvement when the number of receive antennas is doubled. Also, MRC yields additional gains over SD and ECG. The proposed methods are mathematically analyzed, then verified by simulation.

We have reached the following conclusions based on our analysis:

- First, SD and EGC yield the same performance. We see an improvement of 3-dB every time the number of antenna is doubled (Figure 1.2-4).
- Second, MRC gives additional gains of 1 to 2 dB compared to SD or EGC (Figure 1.2-5).

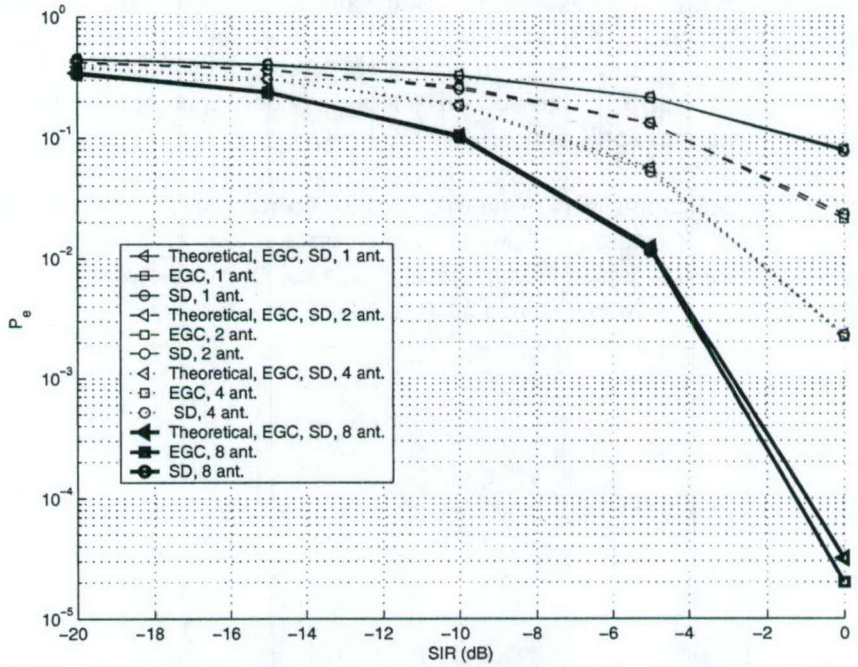

Figure1.2-4 Simulation results of interference mitigation for the performance of EGC and SD for Rayleigh/Fading, showing probabilities of error (Pe) versus signal to interference ration (SIR).

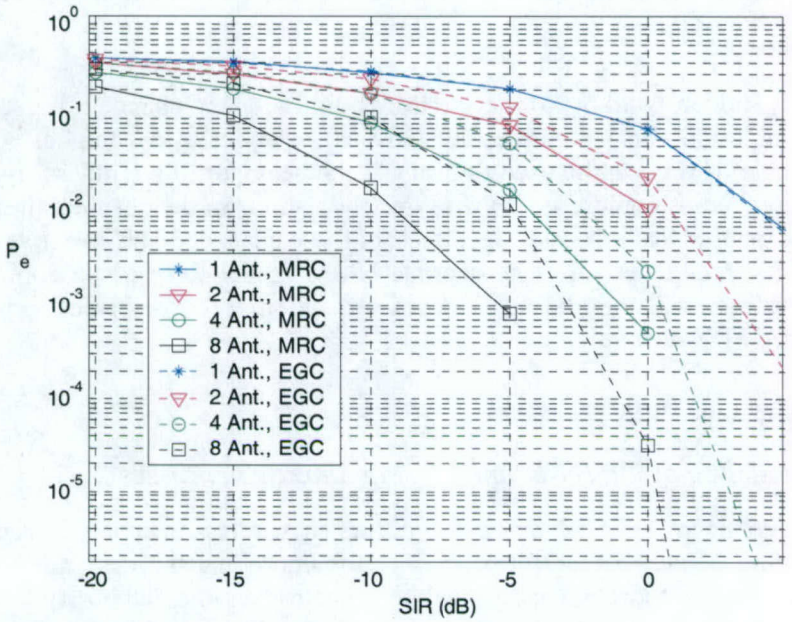

Figure 1.2-5 Simulation results of interference mitigation using MRC vs. EGC for NBI Rayleigh fading.

Schedule:

- January-Summer 2005
  - Finalize two-stage acquisition algorithm
  - Investigate further receiver design strategies
- Summer-Fall 2005
  - Start work on narrowband interference mitigation techniques
  - Start work on UWB tracking
  - Finalize receiver design algorithms
- 1st Quarter 2006
  - Finalize interference work
  - Begin integrating algorithms into hardware
- 2nd Quarter 2006
  - Integration of interference cancellation, synchronization and signal detection into common framework
  -

Personnel:

Jihad Ibrahim – UWB Algorithm Development

Subtask 1.2c Software radio designs for collaborative systems that take advantage of this radio, particularly for interference environments.

Please refer to Section 4.1, TIP #1.

Subtask 1.2d Vector channel models, including Markov Models, and supporting channel measurements.

Task objective: Hidden Markov Models (HMM) for wireless channels are convenient and analytically tractable tools that describe the statistical behavior of a complicated random time series. For example, HMM can be used to evaluate the behavior of a wireless signal in a fading channel. Cognitive radios could use HMM to track variations in the channel; these radios could then respond in a manner that mitigates the effects of these changes. The objective of this subtask is to develop algorithms to establish appropriate HMM model for a given application. These models and algorithms will then be verified via simulation and possibly by experimental data using the advanced SDR receiver.

Accomplishments during reporting period:

Analysis and Modeling of UWB Channels Using Markov Processes

The accurate modeling of error behavior that occurs in wireless channels is necessary for the better understanding of network performance and for improving the design of communication protocols. For example, a thorough understanding of the packet loss and bursty nature of errors is essential for the proper design and parameter tuning of error control protocols, etc.

Discrete channel models are used for simulating the error traces produced by wireless channels. The primary advantage of discrete channel models is fast running time. Discrete channel models with memory can be represented mathematically using discrete time Markov chains, hidden or semi-hidden Markov processes [1]. The primary use of these models allows easy, rapid experimentation and prototyping. Using these models, one can then dynamically generate artificial error patterns for the communication system under study and use these traces to simulate, and thus, better understand the performance of existing system. Due to their ease of use and repeatability, the system engineer can use these error patterns for developing and improving the performance of wireless system.

Although Markov models are used extensively in wireless channel modeling, an important point about these models should be noted. Markov channel models are brittle in the sense that a slight change in system parameters; for example, a change in received SNR, in transmitter-receiver separation, in channel impulse response, in the modulation format, or in the receive signal processing requires that new data be generated and the Markov parameter re-estimated.

UWB error statistics are collected based on channel measurements performed at MPRG. These error statistics are then used as training sequences to train different Markov models. In this report we discuss an important issue that happens in hidden Markov modeling of UWB error sources. A simple block diagram of an N-state HMM is shown in Figure 1.2-6.

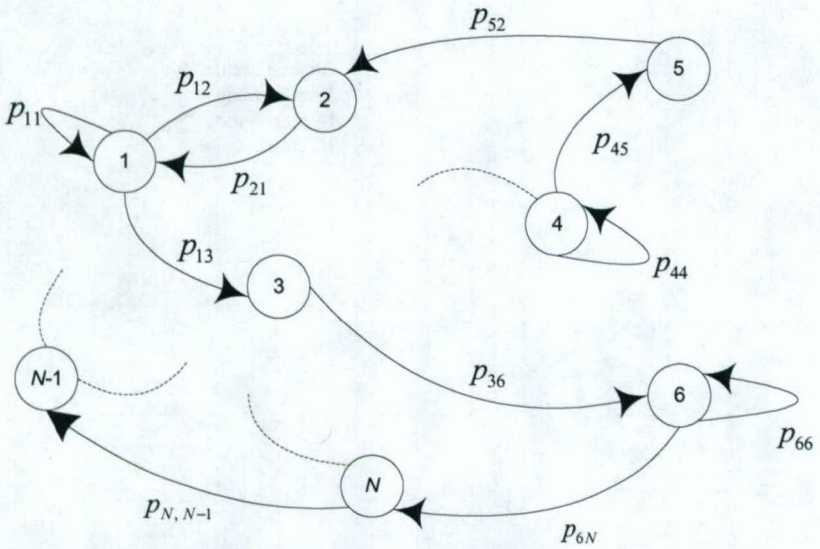

Figure 1.2-6 Illustration of an N-State Hidden Markov model and their transitions.

The use of correct model order is necessary for the accurate analysis of wireless channels. The use of incorrect Markov order might lead to suboptimal design of communication system under investigation. Estimating the correct order of hidden Markov models is a major research area and many publications are devoted to this topic [2-5]. In this report, we use a 2-state, 10-state and 15-state hidden Markov models and evaluate their performance in terms of bit error probability and frequency of error runs and error-free runs.

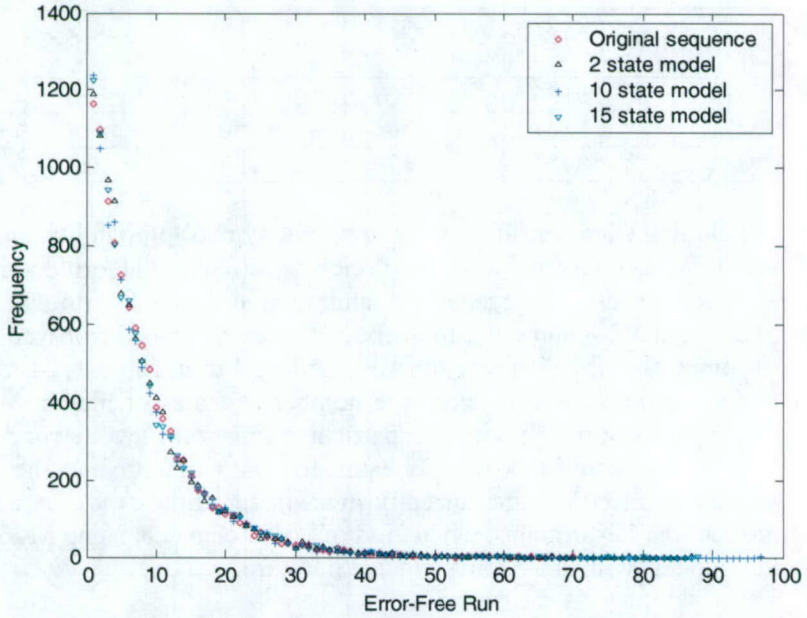

Figure 1.2-7 Simulation results for frequency of error free runs of original and Markov generated sequences.

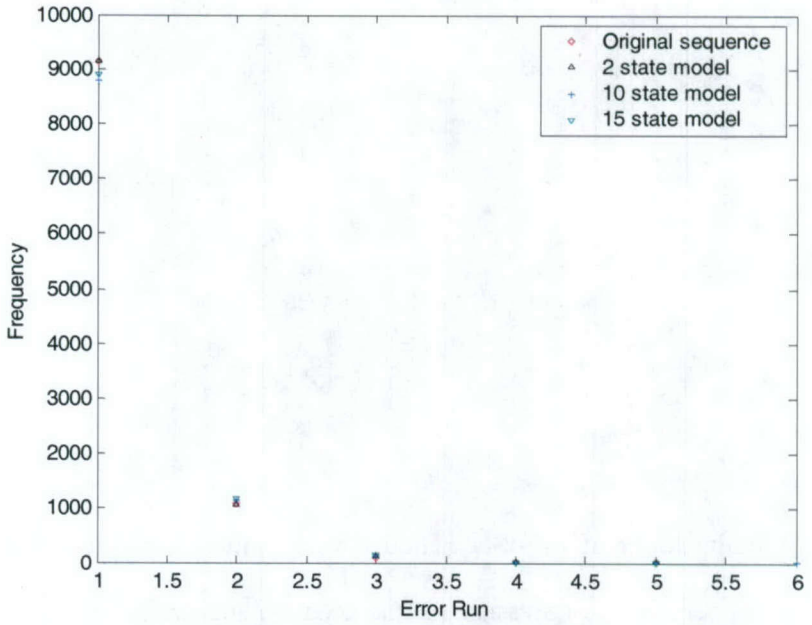

Figure 1.2-8 Simulation results for frequency of error runs of original and Markov generated sequences

Table 1.2-1 Frequency of Error Runs of Original and Markov Generated Sequences

	Length 1	Length 2	Length 3	Length 4	Length 5
Original sequence	9123	1085	112	12	1
2 state HMM	9123	1067	136	15	3
10 state HMM	8801	1144	150	24	1
15 state HMM	8904	1174	153	24	3

Model parameters including state transition matrix, output symbol probability matrix and initial state probability vector are obtained using Baum-Welch re-estimation algorithm [1] with random initial parameters. Error traces are regenerated and then compared with the original error statistics. Figures 1.2-7 and 1.2-8 show the frequency of error runs and error-free runs generated by waveform level simulation for different Markov models. From Table 1.2-1 we can observe some performance degradation as we increase the number of states of hidden Markov models. The 2-state HMM is the closest match with this particular waveform level error sequence. Thus, there exists a need for a consistent Markov order estimator that would give us the correct number of states for a given error trace. We are currently investigating this issue and will address this further in our future reports. Performance evaluation of UWB channels using Markov chains and semi-hidden Markov models will also be investigated in future.

References

1. W. Turin, Digital Transmission Systems: Performance Analysis and Modeling, McGraw-Hill, 1998.

2. P. Billingsley, "Statistical methods in Markov chains," Ann. Math. Statist., vol. 32, 1961.

3. C. Chatfield, "Statistical inferences regarding Markov chain models," Appl. Statist., vol. 22, 1973.

4. R. J. MacKay, "Estimating the order of a hidden Markov model," The Canadian Journal of Statistics, vol. 30, No. 4, 2002, Pages 573-589.

5. S. Khundapur and P. Narayan, "Order Estimation for a Special Class of Hidden Markov Sources and Binary Renewal Processes," IEEE Trans. on Inf. Theory, vol. 48, no. 6, June 2002.

Schedule:

- January-Summer 2005
  - Collect channel measurements
- Summer-Fall 2005
  - Begin model development
- 1st Quarter 2006
  - Simulate performance of the models for UWB communications
- 2nd Quarter 2006
  - Integrate models with SDR Receiver

Personnel:

Ishan Akbar – HMM Algorithm Development

Subtask 1.2e Software radio integration into the AWINN demonstrations.

Task objective: The goal of this subtask is to integrate the software radio developed in Subtask 1.2a into AWINN activities. To achieve this objective, the software radio is being designed with two distinct modes of operation: a communication mode and a data capture mode. The communication mode is currently optimized for impulse UWB signals, however, it is capable of operating using any broadband communication technique (such as DSSS or OFDM). The only limitations on the types of signals that the receiver can handle are: (1) the 2.2 GHz analog input bandwidth limitation of the MAX104 ADCs, (2) the 8 GHz effective receiver sampling frequency, and (3) the processing power of the FPGA.

In the data capture mode, the receiver will simply capture ADC samples and store them in the FPGAs RAM memory. The data can then be processed in non-real time using one of the FPGAs PowerPC processors, or the sample values can be transmitted to a host computer via the USB interface. The number of samples that can be captured is limited by the amount of high-speed RAM memory that can be allocated, but is currently estimated to be around 256,000-512,000 samples—corresponding to about 32-64 μsec of captured data. A trigger signal input allows the receiver to estimate the time of arrival of received samples for ranging, and the ability to synchronize multiple receivers to a common clock signal allows for precise position location.

Accomplishments during reporting period: Several provisions for integrating the software radio into the AWINN activities have been included in the design of both the prototype and full receiver. To facilitate synchronization of several receivers, the clock distribution network was modified to allow for several receivers to be synchronized to a single clock source. A trigger signal input allows the receiver to operate in the data capture mode and measure the time of arrival for UWB pulses. A trigger output allows the FPGA to control an external UWB pulse generator, to facilitate evaluation of the communication system, ranging, and position location algorithms. Finally, FPGA code for the data capture mode is under development and will be implemented on the prototype receiver board.

Schedule:

- August/September 2005 – Evaluate Prototype Receiver
  - Verify that the receiver operates in all modes
  - Verify FPGA code for data capture as well as PowerPC processing
- October-December 2005 – Refine FPGA/PowerPC code for ranging and/or position location
  - Support code development with measurements either from lab equipment or the prototype receiver
- Spring 2006 – Integrate Full Receiver into AWINN Activities
  - Crane demonstration
  - Position location
  - Imaging
  - Channel measurements

Personnel:

Chris R. Anderson – Transmitter and Receiver Hardware Development
Deepak Agarwal – Receiver FPGA Code Development

Subtask 1.2f UWB applications to technology development applicable to Sea-Basing: position location, ranging, and imaging.

Please refer to Section 4.2, TIP #2

1.2.3 Importance/Relevance

The simulation results from the SDR testbed simulations demonstrate that the time-interleaved sampling approach is a viable hardware architecture. The use of TI-Sampling with digital demodulation provides a tremendous amount of flexibility in the receiver operation. Even though the receiver is optimized for impulse UWB communication, it should be capable of using almost any broadband communication scheme.

The UWB SDR algorithm design is investigating ways of improving signal acquisition and tracking, as well as operation in multipath environments. Ship-based environment tend to generate a large number of multipath signals and represent a tremendous amount of energy available for the receiver to capture. Using a pilot-based matched filter topology, the receiver can capture a large percentage of the available energy without resorting to the complex tracking algorithms required by Rake receivers.

The distributed MIMO architecture investigated in this task will allow a number of UAVs to coordinate their transmissions and take advantage of space-time coding performance gains. These performance gains are available even if the various UAVs are not perfectly synchronized—an important consideration if the transmission involves a UWB signal. Combining UWB with distributed MIMO, we believe that long-range transmissions should be possible while still maintaining the LPI properties of UWB signals.

Finally, UWB signals have been demonstrated to have precision ranging and position location properties. Combining 3D ranging information with the crane control system should allow for sea-based ship-ship cargo transfer. Additionally, the position location abilities of UWB will

allow for inventory control and tracking, as well as the precision maneuvering required to establish the ship-ship cargo transfer.

Smart antenna radios are radio systems which use multiple antenna elements with smart signal processing that helps improve range, capacity and reliability of a wireless system. Smart antenna technology has seen adoption in wireless military applications and in commercial cellular base stations. Most recently they have also been considered for WLANs using MIMO technology which is a type of smart antenna technology.

Smart Antenna API Update

There are many flavors of smart antenna implementations some of which include beamforming, space-time coding and multi-antenna multi-user detection. Software defined radios are designed to have multi-mode capability with support for multiple standards and waveforms. This philosophy of design needs to be extended to radios with multiple antennas that in turn are capable of operating under different types of smart antenna technology. Hence the standardization and identification of API interfaces for use of smart antennas lends itself to SDR design effort.

The smart antenna API (SA-API) WG at SDRForum is working towards standardization of the APIs for SDR systems to include smart antennas. With a variety of smart antenna systems available today and the growing number of standards with each having their own implementation and interface issues it is difficult to create APIs that cover every possible scenario. At the same time it is also important to figure out how the introduction of a smart antenna system would affect the current SCA radio framework. Towards this goal the SA-APIa WG led by Virginia Tech and Hanyang University are collecting use case scenarios for different types of smart antenna implementations. The use case scenarios will help identify generic modules required for different types of implementations and the specific ones. This then will help set a framework for smart antennas within a SDR. Once the framework is available it will become easier to specify the interfaces for smart antenna modules that are general purpose in nature and can be extended to specific implementations.

At the current meeting the ongoing effort on collection of use cases was presented that highlighted different types of smart antenna implementations for different waveform applications. The presentation also talked about the issues stated above on the challenges in creating general purpose SA-APIs. The importance of creating a smart antenna framework before looking into specific APIs was brought forward.

1.2.4 Productivity

Journal publications

1. J. Ibrahim and R.M. Buehrer, "Two-Stage Acquisition for UWB in Dense Multipath," submitted to *IEEE Journal on Selected Areas in Communications*, UWB Communications Special Issue.

Conference Publications

1. J. Ibrahim, B. Donlan, and R.M. Buehrer, "Interference Rejection Techniques for UWB Systems," Embedded Systems Conference, San Francisco, CA, USA, March 8-10 2005.

2. R. Menon, J. Ibrahim, and R.M. Buehrer, "UWB Signal Detection Based on Sequence Optimization," WIRELESSCOM 2005, June 13-16, 2005.

3. J. Ibrahim and R.M. Buehrer, "A Data-Aided Iterative UWB Receiver with LDPC," IEEE Vehicular Technology Conference, Fall 2005.

4. J. Ibrahim, R. Menon, and R.M. Buehrer, "UWB Sequence Optimization for Enhanced Energy Capture and Interference Mitigation," submitted to IEEE Military Communication Conference, October 2005.

5. J. Ibrahim and R.M. Buehrer, "Two-Stage Acquisition for UWB in Dense Multipath," submitted to IEEE Military Communication Conference, October 2005.

6. C.R. Anderson and J.H. Reed. "Performance analysis of a time-interleaved sampling of architecture for a software defined ultra wideband receiver," to appear in *2005 Software Defined Radio Technical Conference*, November 2005.

7. J. Ibrahim and R.M. Buehrer, "A Novel NBI Suppression Scheme for UWB Communications Using Multiple Receive Antennas," submitted to IEEE Radio and Wireless Symposium, January 2006.

Students supported

Chris R. Anderson, Jan. 15, 2005 – present
Jihad Ibrahim, Jan. 15, 2005 – present
Swaroop Venkatesh, Jan. 15, 2005 – present
Maruf Mohammad, Jan. 15, 2005 – present

Faculty supported

Jeffrey H. Reed, Jan. 15, 2005 – present
R. Michael Buehrer, Jan. 15, 2005 – present
William H. Tranter, Jan. 15, 2005 – present

1.2.5 Timeline Chart

Task 1.2 Advanced Software Radio

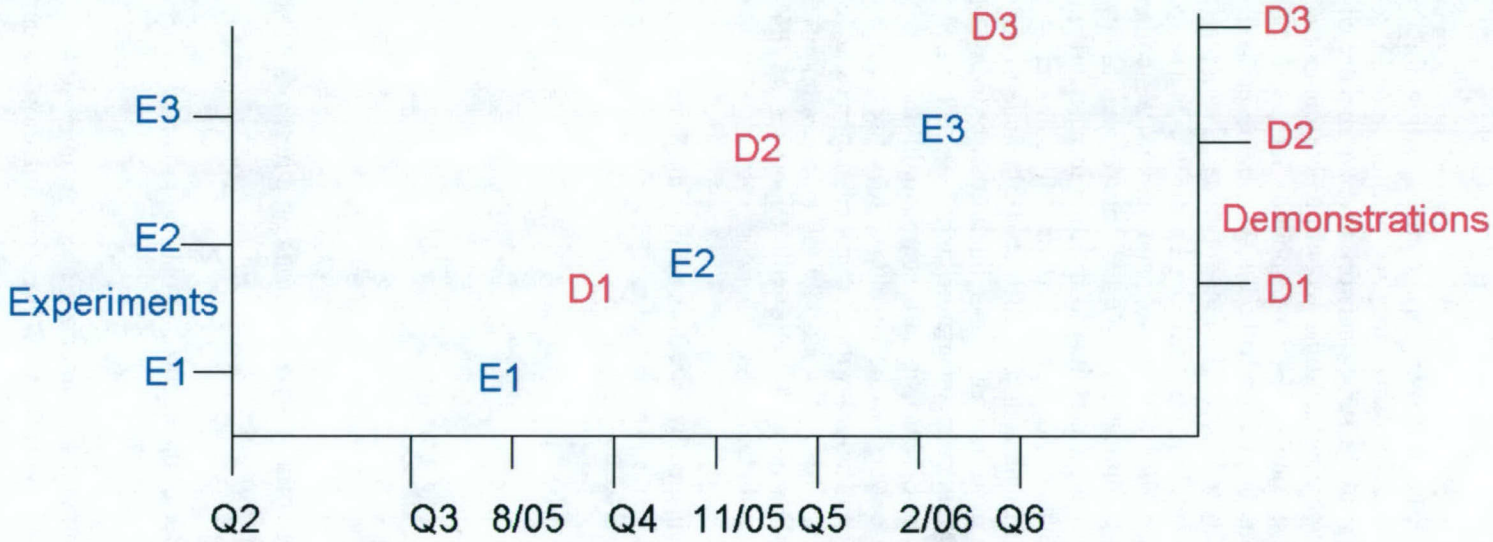

E1: Prototype receiver evaluation.
E2: Ranging & MIMO with prototype receiver.
E3: Full receiver evaluation.

D1: UWB Communication using prototype receiver.
D2: Crane and D-MIMO integration using prototype receiver.
D3: Crane, D-MIMO, and UWB communication using full reciever.

1.3 Task 1.3 Collaborative and Secure Wireless Communications

1.3.1 Overview

Task Goal: We will investigate improving the communication link performance between a (mobile) base station and a spatially distributed, and possibly mobile, sensor network. We will exploit the collective behavior of the sensor network to solve specific communications problems collaboratively. Utilizing emerging run-time reconfigurable computing technology, the radio infrastructure of a compact sensing node (fixed, mobile, floating, airborne, or submerged) can satisfy the diverse communications modes without a sizable impact on size, weight or power. By expanding this nodal capability to a network of autonomous sensing platforms, new opportunities for communications and computing research can be created that directly benefit the overall communications infrastructure. We will research and demonstrate collaborative communication techniques for remote sensing applications. We will investigate link-level strategies in which a network of sensing vehicles can be exploited to improve link performance. We will develop a communication scheme for inter-sensor message passing. The investigators, in collaboration with Task 1.1 and Task 1.2, will implement and characterize a node-to-node link. We will deploy hardware encryption for the protection of sensor intellectual property. In cooperation with the investigators of Task 1.1 on antenna integration and Task 1.2 on SDR integration, we will implement sensor-to-sensor link, sensor-to-base station link, and possibly sensor-to-GEO link (GPS). A multi-mode transceiver will be developed to satisfy: (a) communications between network members, (b) communications with the ground-station, and (c) communications with external factors, such as GPS. We will work with the investigators of Task 2.1 to use a sensor network as a deployable ad-hoc network. We will support the AWINN integration, including ground-based demonstration of a mobile sensor network system.

Organization: This task is managed by Directors of Virginia Tech Configurable Computing Lab using the following personnel:

Peter Athanas, Co-Director
Mark Jones, Co-Director
Deepak Agarwal, GRA
Brian Marshall, GRA
Matt Blanton, GRA

1.3.2 Task Activities for the period

Primary effort this quarter was directed towards Task 1.3f.

Subtask 1.3a Simulation of collaborative methods on a network of sensor platforms using data collected from laboratory prototypes.

The simulation system has been implemented; it may be modified as we gather results from our robotic hardware.

Subtask 1.3b Demonstration and characterization of an inter-sensor link between to or more (mobile) nodes, including a low-power UWB communication scheme for inter-sensor messaging.

This task is awaiting board fabrication and testing.

Subtask 1.3c In cooperation with Tasks 1.1 and 1.2, implement and characterize a node-to-node link.

This task has not been started. This task depends upon tasks 1.3a and 1.3b.

Subtask 1.3d Create two or more multi-mode radio prototypes that can be deployed in a meaningful way on the campus to demonstrate the communications modes.

Subtask 1.3e In cooperation with Task 2.1, perform a simulation that illustrates the network being transformed into an ad hoc network using a node model.

This task has not been started.

Subtask 1.3f Demonstrate a multi-node system comprised of commodity robotic devices to emulate behavior of a loosely coupled mobile sensor network.

The objective for Task 1.3f is to demonstrate a multi-node system comprised of commodity robotic devices to emulate behavior of a loosely coupled mobile sensor network. Guided by simulation results from Task 1.3a, we are designing a distributed control system for mobile, autonomous robot surveillance based on the principles of swarm intelligence. The system's goal is to locate and gather information from mobile targets in an unknown and possibly harsh environment. Swarm Intelligence uses the cooperation of multiple agents with limited local knowledge to accomplish a global task. Swarms have no centralized controlling agent, which is particularly useful in a harsh environment. Any robotic agent can be destroyed and the system remains capable of accomplishing its goals. Also due to the agents' simplicity, their cost will be lower.

To demonstrate the system, we have chosen mobile robotic hardware manufactured by Evolution Robotics. The ER1 Personal Robotic System uses a laptop for controlling the drive motors, IR sensors, and image recognition. During this reporting period, the programming of these robots was completed. The robots now move in a random fashion in a designated area while avoiding any obstacles. If one robot identifies a potential target, it will enter an observing state as well as alert other robots to "swarm" to its location. In the observing state, a robot will change its orientation to improve its view of the target.

We have a large room and wireless router for the testing of groups of the robots. The testing of independent robots is complete. The performance of the swarming robots will be measured against independent non-swarming robots in future tests.

In addition to implementing the robot control software, we began improving the navigation capability of the robots. Currently, the robots navigate by counting wheel rotations; this method tends to lose accuracy over time and only provides information on relative movement. We are augmenting the robots with the O-navi Phoenix-AX board (shown in Fig. 1.3-1) that provides accelerometer, gyroscope, and GPS data. This will improve the accuracy of location information to the point that operations such as cooperative beamforming are feasible. We plan to complete the integration of this board into the robotic software API during the coming quarter.

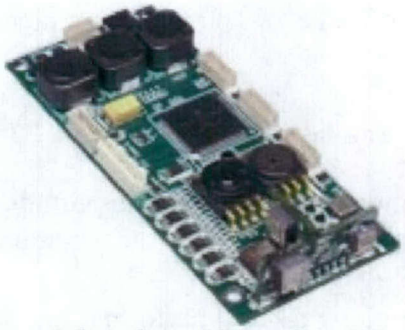

Figure 1.3-1 O-navi Phoenix-AX board

Accomplishments during reporting period:

1. Control software for robots implemented.
2. Benchmark tests for independent robot behavior completed.

Links to other tasks: This is prerequisite work for tasks 1.3b, 1.3c and 1.3e.
Schedule: This will continue throughout Year 1.
Personnel: Brian Marshall, GRA & Matt Blanton, GRA

1.3.3 Importance/Relevance

Mobile sensor networks composed of many inexpensive nodes with limited capabilities have the potential to perform more robustly than networks composed of a smaller number of very capable nodes. Such large networks offer the promise of improved communication reliability and range. This quarter's accomplishments have laid the groundwork for the demonstration of communication within such a mobile sensor network.

1.3.4 Productivity

Conference publications

D. Agarwal, P. Athanas, "An 8 GHz UWB Transceiver Prototyping Testbed," IEEE International Rapid Systems Prototyping Conference (Montreal, Canada), June 8-12, 2005.

Students supported

Deepak Agarwal: 2/2005 – 6/2005
Matt Blanton: 6/2005 – present

1.3.5 Summary Quad Chart

AWINN Task 1.3 – Anvanced Wireless Technologies

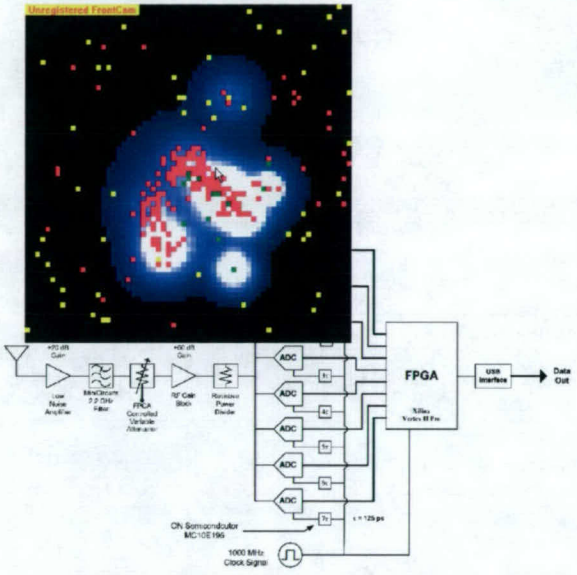

Task 1.3 Collaborative and Secure Wireless Communications

- Demonstration and characterization of an inter-sensor link between two or more (mobile) nodes, including a low-power UWB communication scheme for inter-sensor messaging
- Simulation of collaborative methods on a network of sensor platforms using data collected from laboratory prototypes.
- In cooperation with Tasks 1.1 and 1.2, implement and characterize a node-to-node link.

Task 1.3 Expected Benefits

- Extended Range and/or Battery Life
- Surveillance
- Emergency Early Response
- Network Relay Points
- Fault Tolerant Remote Sensing

Approach

- Create two or more multi-mode radio prototypes that can be deployed in a meaningful way on the campus to demonstrate the communications modes.
- In cooperation with Task 2.1, perform a simulation that illustrates the network being transformed into an ad hoc network using a node model.
- Demonstrate a multi-node system comprised of commodity robotic devices to emulate behavior of a loosely coupled mobile sensor network

Principal Investigators

Dr. Peter Athanas
Dr. Mark Jones

1.3.6 Timeline Chart

Task 1.3 Collaborative and Secure Wireless Communications

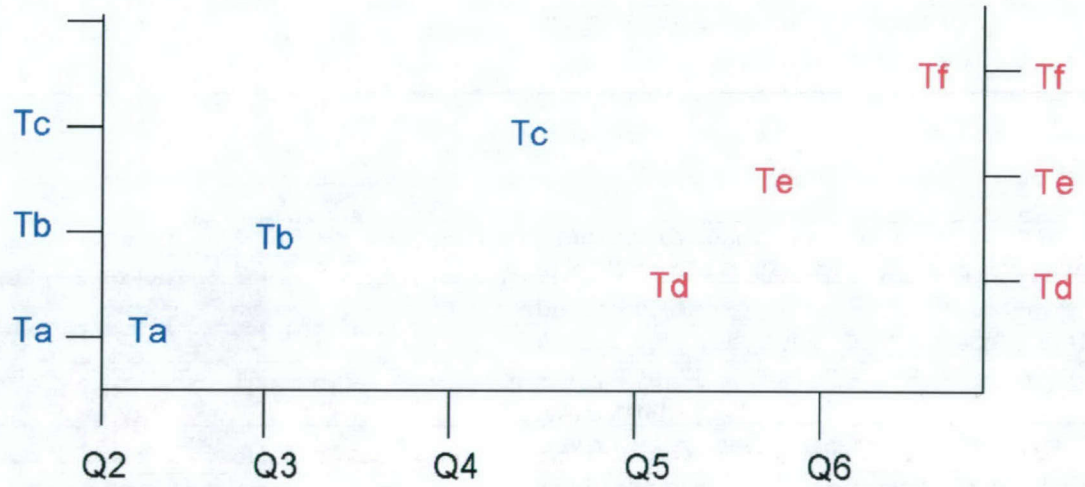

Ta: Collaborative Behavior Simulation

Tb: Mobile UWB Radio Link

Tc: Demonstrate Node-to-Node Radio Link

Td: Multi-Mode Radio Prototypes

Te: Simulate Mobile Ad-Hoc Network

Tf: Demonstrate Multi-Node Mobile System

2. TASK 2 Secure and Robust Networks

2.1 Task 2.1 Ad Hoc Networks

2.1.1 Overview

Task Goal: This task investigates core network capabilities for quality of service (QoS), security, and routing in ad hoc networks, especially mobile ad hoc networks (MANETs).

Organization: This task is managed by Scott Midkiff and involves the following personnel:

Scott F. Midkiff, task director
Luiz A. DaSilva, faculty
Nathaniel J. Davis, IV, faculty
Y. Thomas Hou, faculty
Shiwen Mao, post-doctoral research associate
Waltemar M. de Sousa, GRA (5/15/05-6/30/05)
George C. Hadjichristofi, GRA (4/1/05-5/14/05)
Unghee Lee, GRA (33% for 4/1/05-5/14/05, 100% for 5/15/05-6/30/05)
Xiaojun Wang, GRA

Summary: This quarter we focused on completing work on security mechanisms for ad hoc networks, design and initial implementation of combined routing and medium access control (MAC) protocols for ad hoc networks, planning work on policy-based network management with an emphasis on QoS, and initial implementation of test bed conversion to support Internet Protocol version 6 (IPv6). In this section, we also report on accomplishments in the area of carrying multiple description (MD) video across ad hoc networks. The accomplishments and other details are provided in Section 2.1.2 below.

2.1.2 Task Activities for the Period

Subtask 2.1a Policy-based Quality of Service

Task Objective: The objectives of this subtask are to investigate and develop quality of service mechanisms that provide differential bandwidth allocation and scheduling based on traffic type, node type, and the current network environment. We seek to increase the adaptability of the QoS mechanisms to operate more robustly in a variety of environments. We will also explore automatic adaptation at the physical and data link layers in response to application and network-layer demands, as an initial exploration of cognitive networks as an approach to cross-layer optimization.

Accomplishments during reporting period: Initial investigation and planning for this task began during this quarter. We began with reevaluating work done and software developed for policy-based network management (PBNM) during the NAVCIITI project and in investigating relevant literature in the field.

Links to other tasks: This subtask has natural synergies with Task 2.4 (Cross-Layer Optimization), as the mechanisms that support QoS in mobile ad hoc networks span the physical, data link, network and application layers. It also integrates with Task 2.2 (Real-Time Resource Management, Communication, and Middleware) as some of the QoS mechanisms developed here

will support real-time applications and must integrate with the real-time middleware developed in Task 2.2.

Schedule: The schedule for this subtask is as follows.
- Develop extended policy-based QoS mechanism (April-August 2005)
- Explore adaptability methods (July-December 2005)
- Integrate cross-layer design features (July-September 2005)
- Realize prototype implementation (July-December 2005)
- Integrate protocols using test bed (January-March 2006)
- Refine protocols based on performance evaluation and demonstrations (April-June 2006)
-

Personnel: The following personnel were assigned to this subtask.
Luiz A. DaSilva, faculty
Scott F. Midkiff, faculty
Waltemar de Sousa, GRA (5/15/05-6/30/05)

Subtask 2.1b Security Mechanisms for Ad Hoc Environments

Task Objective: The objectives of this subtask are to investigate and, where feasible and deemed appropriate, develop security mechanisms that are efficient for ad hoc network environments. Our initial emphasis considers a distributed key management system (KMS) and associated shared trust schemes.

Accomplishments during reporting period: Activities during this quarter focused on completion and evaluation of a distributed certificate authority (DCA) and trust management scheme. We evaluated the probability of node being able to complete authentication using "out-of-band" mechanisms under different assumptions in a mobile ad hoc environment. In particular, our objective was to assess the need and effectiveness of a control plane for DCAs and trusted certificate authorities (TCAs). The analysis was carried out to investigate the time that it would take for a node to come within close proximity of a DCA or TCA and, thus, obtain a certificate via out-of-band methods. Reports on this research were made in two conference papers (see Section 2.1.4). George Hadjichristofi also successfully defended his Ph.D. dissertation on this topic in June 2005 (a copy of the dissertation can be provided on request). Note that Dr. Hadjichristofi will temporarily rejoin the project as a post-doctoral associate in July 2005.

Links to other tasks: This subtask has synergies with Subtask 2.1c and Task 2.4 (Cross-Layer Optimization) as link layer and, especially, network layer information can be employed to improve key management and other security functions. We will deploy a prototype for evaluation in the test bed developed in Subtask 2.1e and use tools of Subtask 2.1f.

Schedule: The schedule for this subtask is as follows.
- Develop DCA and trust management system (January-June 2005)
- Integrate cross-layer design features (July-September 2005)
- Realize prototype implementation (July-December 2005)
- Integrate protocols using test bed (January-March 2006)
- Refine protocols based on performance evaluation and demonstrations (April-June 2006)

Personnel: The following personnel were assigned to this subtask.
Nathaniel J. Davis, IV, faculty
Scott F. Midkiff, faculty

George C. Hadjichristofi, GRA (4/1/05-5/14/05)

Subtask 2.1c Ad Hoc Routing Optimization

Task Objective: The objectives of this subtask are to investigate schemes to improve routing and to use network layer functionality to improve other network services.

Accomplishments during reporting period: During the current reporting period, our focus was on employing cross-layer design of the medium access control and routing layers and in jointly supporting both Internet Protocol version 4 (IPv4) and IPv6. In particular, we extended the Open Shortest Path First with Minimum Connected Dominating Sets (OSPF-MCDS) MANET routing protocol to support multiple channels operating with IPv4. We call the new protocol OPSF-MCDS-Multiple Channel (OSPF-MCDS-MC or, more simply, OMM). Note that OSPF-MCDS was developed as part of the NAVCIITI program. Further testing and refinement and extension to support IPv6 are needed in the subsequent quarter. We have also extended the Naval Research Laboratory (NRL) version of the Optimized Link State Routing (OLSR) protocol to operate with multiple channels in an IPv4 and IPv6 environment. We call the new protocol OLSR-Multiple Channel (OLSR-MC). Note that the conversion to IPv6 was less of an issue with OLSR-MC than with OMM since the NRL version of OLSR supports both IPv4 and IPv6. Further testing and refinement of OLSR-MC are needed in the subsequent quarter.

Initial results on this work concerning the extension of the Destination-Sequenced Distance-Vector (DSDV) to a multi-channel version, DSDV-Multiple Channel (DSDV-MC) were reported in a conference paper in April 2005 (see Section 2.1.4).

Links to other tasks: This subtask has direct ties to Task 2.4 (Cross-Layer Optimization) as our focus makes the network layer a key part of our cross-layer optimization schemes. In addition, we will explore synergy with Task 2.2 (Real-Time Resource Management, Communication, and Middleware). We are deploying a prototype for evaluation in the test bed developed in Subtask 2.1e and use tools of Subtask 2.1f.

Schedule: The schedule is as follows.
- Extend DSDV to support multi-channel MAC (January-March 2005)
- Extend OSPF-MCDS to support multi-channel MAC (April-June 2005)
- Extend Optimized Link State Routing (OLSR) to support multi-channel MAC (May-June 2005)
- Realized prototype implementation in Linux, including IPv6 support (July-September 2005)
- Provide enhanced support for policy-based network management (PBNM) (July-September 2005)
- Provide enhanced support for security services (October-December 2005)
- Integrate additional cross-layer enhancements (October-December 2005)
- Integrate protocols using test bed (January-March 2006)
- Refine protocols based on performance evaluation and demonstrations (April-June 2006)

Personnel: The following personnel were assigned to this subtask.
Scott F. Midkiff, faculty
Unghee Lee, GRA (33% for 4/1/05-5/14/05, 100% for 5/15/05-6/30/05)

Subtask 2.1d Cross-Layer Approach for Routing of Multiple Description Video over Ad Hoc Networks

Task Objective: The objectives of this subtask are to investigate a theoretical foundation for cross-layer approaches for carrying MD video over ad hoc networks and to build on this foundation to demonstrate key concepts via a prototype implementation.

Accomplishments during reporting period: As developments in wireless ad hoc networks continue, there is an increasing expectation with regard to supporting content-rich multimedia communications (e.g., video) in military ad hoc networks. The recent advances in multiple description (MD) video coding have made multimedia applications feasible in such networks. We have studied the important problem of multi-path routing for MD video in wireless ad hoc networks. We followed an application-centric cross-layer approach and formulated an optimal routing problem that minimizes the application layer video distortion. We have shown that the optimization problem has a highly complex objective function and an exact analytic solution is not obtainable. However, we find that a meta-heuristic approach, such as genetic algorithms (GAs), is effective in addressing this type of complex cross-layer optimization problem. We have developed a detailed solution procedure for the GA-based approach, as well as a tight lower bound for video distortion. We have run numerical results to demonstrate the superior performance of the GA-based approach and have compared it to several other approaches. This effort provides an important methodology for addressing complex cross-layer optimization problems, particularly those involving application and network layers.

Links to other tasks: This subtask has direct ties to Task 2.4 (Cross-Layer Optimization) as it considers cross-layer optimization schemes that involve applications, in this case, video. We are deploying a prototype for evaluation and this will be integrated into the test bed developed in Subtask 2.1e.

Schedule: The schedule is as follows.

- Develop foundation for cross-layer optimization (January-July 2005)
- Develop prototype system (June-September 2005)
- Integrate prototype system into interoperability test bed (October-December 2005)
- Conduct experiments with interoperability test bed (January-March 2006)
- Refine protocols based on performance evaluation and demonstrations (April-June 2006)

Personnel: The following personnel were assigned to this subtask.

Y. Thomas Hou, faculty
Shiwen Mao, post-doctoral research associate
Xiaojun Wang, GRA

Subtask 2.1e Test Bed Evaluation and Demonstration

Task Objective: The objectives of this subtask are to integrate and demonstrate through research prototype implementations key ideas from Subtasks 2.1a, 2.1b, 2.1c, and 2.1d and, as feasible and appropriate, from Task 2.2 (Real-Time Resource Management, Communication, and Middleware), Task 2.3 (Network Interoperability and Quality of Service), and Task 2.4 (Cross-Layer Optimization). The objective includes exploring interactions between different components and functions and to evaluate and demonstrate both functionality and performance.

Accomplishments during reporting period: We began to test components and plan for the evolution of the test bed from supporting only IPv4 to supporting both IPv6. Some minor issues

were uncovered and addressed in this quarter. The majority of the task will consist of: (i) upgrading the operating system in test bed nodes to a recent version of Red Hat Fedora Core Linux; and (ii) testing test bed software and making fixes, as needed. Note that it may not be efficient to support all "legacy" test bed capabilities from the NAVCIITI task because some third-party software packages, such as COPS, do not support IPv4 and it would be well beyond the scope of this project to make such modifications.

Links to other tasks: The test bed evaluation and demonstrations rely on results from Subtasks 2.1a, 2.1b, 2.1c, and 2.1d, as well as Tasks 2.2, 2.3, and 2.4.

Schedule: The schedule for this subtask is as follows.
- Identify and clarify needs (July-September 2005)
- Acquire and deploy test bed hardware (October-December 2005)
- Deploy technologies in test bed (January-March 2006)
- Final performance evaluation and demonstrations (April-June 2006)

Personnel: The following personnel were assigned to this subtask.
Scott F. Midkiff, faculty
Unghee Lee, GRA (33% for 4/1/05-5/14/05, 100% for 5/15/05-6/30/05).

Subtask 2.1f Configuration and Monitoring Tools

Task Objective: The objectives of this subtask are to investigate and develop software configuration and monitoring tools to facilitate network testing and demonstration.

Accomplishments during reporting period: There were no substantial activities for this subtask in the reporting period.

Links to other tasks: The tools support the test bed described above for Subtask 2.1e.

Schedule: The schedule for this subtask is as follows.
- Identify and clarify needs (April-June 2005)
- Implement and test tools (July-December 2005)
- Utilization and refinement of tools (January-June 2006)

Personnel: No personnel were assigned to this subtask for the reporting period.

2.1.3 Importance/Relevance

Ad hoc networks are of particular importance to the Navy and other Department of Defense (DoD) units because of their ability to be quickly configured and operate without infrastructure. Research in ad hoc networks to date has been dominated by solutions to particular, specific problems and not to general system and network infrastructure issues. This task focuses on making ad hoc network operate successfully as a system with efficient routing, the ability to offer quality of service, and the robustness and security required of military networks. We also examine the challenging problem of delivering video, specifically MD video, in an ad hoc network.

Scott Midkiff and Luiz DaSilva met with personnel at the Naval Research Laboratory on May 23, 2005 (hosted by Raymond Cole of NRL). We identified potential areas of collaboration and

opportunities for each group to leverage the work of the other. In particular for our effort, we have already started making use of the NRL version of OLSR, as discussed above.

2.1.4 Productivity

Conference publications

1. S. Mao, S. Kompella, Y.T. Hou, and S.F. Midkiff, "A fast greedy algorithm for routing concurrent video flows," *IEEE International Symposium on Circuits and Systems (ISCAS 2000)*, Kobe, Japan, May 23–May 26, 2005, pp. 3535-3538.
2. S. Mao, S. Kompella, Y. T. Hou, H. D. Sherali, S.F. Midkiff, "Routing for multiple concurrent video sessions in wireless ad hoc networks," *Proceedings IEEE International Conference on Communications (ICC)*, May 16–20, 2005, Seoul, Korea (presented by Kompella).
3. S. Mao, X. Cheng, and Y.T. Hou, H.D. Sherali, and J.H. Reed, "Joint routing and server selection for multiple description video in wireless ad hoc networks," *IEEE International Conference on Communications (ICC)*, May 16–20, 2005, Seoul, Korea (presented by Hou).
4. M. X. Gong, S. F. Midkiff, and S. Mao, "Design Principles for Distributed Channel Assignment in Wireless Ad Hoc Networks," *IEEE International Conference on Communications (ICC)*, Seoul, Korea, May 16-20, 2005 (presented by Midkiff).
5. L. A. DaSilva, S. F. Midkiff, N. J. Davis, J. S. Park, G. C. Hadjichristofi, K. Phanse, and T. Lin, "Interoperable security, routing and quality of service for ad hoc network mobility," *Information Systems Technology Panel Symposium on Military Communications*, NATO Research and Technology Agency, Rome, Italy, April 18-19, 2005, 12 pages in web proceedings (presented by Midkiff).
6. U. Lee, S. F. Midkiff, and J. S. Park, "A proactive routing protocol for multi-channel wireless ad-hoc networks (DSDV-MC)," *International Conference on Information Technology: Coding and Computing (ITCC)*, Vol. 2, Las Vegas, NV, April 4-6, 2005, pp. 710-715 (presented by Lee).
7. G. C. Hadjichristofi, W. J. Adams, and N. J. Davis, "A framework for key management in mobile ad hoc networks," *International Conference on Information Technology: Coding and Computing (ITCC)*, Vol. 2, Las Vegas, NV, April 4-6, 2005, pp. 568-573 (presented by Hadjichristofi).
8. W. J. Adams, G. C Hadjichristofi, and N. J. Davis, "Calculating a node's reputation in a mobile ad hoc network," *IEEE Performance, Computing, and Communications Conference (IPCCC)*, Phoenix, AZ, April 2005, pp. 303-307 (presented by Adams).

The conference publications listed below should have been included in the quarterly report for January-March 2005 but were omitted due to an oversight.

1. S. Mao, Y. T. Hou, X. Cheng, H. D. Sherali, S. F. Midkiff, "Multipath routing for multiple description video in wireless ad hoc networks," *IEEE INFOCOM*, March 13-17, 2005, Miami, FL.
2. Y. T. Hou, Y. Shi, H. D. Sherali, J. E. Wieselthier, "Online lifetime-centric multicast routing for wireless ad hoc networks with directional antennas," *IEEE INFOCOM*, March 13-17, 2005, Miami, FL.

3. S. Mao, S. S. Panwar, and Y. T. Hou, "On optimal partitioning for realtime traffic over multiple paths," *IEEE INFOCOM*, March 13-17, 2005, Miami, FL.

Students supported

George Hadjichristofi, 1/15/05-5/14/05
Unghee Lee, 1/15/05-5/14/05 (33%), 5/15/05-6/30/05 (100%)
Xiaojun Wang, 1/15/05-6/30/05

Faculty supported

Scott F. Midkiff, 1/15/05–6/30/05
Luiz A. DaSilva, 1/15/05–6/30/05
Nathaniel J. Davis, 1/15/05–6/30/05
Y. Thomas Hou, 1/15/05–6/30/05
Shiwen Mao, 1/15/05–6/30/05 (post-doctoral associate)

2.2 Task 2.2 Real-Time Resource Management, Communications, and Middleware

This report discusses the progress of Task 2.2 during the second quarter – April through June, 2005. The report has four sections: (1) task overview, (2) task activities for the period, (3) importance to the Navy, and (4) productivity.

2.2.1 Task Overview

The objectives of Task 2.2 include:
Develop time/utility function (TUF)/utility accrual (UA) scheduling algorithms for scheduling Real-Time CORBA 1.2's distributable threads with *assured timeliness properties* under failures.
Develop distributable thread maintenance and recovery (TMAR) protocols that are integrated with such scheduling algorithms.

Develop TUF/UA *non-blocking synchronization mechanisms* for synchronizing distributable threads and single-processor threads for concurrently and mutually exclusively accessing shared objects.

Investigate how TUF/UA scheduling algorithms, synchronization mechanisms, and TMAR protocols can co-reside with policy-based network QoS management schemes, and jointly optimize (with network QoS schemes) UA timeliness optimality criteria, as envisaged in Task 2.3.

Develop the *Distributed Real-Time Specification for Java* (DRTSJ) standard under the auspices of Sun's Java Community Process (JCP)1, incorporating scheduling algorithms, synchronization mechanisms, and TMAR protocols developed in (1) and (2).

Embedded real-time systems that are emerging such as control systems in the defense domain (e.g., Navy's DD(X), Air Force's AWACS) are fundamentally distinguished by the fact that they operate in environments with dynamically uncertain properties. These uncertainties include transient and sustained resource overloads due to context-dependent activity execution times and arbitrary activity arrival patterns. For example, many DoD combat systems include radar-based tracking subsystems that associate sensor reports to airborne object tracks. When significantly large number of sensor reports arrives, it exceeds the system processing capacity, causing overloads that result in important tracks to go undetected.

When resource overloads occur, meeting deadlines of all application activities is impossible as the demand exceeds the supply. The urgency of an activity is typically orthogonal to the relative importance of the activity—e.g., the most urgent activity can be the least important, and vice versa; the most urgent can be the most important, and vice versa. Hence when overloads occur, completing the most important activities irrespective of activity urgency is often desirable. Thus, a clear distinction has to be made between the urgency and the importance of activities, during overloads. (During under-loads, such a distinction need not be made, because deadline-based scheduling algorithms such as EDF are optimal for those situations [hor74]—i.e., they can satisfy all deadlines.)

Deadlines by themselves cannot express both urgency and importance. Thus, we consider the abstraction of time/utility functions (or TUFs) [jlt85] that express the utility of completing an application activity as a function of that activity's completion time. Utility is typically mapped to

---

1 The DRTSJ effort is currently ongoing under a JCP called JSR-50. The core members of the DRTSJ team include those from The MITRE Corporation and Virginia Tech.

application-level quality of service (QoS) metrics such as track quality and track importance in a command and control application. We specify deadline as a binary-valued, downward "step" shaped TUF; Figure 2.2-1(a) shows examples. Note that a TUF decouples importance and urgency—i.e., urgency is measured as a deadline on the X-axis, and importance is denoted by utility on the Y-axis.

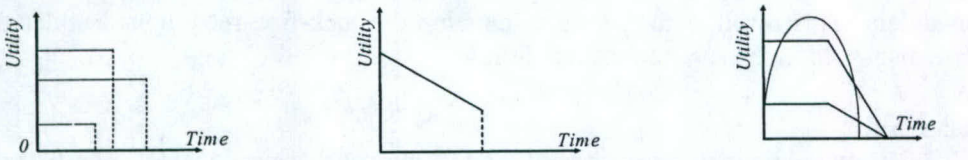

(a) Step TUFs **(b) AWACS TUF** **(c) Air Defense TUFs**

Figure 2.2-1 Example timing requirements specified using Time/Utility Functions

Many embedded real-time systems also have activities that are subject to non-deadline time constraints, such as those where the utility attained for activity completion varies (e.g., decreases, increases) with completion time. This is in contrast to deadlines, where a positive utility is accrued for completing the activity anytime before the deadline, after which zero, or infinitively negative utility is accrued. Figures 2.2-1(b)—2.2-1(c) show example such time constraints from two real applications (see [cjk+99] and the references therein).

When activity time constraints are specified using TUFs, which subsume deadlines, the scheduling criteria is based on accrued utility, such as maximizing sum of the activities' attained utilities. We call such criteria, utility accrual (or UA) criteria, and scheduling algorithms that optimize them, as UA scheduling algorithms.

UA algorithms that maximize summed utility under downward step TUFs (or deadlines) [loc86, cla90, wrjb04] default to EDF during under-loads, since EDF can satisfy all deadlines during those situations. Consequently, they obtain the maximum total utility during under-loads. When overloads occur, they favor activities that are more important (since more utility can be attained from them), irrespective of their urgency. Thus, UA algorithms' timeliness behavior subsumes the optimal timeliness behavior of deadline scheduling.

The major Task 2.2 accomplishments of this quarter include the establishment of tradeoffs between lock-free and lock-based synchronization for TUF/UA scheduling, for dynamic real-time systems, including those that are subject to resource overloads and arbitrary activity arrivals. We model activity arrival behaviors using the unimodal arbitrary arrival model (or UAM). UAM embodies a "stronger" adversary than most traditional arrival models. We establish the fundamental tradeoffs between lock-free and lock-based object sharing under UAM – the first such result. Our tradeoffs include analytical conditions under which activities' accrued timeliness utility is greater under lock-free than lock-based, and the consequent upper bound on the increase in accrued utility that is possible with lock-free. Our implementation experience on a POSIX RTOS reveals that the lock-free scheduling algorithm yields higher accrued utility, by as much as 65%, and critical time satisfactions, by as much as 80%, over lock-based.

We summarize this result in Section 2.2.2.

2.2.2 Task Activities for the Period: Tradeoffs between Lock-Free and Lock-Based Synchronization for TUF/UA Scheduling

- Bounding Retries Under UAM

To derive lock-free RUA's retry bound under the UAM, we first describe our task model, and overview lock-based RUA. We then derive the upper bound on the number of preemptions under UA schedulers. This result is then used to develop the lock-free retry bound under the UAM. These are discussed in the subsections that follow.

- Task Model

Figure 2.2-2 shows the three dimensions of the task model that we consider. The first dimension is the arrival model. We consider the UAM, which is more relaxed than the periodic model, but more regular than the aperiodic model. Hence it falls in between these two ends of the (regularity) spectrum of the arrival dimension. For a task T_i, its arrival using UAM is defined as a tuple $<l_i, a_i, W_i>$, meaning that the maximal number of job arrivals of the task during any sliding time window W_i is a_i and the minimal number is l_i [hl98]. Jobs may arrive simultaneously. The periodic model is a special case of UAM with $<1,1, W_i>$.

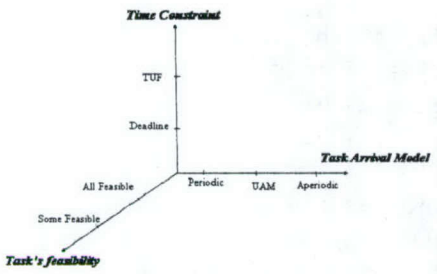

Figure 2.2-2 Three dimensions of Task Model

We refer to the j^{th} job (or invocation) of task T_i as $J_{i,j}$. The basic scheduling entity that we consider is the job abstraction. Thus, we use J to denote a job without being task specific, as seen by the scheduler at any scheduling event. A job's time constraint, which forms the second dimension, is specified using a TUF. A TUF subsumes deadline as a special case---i.e., binary-valued, downward step TUF. Jobs of a task have the same TUF. We use $U_i()$ to denote task T_i 's TUF. Thus, completion of task T_i at a time t will yield an utility $U_i(t)$.

TUFs can take arbitrary shapes, but must have a (single) "critical time." Critical time is the time at which the TUF has zero utility. For the special case of deadlines, critical time corresponds to the deadline time. We denote the critical time of task i's $U_i(t)$ as C_i, and assume that $C_i \leq W_i$.

The third dimension is feasibility. Feasibility includes under-load situations, during when all tasks can be completed before their critical times, and overloads, during when only a subset of the tasks (including possibly none) can be done so. Our model includes overloads, the UAM, and TUFs.

- Preemptions Under UA Schedulers

Under fixed priority schedulers such as rate-monotonic (RM) [ll73], a lower priority job can be preempted at most once by each higher priority job if no resource dependency (that arises due to concurrent object sharing) exists. This is because a job does not change its execution eligibility until its completion time. However, under UA schedulers such as RUA, execution eligibility of a job dynamically changes.

In Figure 2.2-3, assume that two jobs $J_{1,1}$ and $J_{2,1}$ arrives at time t_0. Scheduling events are assumed to happen at t_1, t_2, and t_3. Δt corresponds to t_2- t_1. In the figure, $J_{2,1}$ occupies CPU at time t_0 and is preempted by $J_{1,1}$ at t_1. Subsequently, $J_{1,1}$ is preempted by $J_{2,1}$ at t_2, which does not happen under RM scheduling. Here, we assume that some events which invoke the scheduler happens at time t_1 and t_2, caused by other jobs in the system. Under RUA, a simple condition causing this mutual preemption, where a job which has preempted another job can be subsequently preempted by the other job, can be determined as follows:

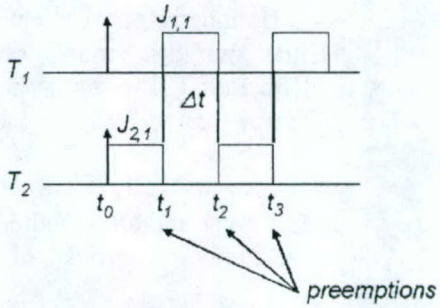

Figure 2.2-3 Mutual Preemption

The PUD of a task i at time t is given by $U_i(c_i)/(c_i - t)$, where c_i is task i's expected completion time, $U_i(c_i)$ is task i's utility at time c_i, and t is the current time. Suppose that $J_{1,1}$ and $J_{2,1}$ have the same critical time and only one of them is feasible. RUA will now select the higher PUD job among $J_{1,1}$ and $J_{2,1}$. Assuming that RUA is invoked at times t_0, t_1, and t_2 by the arrival of other low PUD jobs, PUDs of jobs $J_{1,1}$ and $J_{2,1}$ can be computed as follows:

$$t_0 : PUD_1(t_0) = \frac{U_1(c_1)}{c_1 - t_0} < PUD_2(t_0) = \frac{U_2(c_2)}{c_2 - t_0}$$

$$t_1 : PUD_1(t_1) = \frac{U_1(c_1 + \Delta t)}{c_1 - t_0} > PUD_2(t_1) = \frac{U_2(c_2)}{c_2 - (t_0 + \Delta t)}$$

$$t_2 : PUD_1(t_2) = \frac{U_1(c_1 + \Delta t)}{c_1 - (t_0 + \Delta t)} < PUD_2(t_2) = \frac{U_2(c_2 + \Delta t)}{c_2 - (t_0 + \Delta t)}$$

Since $PUD_2(t_0) < PUD_2(t_1)$, $PUD_1(t_1)$ should be greater than $PUD_1(t_0)$, which means that $U_1(c_1+\Delta t)$ should be greater than $U_1(c_1)$. In the same way, since $PUD_1(t_1) < PUD_1(t_2)$, $U_2(c_2+\Delta t)$ should be greater than $U_2(c_2)$.

As indicated previously, one of the simple cases for RUA to allow the mutual preemption is when TUFs of two jobs are increasing. In other words, two jobs scheduled by RUA may preempt each other repeatedly if the jobs have increasing TUFs. This potential mutual preemption distinguishes RUA from traditional priority schedulers such as RM, where a job can be preempted by another job at most once. Hence, the maximum number of preemptions under RM that a job may suffer can be bounded by the number of releases of other jobs during a given time interval [ajs97]. However, this is not true with RUA, as one job can be preempted by another job more than once. Therefore, the maximum number of preemptions that a job may experience under RUA is bounded by the number of events that invoke the scheduler, and not by the number of released jobs as computed for traditional schedulers such as RM in [arj97].

Lemma 2.2-1 [Preemptions Under UA scheduler] During a given time interval, a job scheduled by a UA scheduler can experience preemptions by other jobs at most the number of the scheduling events that invoke the scheduler.

Proof: Assume that preemptions happen more than the scheduling events during a given time interval. It means that preemptions can occur without invoking the scheduler, which is not true.

Lemma 2.2-1 helps compute the upper bound of the number of retries on lock-free objects for our task model. This is also true with other UA schedulers such as [cla90,loc86], simply because it is impossible for more preemptions to occur than scheduling events.

- Bounded Retry Under UAM

Under our task model, jobs arrive under the UAM, are subject to TUF time constraints, and sufficient CPU time may not always be available to complete all jobs before their critical times. We now bound lock-free RUA's retries under this model.

Theorem 2.2-2 [Lock-Free Retry Bound Under UAM] Suppose that jobs arrive under the UAM $<1, a_i, W_i>$ and are scheduled by RUA. When a job J_i accesses more than one lock-free object, the total number of retries f_i of J_i is bounded as:

$$f_i \leq 3a_i + \sum_{j=1, j\neq i}^{N} 2a_j \left(\left\lceil \frac{C_i}{W_j} \right\rceil + 1 \right)$$

where N is the number of tasks.

Proof: The proof is long and is not presented here.

Note that f has nothing to do with the number of lock-free objects in J_i in Theorem 2.2-2, even when J_i accesses more than one lock-free object. This is because no matter how many objects J_i accesses, f cannot exceed the number of events. Further, even if J_i accesses a single object, the retry can occur only as many times as the number of events.

Theorem 2.2-2 also implies that the sojourn time of J_i is bounded. The sojourn time of J_i is computed as the sum of J_i 's execution time, the interference time by other jobs, the lock-free object accessing time, and f retry time.

- Lock-Based versus Lock-Free

We now formally compare lock-based and lock-free sharing by comparing job sojourn times. We do so, as sojourn times directly determine critical time-misses and accrued utility. The comparison will establish the tradeoffs between lock-based and lock-free sharing: Lock-free is free from blocking times on shared object accesses and scheduler activations for resolving those blockings', while lock-based suffers from these. However, lock-free suffers from retries, while lock-based does not.

We introduce some notations, which are the same as that in [ajs97]. We assume that all accesses to lock-based objects require r time units, and to lock-free objects require s time units. The computation time J_i J_i c_i of a job J_i can be written as $c_i = u_i + m_i t_{acc}$, where u_i is the computation time not involving accesses to shared objects; m_i is the number of shared object accesses by J_i; and t_{acc} is the maximum computation time for any object access---i.e., r for lock-based objects and s for lock-free objects.

The worst-case sojourn time of a job with lock-based objects is u_i+I+rm_i+B, where B is the worst-case blocking time and I is the worst-case interference time. In [wrjb04], it is shown that a job J_i under RUA can be blocked for at most $min(m,n)$ times, where n is the number of jobs that could block J_i and m is the number of resources (or objects) that can be used to block J_i. Therefore, B can be computed as $r \times min(m,n)$.

On the other hand, the worst-case sojourn time of a job with lock-free objects is u_i+I+sm_i+R, where R is the worst-case retry time. R can be computed as $s \times f$ by Theorem 2.2-2. Thus, the difference between $r \times m_i+B$ and $s \times m_i+R$ is the sojourn time difference between lock-based and lock-free sharing.

Theorem 2.2-3 [Lock-Based versus Lock-Free Sojourn] Let jobs arrive under the UAM and be scheduled by RUA. Now, if

$$\begin{cases} \left(\frac{s}{r} < \frac{2}{3}\right) \wedge \left(\frac{1}{\frac{2r}{s} - 1}(3a_i + 2x) < m_i < 2a_i + x \right), m_i \le n \\ \left(\frac{s}{r} < 1\right) \wedge \left(\frac{s}{r}(3a_i + 2x) < \left(1 - \frac{s}{r}\right) m_i + x \right), \quad m_i > n \end{cases}$$

then the sojourn time of job J_i with lock-free objects is shorter than with lock-based objects, where

$$x = \sum_{j=1, j \neq i}^{N} a_j \left(\lceil C_i / W_j \rceil + 1 \right).$$

Proof: The proof is long and is not presented here.

Theorem 2.2-3 shows that at least $s/r<2/3$ for jobs to obtain a shorter sojourn time under lock-free. Note that while r includes the time of the scheduler invocations, s does not. In [ajs97], Anderson *et al.* show that s is typically much smaller than r in comparison with various lock-free objects. In particular, RUA's asymptotic time complexity is $O(n^2 log n)$, where n is the number of jobs [wrjb04]. Further, when a deadlock occurs, RUA's time complexity increases to $O(n^4)$ due to deadlock detection and resolution. This high time complexity makes r much longer. However, for the most simple lock-free objects, such as buffers, queues, and stacks, s is much smaller.

Corollary 2.2-4 [Special Case Sojourn] Let jobs arrive under the UAM and be scheduled by RUA. Let r be significantly larger than s. Now, if:

$$\begin{cases} 0 < m_i < 2a_i + x, & m_i \le n \\ & m_i > n \end{cases}$$

then the sojourn time of job J_i with lock-free objects is shorter than that with lock-based objects, where $x = \sum_{j=1, j \neq i}^{N} a_j \left(\lceil C_i / W_j \rceil + 1 \right)$.

Proof: When r is significantly larger than s, s/r converges to 0. Thus, Theorem 2.2-3 simplifies.

Shorter sojourn times always yields higher utility with non-increasing TUFs, but not always with increasing TUFs. However, it is likely to improve performance at system level because each job can save more CPU resources for other jobs to execute.

As r is larger than s, lock-free sharing is more likely to perform better than lock-based sharing, according to Corollary 2.2-4. Further, when m_i is larger than n, the sojourn time of a job with lock-free object always outperforms its lock-based counterpart. Thus, lock-free sharing is very attractive for UA scheduling as most UA schedulers' object sharing mechanisms have higher time complexity.

Shorter sojourn times for a job under lock-free sharing will only increase the job's accrued utility under non-increasing TUFs. However, this does not directly imply that lock-free sharing will yield higher *total* accrued utility than lock-based sharing. This is because Theorem 2.2-3 does not reveal anything regarding aggregate system-level performance, but only job-level performance. Since RUA's objective is to maximize total utility, we now compare lock-based and lock-free sharing in terms of accrued utility ratio (or AUR). AUR is the ratio of the actual accrued total utility to the maximum possible total utility.

Lemma 2.2-5 [Lock-Based versus Lock-Free AUR] Let jobs arrive under the UAM and be scheduled by RUA. If all jobs are feasible and their TUFs are non-increasing, then the difference in AUR between lock-free and lock-based sharing, $\Delta AUR = AUR_{lf} - AUR_{lb}$ is:

$$\sum_{i=1}^{N} \frac{U_{i,lf}(s_{0,lf} + R) - U_{i,lb}(s_{0,lb})}{U_i(0)} \leq \Delta AUR \leq \sum_{i=1}^{N} \frac{U_{i,lf}(s_{0,lf} + R) - U_{i,lb}(s_{0,lb} + B)}{U_i(0)}$$

Proof: The proof is straightforward. Both the blocking time B and the retry time R are computed for the worst-case. In the best-case, both are zero. With non-increasing TUFs, job sojourn times can be directly mapped to accrued utility. Since all jobs are assumed to be feasible and hence will not be aborted, the AUR can be calculated from each job of the task.

The fact that B and R are the worst-case values make it highly likely for lock-free sharing to outperform lock-based sharing. Even when jobs access several shared objects, it is highly likely that there may be no or a few interferences or retries. Such few interferences are very likely to actually occur because r and s are significantly smaller than job execution times. Lock-based sharing, on the contrary, will invoke the scheduler for these cases, since object access is an automatic scheduling event, resulting in increased overhead.

- Implementation Experience

We implemented lock-based and lock-free objects with RUA in the *meta-scheduler* scheduling framework [lrsf04], which allows middleware-level real-time scheduling atop POSIX RTOSes. We used QNX Neutrino 6.3 RTOS running on a 500 MHz, Pentium-III processor in our implementation, which provides an atomic memory-modification operation, the CAS (Compare-And-Swap) instruction. In our study, we used queues, one of the common shared objects, to validate our theorems. We used a well-known lock-free queue introduced in [mmms98] to compare lock-free objects and their lock-based counterparts in our environment.

- Object Access Times

As shown in Theorem 2.2-3, one of the critical elements that affect the tradeoff between lock-based and lock-free sharing is the time needed for object access---i.e., lock-based object access time r, and lock-free object access time s. We measure r and s for lock-based and lock-free RUA, respectively, with a 10 task set. Each measurement is an average of approximately 2000 samples.

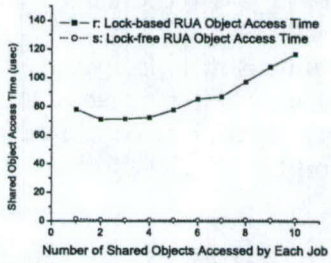

Figure 2.2-4 Lock-Based and Lock-Free shared object access time.

Figure 2.2-4 shows r and s under increasing number of shared objects accessed by jobs. From the figure, we observe that r is significantly larger than s. Note that r includes the time for lock-based RUA's resource sharing mechanism.

When $r >> s$, Theorem 2.2-3 implies that lock-free sharing is likely to perform better than lock-based sharing. Furthermore, when the number of objects m_i increases, it increases the likelihood

for satisfying Corollary 2.2-4's Case 2 and lock-free sharing becomes increasingly advantageous than lock-based consequently.

- Critical Time-Miss Load

The impact of r and s on lock-based RUA's and lock-free RUA's performance, respectively, can be measured by evaluating the load at which the schedulers miss task critical times. We measure this using a metric called *Critical time-Miss Load* (or CML). The CML of a scheduler is defined as the approximate load *after which* the scheduler begins to miss task critical times. We define approximate load as $AL = \sum_{i=1}^{n} u_i / C_i$, where u_i is the task computation time excluding shared object access time, and C_i is the task critical time.

We exclude object access time in this load definition, because an ideal implementation of objects for synchronization must have negligibly small ---almost zero--- object access time. If so, the implementation is ideal in the sense that the scheduler's performance with the (ideal) implementation is the same as that under no object sharing. For no object sharing, RUA's CML is 1 (or 100%) if RUA's overhead is almost zero, as the algorithm defaults to EDF for that case, and thereby will miss critical times only during overloads.

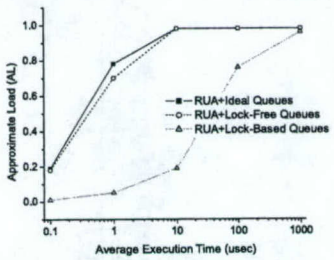

Figure 2.2-5 Critical time miss load

We consider a task set of 10 tasks, accessing 10 shared queues, and measure the CML of lock-free RUA, lock-based RUA, and ideal RUA under increasing average job execution times. Figure 2.2-5 shows the results. We observe that lock-free RUA yields almost the same CML as that of ideal RUA, as it exploits the eliminated blocking times and achieves almost the same performance of RUA without object sharing. Note that the ideal queue and RUA achieve the CML of 1, only at ≈10 *usec* of average execution time. This is because of the algorithm's overhead for scheduling. (RUA's and EDF's CML of 1 is valid at zero job execution times under the assumption of no system overheads, which is not true in practice).

On the other hand, lock-based RUA's CML converges to 1, only at ≈1 millisecond. This is precisely because of lock-based RUA's complex operations for resolving jobs' contention for object locks and consequent higher overhead, as manifested by its higher asymptotic complexity and higher object access times in Figure 2.2-4.

- Accrued Utility and Critical Time-Meets

We now measure the AUR and the critical time-meet ratio (CMR) of lock-free RUA and lock-based RUA for average job execution times in the range of 30 *usec* – 1000 *usec*. CMR is the ratio of the number of tasks that meet their critical times to the total number of task releases. We consider a task set of 10 tasks, accessing 10 shared queues. Each experiment is repeated to obtain AUR and CMR averages from more than 5000 task arrivals. We consider two classes of TUF shapes in this study: step and a heterogenous class including step, parabolic, and linearly-decreasing shapes.

Figure 2.2-6 shows the AUR and CMR of lock-based and lock-free RUA for heterogenous TUFs during under-loads (AL =≈0.4), under increasing number of shared objects. Figure 2.2-7 shows similar results during overloads (AL = ≈1.1).

As expected, the figures show that the AUR and CMR of lock-based RUA sharply decreases, eventually reaching 0% during overloads, as the number of objects increases. This is because, as the number of objects increases, greater number of task blockings' occurs, due to the large *r*, resulting in increased sojourn times, critical time-misses, and consequent abortions.

The performance of lock-free RUA, on the contrary, does not degrade as the number of objects increases. During under-loads, lock-free RUA achieves almost 100% AUR and CMR, whereas during overloads, the algorithm achieves higher AUR by as much as ≈65% and higher CMR, by as much as ≈80% than lock-based. This better performance is directly due to the short *s* of lock-free objects, which results in few retries and thus reduced interferences.

(a) AUR (b) CMR

Figure 2.2-6 AUR/CMR during underload, heterogeneous TUFs.

(a) AUR (b) CMR

Figure 2.2-7 AUR/CMR during overload, heterogeneous TUFs.

(a) AUR (b) CMR

Figure 2.2-8 AUR/CMR during increasing readers, heterogeneous TUFs.

We repeated similar experiments for increasing number of reader tasks (instead of increasing shared objects) and observed exact similar trends and consistent results. Figure 2.2-8 shows a snapshot of these results (Heterogeneous TUFs, AL=0.1-1.1), further illustrating lock-free RUA's superior performance over lock-based. Lock-based RUA starts to lose AUR/CMR earlier than

Lock-free because its heavy overhead makes the earlier overload. We omit more results as they show the same trend and consistency. We emphasize again that the lock-free RUA's superiority over lock-based RUA is mainly because s is much smaller than r, which is highly likely to happen in most systems, and lock-free approaches are optimistic.

References

[cla90] R. K. Clark, "Scheduling Dependent Real-Time Activities," PhD thesis, CMU CS Dept., 1990

[cjk+99] R. K. Clark, E. D. Jensen, et al., "An adaptive, distributed airborne tracking system," In *IEEE WPDRTS*, pages 353--362, April 1999

[hor74] W. Horn, "Some Simple Scheduling Algorithms," *Naval Research Logistics Quarterly*, 21:177--185, 1974.

[jlt85] E. D. Jensen, C. D. Locke, and H. Tokuda, "A time-driven scheduling model for real-time systems," In *IEEE RTSS*, pages 112--122, December 1985

[loc86] C. D. Locke, "Best-Effort Decision Making for Real-Time Scheduling," PhD thesis, Carnegie Mellon University, 1986

[wrjb04] H. Wu, B. Ravindran, E. D. Jensen, and U. Balli, "Utility Accrual Scheduling Under Arbitrary Time/Utility Functions and Multiunit Resource Constraints," *IEEE Real-Time Computing Systems and Applications*, April 2004

[srl90] L. Sha, R. Rajkumar, and J P. Lehoczky, "Priority inheritance protocols: An approach to real-time synchronization," *IEEE Trans. Computers*, 39(9):1175--1185, 1990

[kr93] H. Kopetz and J. Reisinger, "The non-blocking write protocol NBW", *IEEE RTSS*, 131--137, 1993

[cb97] J. Chen and A. Burns, "A fully asynchronous reader/writer mechanism for multiprocessor real-time systems," *Technical Report YCS-288*, CS Dept., University of York, May 1997.

[hps02] H. Huang, P. Pillai, and K. G. Shin, "Improving wait-free algorithms for interprocess communication in embedded real-time systems," *USENIX Annual Technical Conference*, pages 303--316, 2002

[arj97] J. H. Anderson, S.~Ramamurthy, and K. Jeffay, "Real-time computing with lock-free shared objects," *ACM TOCS*, 15(2):134--165, 1997

[crj05] H. Cho, B. Ravindran, and E. D. Jensen, "A space-optimal, wait-free real-time synchronization protocol," *IEEE ECRTS*, 2005.

[hl98] J.-F. Hermant, G. Le Lann, "A Protocol and Correctness Proofs for Real-Time High-Performance Broadcast Networks," *IEEE ICDCS*, 1998

[ll73] C. L. Liu, J. W. Layland, " Scheduling Algorithms for Multiprogramming in a Hard Real-Time Environment," *Journal of the ACM*, 1973

[ajs97] J. H. Andrson, R. Jain, S. Ramamurthy, "Wait-free object-sharing schemes for real-time uniprocessors and multiprocessors," *IEEE RTSS*, 1997

[lrsf04] P. Li, B. Ravindran, others, " A Formally Verified Application-Level Framework for Real-Time Scheduling on POSIX Real-Time Operating Systems," *IEEE Trans. Software Engineering,* 2004

[mmms98] M. M. Michael, M. L. Scott, " Non-Blocking Algorithms and Preemption-Safe Locking on Multiprogrammed Shared Memory Multiprocessors," *Journal of Parallel and Distributed Computing,* 1998

2.2.3 Importance to the Navy

We believe that the TUF/UA real-time technology developed in this task is directly relevant to DoD's network-centric warfare concept, Navy combatant systems including DD(x), and other DoD systems such as Air Force's next generation command and control aircrafts. In fact, the fundamental aspects of this class of real-time problems include:

1. Need for transparent programming and scheduling abstractions for distributed computation workflows that are subject to time constraints.
2. Systems that are subject to significant run-time uncertainties that are often manifested in execution and communication times, and event and failure occurrences that are non-deterministically distributed.
3. Systems that are subject to transient and permanent overloads.
4. Need for time-critical and mission-oriented resource management (i.e., timely management of resources in the best interest of the current application mission).
5. Need for industry/commercial standards- and COTS-based solutions for portability, robustness, and maintainability.

All these aspects are directly addressed by Task 2.2 research. In particular, Real-Time CORBA 1.2's and DRTSJ's distributable threads abstraction provides a transparent programming and scheduling abstraction for distributed real-time computation workflows. Further, the class of TUF/UA scheduling algorithms, TMAR protocols, synchronization mechanisms, and policy-based network QoS management schemes target application activities, whose execution/communication latencies and event/failure occurrences are non-deterministically distributed and are subject to overloads. TUF/UA algorithms provide time-critical and mission-oriented resource management by (system-wide) scheduling to maximize system-wide accrued utility, where utility is mapped to application-level QoS. Consequently, utility maximization leads to managing system resources to maximize utility achieved for the users by the system. Furthermore, Task 2.2's work on the DRTSJ industry standard directly promotes industry/commercial standards and COTS-based solutions.

Thus, we believe that Task 2.2 research is directly relevant to Navy systems and other DoD systems.

DD(X) is currently using RTSJ, and is building a distributed real-time infrastructure using RTSJ. The DD(X) team has expressed significant interest in using DRTSJ – in particular, the distributable threads abstraction and end-to-end timing analysis capability. We believe that DD(X) can directly leverage DRTSJ's advanced adaptive time-critical (TUF/UA) resource management techniques, and DRTSJ's synergy with RTSJ.

2.2.4 Productivity

Journal publications

1. K. Channakeshava, B. Ravindran, and E. D. Jensen, "Utility Accrual Real-Time Channel Establishment in Multi-hop Networks," *IEEE Transactions on Computers*, Accepted with minor revisions, May 2005
2. P. Li, H. Wu, B. Ravindran, and E. D. Jensen, "A Utility Accrual Scheduling Algorithm for Real-Time Activities With Mutual Exclusion Resource Constraints," *IEEE Transactions on Computers*, Accepted with minor revisions, July 2005

Conference publications

1. B. Ravindran, E. D. Jensen, and P. Li, "On Recent Advances in Time/Utility Function Real-Time Scheduling and Resource Management," *IEEE International Symposium on Object-oriented Real-time distributed Computing (ISORC)*, Seattle, Washington, USA, May 18-20, 2005
2. P. Li, H. Cho, B. Ravindran, and E. D. Jensen, "Stochastic, Utility Accrual Real-Time Scheduling with Task-Level and System-Level Timeliness Assurances," *IEEE International Symposium on Object-oriented Real-time distributed Computing (ISORC)*, Seattle, Washington, USA, May 18-20, 2005
3. H. Cho, B. Ravindran, and E. D. Jensen, "On Lock-Free Synchronization for Dynamic Embedded Real-Time Software," *IEEE Real-Time Systems Symposium (RTSS)*, Submitted May 2005 (under review)
4. H. Wu, B. Ravindran, and E. D. Jensen, "Utility Accrual, Real-Time Scheduling with Energy Bounds," *IEEE Real-Time Systems Symposium (RTSS)*, Submitted May 2005 (under review)
5. H. Wu, U. Balli, B. Ravindran, and E. D. Jensen, "Utility Accrual Real-Time Scheduling Under Variable Cost Functions," *IEEE International Conference on Embedded and Real-Time Computing Systems and Applications (RTCSA)*, Hong Kong, August 17-19, 2005, Accepted May 2005, To appear
6. K. Channakeshava, K. Phanse, L. A. DaSilva, B. Ravindran, S. F. Midkiff, and E. D. Jensen, "IP Quality of Service Support for Soft Real-Time Applications," *International Workshop on Real-Time Networks (RTN)*, *IEEE Euromicro Conference on Real-Time Systems (ECRTS)*, Palma de Mallorca, Balearic Islands, Spain, July 6-8, 2005
7. H. Wu, B. Ravindran, and E. D. Jensen, "The Impact of Scheduler Overhead on the Performance of Mobile, Embedded Real-Time Systems," *Work-In-Progress (WIP) Session, IEEE Euromicro Conference on Real-Time Systems (ECRTS)*, Palma de Mallorca, Balearic Islands, Spain, July 6-8, 2005
8. H. Cho, B. Ravindran, and E. D. Jensen, "A Space-Optimal, Wait-Free Real-Time Synchronization Protocol," *IEEE Euromicro Conference on Real-Time Systems (ECRTS)*, Palma de Mallorca, Balearic Islands, Spain, July 6-8, 2005

Students supported

Jonathan Anderson, Jan. 15, 2005 – present
Hyeonjoong Cho, Jan. 15, 2005 – present
Edward Curley, May 2005 – present

2.2.6 Summary Quad Chart

AWINN Task 2.2 – Real-Time Resource Management, Communication, and Middleware

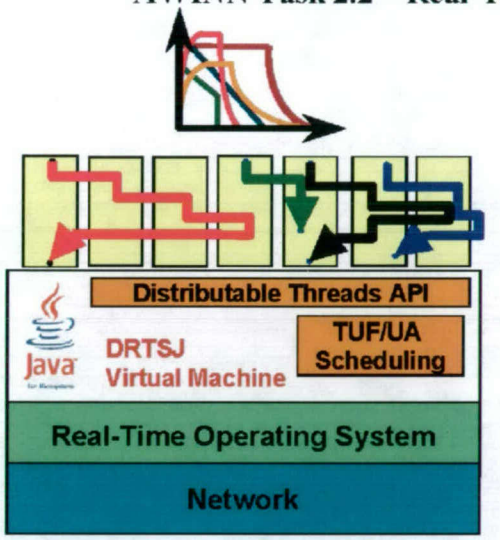

Task Objectives

- Develop TUF/UA Algorithms for RT-CORBA's distributable threads
- Develop TUF/UA non-blocking synchronization algorithms for distributable threads
- Develop Distributed Real-Time Specification for Java (DRTSJ) under Sun's JCP

Team

Dr. Binoy Ravindran Hyeonjoong Cho
Ed Curley Jonathan Anderson
Collaboration on DRTSJ with the MITRE Corp.

Description and Motivation

Develop TUF/UA scheduling and synchronization algorithms and provide implementations of new real-time programming facilities appropriate to support construction of dynamic, distributed real-time systems as envisioned by the US Navy DD(X) program. This work will be done in the context of the Real-Time Specification for Java (RTSJ), the target platform for DD(X), and its extension, the Distributed Real-Time Specification for Java (DRTSJ).

Milestones

Q3 2005
DRTSJ Increment 1 Release – Draft Level 1 Spec

Q4 2005
DRTSJ Increment 2 & 3 Public Releases
Draft Level 2 Specification (TMAR, DThreads, Scheduling)
Initial TUF/UA Scheduling & Synchronization Algorithms
Initial Command & Control Demo Capability

Q1 2006
DRTSJ Increments 4-6 Public Releases (Level 2 Features)
Final Command & Control Demo
TUF/UA – MANET Routing
Initial Integrated Demonstration w/ Task 2.1

Q2 2006
DRTSJ Final Release
Advanced TUF/UA Scheduling & Synchronization Algorithms
Final Integrated Demonstration w/ Task 2.1

Q3 2006
Submission of JSR-50/DRTSJ to Sun's JCP

2.2.6 Timeline Chart

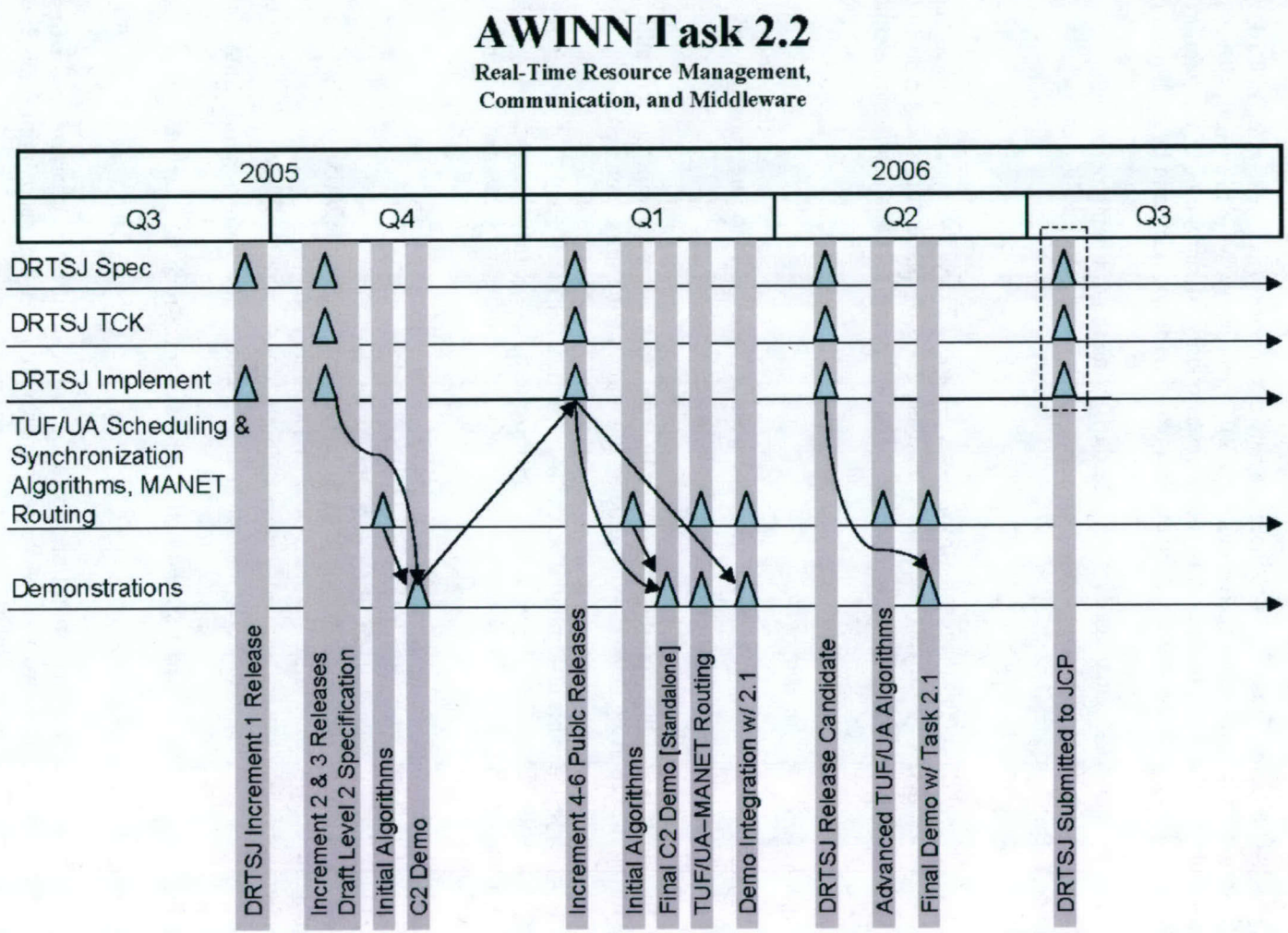

2.3 Task 2.3 Network Interoperability and Quality of Service

2.3.1 Overview

Task Goal: The goal of Task 2.3 is to integrate network services (as investigated in Task 2.1) with real-time middleware (as investigated in Task 2.2). Specifically, we will investigate and develop methods and mechanisms to integrate policy-based quality of service (QoS) capabilities at the network level, and perhaps at the link layer, with real-time services offered by middleware.

Organization: This task is managed by Scott Midkiff using the following personnel:
Scott F. Midkiff, task director
Luiz A. DaSilva, faculty
Binoy Ravindran, faculty

Summary: Task 2.3 integrates results from Tasks 2.1 and 2.2. As these tasks are just beginning, no significant activity specifically in support of Task 2.3 took place during the reporting period beyond beginning of planning for integration. The following sections summarize subtasks and schedule.

2.3.2 Task Activities for the Period

Task Objective: As stated in Section 2.3.1, the goal of Task 2.3 is to integrate network services (from Task 2.1) with real-time middleware (from Task 2.2).

Accomplishments during reporting period: Minimal activities pertaining to this subtask took place during the reporting period. We did begin planning integration of the two tasks.

Links to other tasks: This task integrates results from Task 2.1 and Task 2.2. It is also potentially synergistic with Task 2.4 (Cross-Layer Optimization) as it may be possible to integrate optimizations at the link and network layer with requirements presented by the real-time middleware.

Schedule: The schedule for this task is as follows.
- Plan integration approach (April-August 2005)
- Begin integration based on preliminary results (August-December 2005)
- Integrate cross-layer design features (October-December 2005)
- Integrate protocols using test bed (January-March 2006)
- Refine protocols based on performance evaluation and demonstrations (April-June 2006)

Personnel: No personnel were assigned to this subtask for the reporting period.

2.3.3 Importance/Relevance

Many military systems rely on real-time operation, but can often be characterized using "soft" real-time constraints. This work paves the way to providing real-time capabilities, based on time-utility functions (TUFs), in an ad hoc network environment.

2.3.4 Productivity

There is currently no productivity items to report for Task 2.3.

2.4 Task 2.4 Cross-Layer Optimization

2.4.1 Overview

Task Goal: The goal of this task is to investigate and develop methods and metrics to characterize and evaluate the interaction between physical, data link, network and application layer protocols. This will be accomplished through two specific applications (a) position location networks and (b) collaborative radio networks

Organization: This task is managed by Dr. R. Michael Buehrer and Dr. Scott Midkiff.

Dr. R. Michael Buehrer, faculty
Dr. Scott Midkiff, faculty
Dr. Tom Hou, faculty
Qiao Chen, GRA
Swaroop Venkatesh, GRA

Summary: This quarter we focused on two subtasks: (a) Cross-layer design for UWB position-location networks and (b) collaborative radio networks.

2.4.2 Task Activities for the Period

Subtask 2.4.1 Cross-Layer Design for Ultra-Wideband Position-Location Networks

In the past quarter, we examined the design of MAC protocols for UWB Position Location Networks (PoLoNets). Specifically, we examined the design of MAC protocols from the perspectives of localization accuracy and convergence-time of location estimates, and present results indicating that time-hopped CDMA-based multiple access would be more suitable for these applications than CSMA-based MAC schemes.

In this work, we are investigating *infrastructure-based UWB Position-Location Networks* (PoLoNets). This implies the presence of fixed UWB radios or *reference nodes* in the area of interest whose locations are known *a priori*. (We are addressing the localization of the reference nodes separately.) These reference nodes aid the estimation of the locations of *mobile nodes* entering the area of interest via ranging and triangulation. The network of reference nodes provides TOA-based range estimates at the mobile node, which are used to estimate its location (in terms of 2D-coordinates). The mobile nodes periodically update their location estimate by ranging to reference nodes in order to maintain accuracy of location estimates. The deployed reference nodes also serve as a multi-hop communication network to relay position information to and instructions from a data sink (possibly C&C) as shown in Figure 2.4-1.

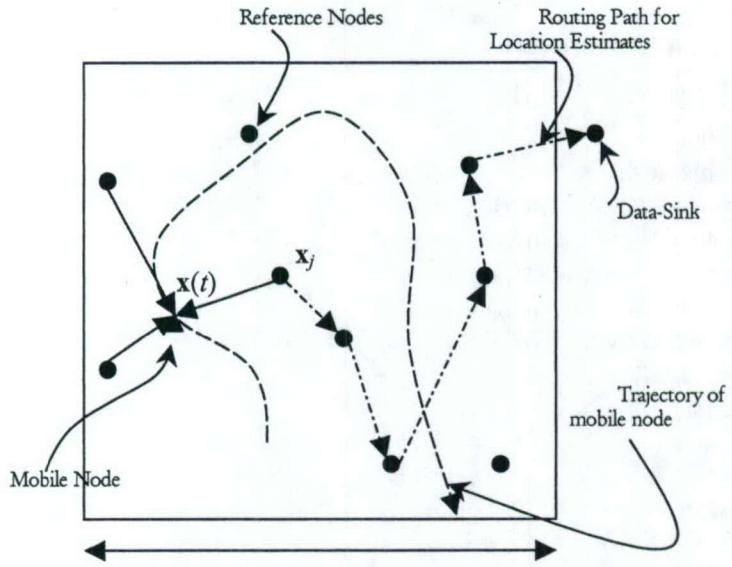

Figure 2.4-1 Position location network architecture.

The mechanism for ranging between two nodes is via a packet-handshake as discussed in [Lee2002] and shown in Figure 2.4-2. Using this mechanism, nodes can not only determine the distance between them, but also exchange data and parameters, such as other ranges and coordinates of other nodes in the network. This feature is critical to propagating location information across the network.

The mechanism of two-way ranging between nodes of a network is comprised of a packet-handshake. Suppose node A of the network would like to know the range R_{AB} to node B. Node A first transmits a packet, called the "range-initiate" (RI) packet at time t_0, with an acquisition header of length $N_c T_f$ spread using a TH-code C_A, which contains N_c pulses with a pulse repetition interval T_f, as shown in Figure 2.4-2 and keeps track of the times $t_s(n) = t_0 + nN_cT_f$, where n is an integer. If $t_c = R_{AB}/c$ is the propagation delay, the packet reaches B at $t_a = t_0 + t_c$. Assuming B knows the TH-code C_A and listens on C_A, it uses the acquisition header and synchronizes itself to the *leading edge* of the acquisition header t_a and keeps track of the times $t_r(n) = t_a + mN_cT_f = t_0 + t_c + mN_cT_f$, where m is an integer. Then node B sends a "range-response" (RR) packet at $t_r(N)$ where N is an integer. Node A receives the response packet and determines the time of the leading edge of the received acquisition header $t_{r2} = t_r(N) + t_c = t_0 + 2t_c + NN_cT_f$. Node A then computes the difference $\Delta t = t_{r2} - t_s(N) = 2t_c$. The range R_{AB} can be computed using $R_{AB} = c\Delta t/2$, where c is the speed of light.

When the packet handshake described above is successfully completed, we say node A has successfully "ranged" to node B. A useful feature of this scheme is that any data can be sent in the data portion of the header, since only the acquisition header is used for ranging. With $T_f = 100$ ns, the duration of each packet is on of the order of 10 milliseconds. Note that any ambiguity in interpreting the range is eliminated by ensuring $R_{AB} >> cN_cT_f$. The above equations assume the absence of processing delays, but these can be eliminated via calibration.

Using this process, nodes are able to obtain the coordinates of, and ranges to, other localized nodes in the network. Based on this information, the locations of these nodes can be estimated. In the next section, we derive bounds on the estimation of a node's location, given noisy ranges and coordinates of the reference nodes.

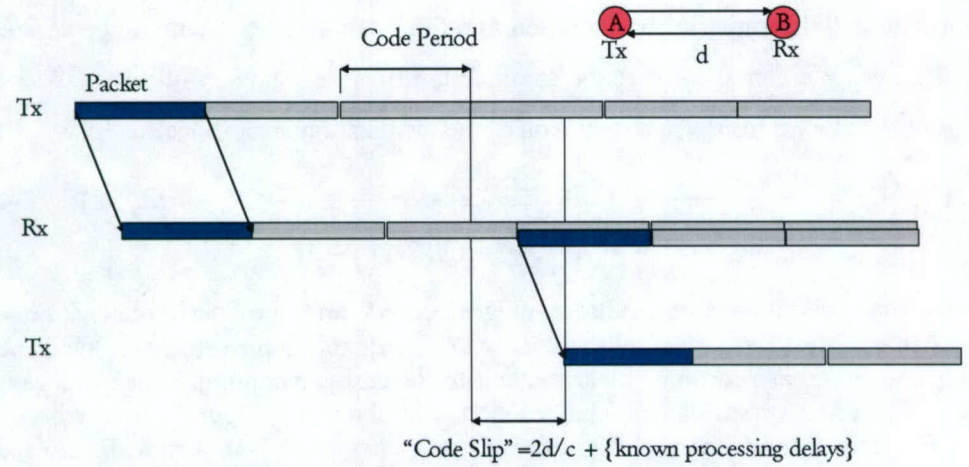

Figure 2.4-2 TOA-based ranging mechanism.

Bounds on Location Estimation

Assuming that noisy estimates of the ranges to reference nodes with known coordinates are available via the ranging mechanism described above, the Cramer-Rao Bound (CRB) on the estimation of the mobile nodes' location can be derived, assuming that the range estimates are unbiased and Gaussian distributed. This bound is represented by the minimum achievable "localization error" Ω_x, which is defined as the sum of the variances of the estimate in the x and y directions:

$$\Omega_x = \sigma_x^2 + \sigma_y^2 \tag{2.4-1}$$

It can be shown that the minimum achievable localization error is given by

$$\Omega_x(m) = \frac{\sum_{i=1}^{m} \frac{1}{\sigma_i^2}}{\sum_{i=1}^{m} \sum_{j=1, j>i}^{m} \frac{\sin^2(\alpha_i - \alpha_j)}{\sigma_i^2 \sigma_j^2}} = \frac{\gamma_m}{\psi_m} \tag{2.4-2}$$

where m is the number of range estimates available, $\{\sigma_i^2\}$ are the variances of the range estimates and $\{\alpha_i\}$ defines the orientation of the reference nodes relative to the node whose location is being estimated, as shown in Figure 2.4-3. It must be noted that in the above equation, we have used the following definitions:

$$\gamma_m = \sum_{i=1}^{m} \frac{1}{\sigma_i^2}, \quad \psi_m = \sum_{i=1}^{m} \sum_{j=1, j>i}^{m} \frac{\sin^2(\alpha_i - \alpha_j)}{\sigma_i^2 \sigma_j^2} \tag{2.4-3}$$

From (2.4-2), the localization error is a function of (**a**) the number of range estimates m, (**b**) the accuracy of the range estimates (σ_i^2, i = 1, 2,...,m) and (**c**) the geometry of reference nodes (α_i, i = 1, 2, ... ,m).

Suppose we have an initial geometric configuration of reference nodes $\{\alpha_i\}$ with range variances $\{\sigma_i^2\}$, $i = 1, 2, \ldots, m$. We can show that the introduction of a new node with orientation and variance $(\alpha_{M+1}, \sigma_{M+1}^2)$ always results in a reduction of the localization error. Specifically,

$$\Omega_x(m+1) = \frac{\gamma_{m+1}}{\psi_{m+1}} = \frac{\sigma_{m+1}^2\gamma_m + 1}{\sigma_{m+1}^2\psi_m + \frac{\gamma_m}{2} - \frac{\sqrt{\gamma_m^2 - 4\psi_m}}{2}\cos(2\alpha_{m+1} - 2\upsilon)} \leq \frac{\gamma_m}{\psi_m} = \Omega_x(m) \quad (2.4\text{-}4)$$

Therefore, increasing the number of available ranges always improves performance. For the special case where $\alpha_{m+1} = \alpha_k$, $\sigma_{m+1} = \sigma_k$ where $k \in \{1, 2, \ldots, m\}$, the improvement in localization error can be viewed as a repeated range measurement followed by averaging, which reduces the range variance. The error versus the number of nodes is shown in Figure 2.4-4, where the localization error is shown for different values of m. As predicted by (2.4-4), the localization error decreases as m increases. We also show the localization error obtained by a simple Least-Squares estimator for different values of m, and observe that it follows a pattern similar to the CRB. These observations indicate that the accuracy of localization improves as the number of successful range-packet exchanges increases.

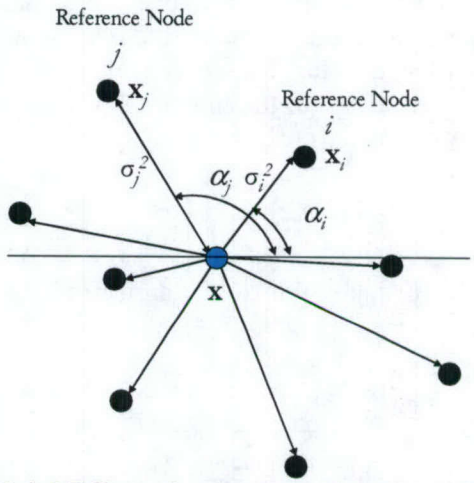

Figure 2.4-3 Effect of geometry on location estimation.

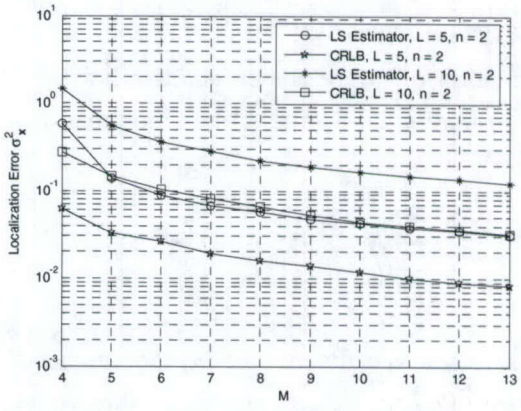

Figure 2.4-4 Effect of m on the localization error. L is the dimension of the area in which reference nodes are randomly distributed and n is the path loss exponent.

MAC Design for UWB Position Location Networks

For the application of emergency location networks, we observe that the desired network is a *unique hybrid of the mobile ad hoc and sensor networks*. Specifically, the data sinks of the network are mainly the mobile and control nodes and the physical quantity being measured by the remaining stationary sensor nodes is the physical location of the mobile nodes. The size of the network grows with time over the area of coverage and therefore automated node discovery and routing are essential. Since the size of the network grows with time, we require the MAC protocol to be scalable. The MAC protocol for this network needs to provide node discovery, fair and reliable multi-hop data transfer between nodes and be able to adapt to the mobility of nodes and to node failure. We also require fairly up-to-date knowledge of the location of the mobile nodes, and therefore we need to ensure that latency requirements are met. As mentioned previously, there is a trade-off between update-rate and reliability, and therefore our MAC protocol should allow us to trade one quantity for another. Since the nodes in the ad hoc network case are designed to be battery-powered, once again the MAC protocol needs to be power-efficient. Another aspect that needs to be considered is the hardware complexity of the nodes. In order to minimize the hardware complexity of the nodes, we enforce the constraint that at any instant, a node can either transmit or receive, but not both. Additionally, each node can listen on only one TH-code at a time.

Another unique feature of the network is the impulse-based UWB physical layer. Due to power constraints on UWB impulse radio, in order for impulse radios to achieve significant transmission ranges, we would have to use several pulses per bit and therefore reduce the data rates of these networks. This low-data rate over a wide transmission bandwidth automatically implies large spreading gains, and therefore we envision Time-Hopped (TH) or Direct Sequence (DS) spreading to be an integral feature of the UWB signals used. Time-Hopped signals for example, allow us to trade area of coverage and reliability of position estimations for the update rate of the estimates, since the number of pulses that represent one bit of information can be controlled. Additionally, TH lowers the power-spectral density of the signals and makes the signals more covert and harder to detect.

Many of the MAC protocols proposed for mobile ad hoc and sensor networks are based on CSMA [Jurdak2004]. CSMA-based MAC protocols are scalable; however, there are several issues with CSMA-based schemes for impulse-radio networks. Time-hopping is predominantly used to lower the power spectral density of impulse-based UWB to within the FCC limits. Therefore, in order for a node sensing the channel to detect channel usage, knowledge of the TH-code of transmission must be known beforehand. In addition, T_b, the time-shift due to data, must be known and even if T_b is known, searching for this time-hopped signal may be highly computationally intensive and time-consuming, i.e., simple energy detection is not sufficient. Additionally, pure CSMA suffers from the Hidden-Node problem, and we need RTS/CTS overheads to alleviate this problem. The additional overhead reduces the energy efficiency of the network. TDMA is a commonly suggested MAC protocol [Oppermann2004] in sensor network literature as it is power efficient and allows for sleep schedules to improve power efficiency, but it is not scalable and thus does not meet our requirements. A subsequent section analytically compares the performance of CSMA with TH-CDMA for a simple network.

MAC Design: Minimizing Localization Error

It is clear from (2.4-4) and Fig. 2.4-4 that the accuracy of a location estimate of an unlocalized node is determined by the number of RR packets (m) it receives from other localized nodes. Therefore, for the design metrics of *location-accuracy* and *estimation-delay*, a MAC protocol that provides a higher *effective throughput* of RR packets allows (1) higher accuracy and (2) quicker

estimation of location by unlocalized nodes. Similarly, in the second phase of the network location estimation, where the estimates of locations of mobile nodes are routed back to a monitoring station, the effective throughput of the MAC protocol affects the update rate of mobile's location estimate or "location refresh rate" at the monitoring station. More precisely, a higher effective throughput reduces the lag between the estimation of the mobile's location and the display of this information at a remote location. A CDMA-based protocol allows simultaneous transmissions by the nodes of the network at the cost of incurring multi-access interference; CSMA on the other hand does not allow nodes in the same vicinity to transmit simultaneously. Figure 2.4-5 shows the effective throughputs in terms of successful packet delivery per second versus the number of nodes in an UWB packet-radio network for two MAC protocols: a TH-spread spectrum scheme and CSMA. The network is assumed to be an ad hoc multi-hop network in which packets (of unit duration) are communicated between the nodes of the network. The effective throughput of the network is determined by the number of packets successfully decoded (based on SNR or SINR) per unit time in the network. We see that the effective throughput of the TH-CDMA scheme is higher than that of CSMA. This suggests that a TH-spread-spectrum MAC protocol would provide a higher location estimate convergence rate than the CSMA protocol.

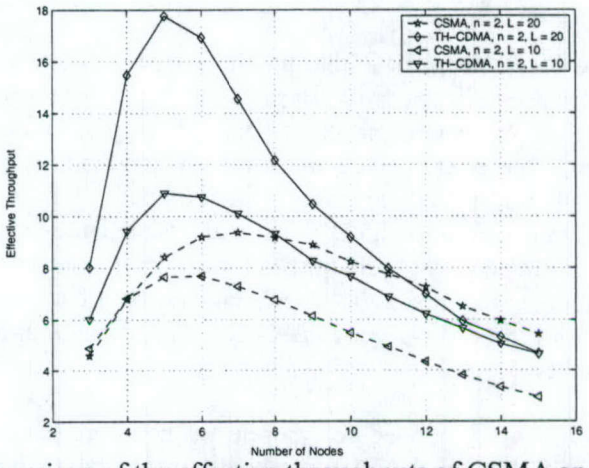

Figure 2.4-5 A comparison of the effective throughputs of CSMA and TH-CDMA MAC schemes.

References

J.-Y. Lee and R. A. Scholtz, "Ranging in a dense multipath environment using an UWB radio link," *IEEE Journal on Selected Areas in Communications*, vol. 20, pp. 1677–1683, December 2002.

R. Jurdak, C. Lopes, and P. Baldi, "A Survey, Classification and Comparative Analysis of Medium Access Control Protocols for Ad Hoc Networks," *IEEE Communications Surveys and Tutorials*, vol. 6, pp. 2–16, Q1 2004.

I. Oppermann, L. Stoica, A. Rabbachin, Z. Shelby, and J. Haapola, "UWB wireless sensor networks: UWEN - a practical example," *IEEE Communications Magazine*, vol. 42, pp. S27–S32, December 2004.

Subtask 2.4.1.b Cross-Layer Design of Cooperative UWB Networks

Based on the accomplishments from Quarter 1, we applied TR-UWB (Time reversal UWB) techniques to improve energy capture at the receiver. It was found that a 3 dB improvement is introduced in SISO UWB scenarios. Next we extended the TR-UWB technique to a collaborative (Distributed MIMO) scenario. Again, we find that the technique improves overall link quality. Finally, a rate adapted cross layer UWB optimization technique is investigated in which a sequence optimization technique is adopted to improve the SINR and throughput in an UWB-based ad hoc network.

TR-UWB

Time reversal (TR) techniques, also known as phase conjugation, have been applied in the field of acoustics for past two decades. The basic principle behind TR is to use the complex conjugate version of time-reversed channel impulse response (CIR) as a prefilter at the transmitter. The benefits of TR techniques in wireless communications can broadly be characterized in three effects: temporal focusing, spatial focusing and channel hardening. Due to the inherent inter-symbol interference (ISI) and co-channel interference suppression capabilities, TR techniques have been extended to MIMO systems. Furthermore, recently the space-time focusing properties of TR have been demonstrated in SISO Ultra-wideband (UWB) channels. It has also been proposed to exploit the TR-shift algorithm to improve channel capacity in multi-user UWB systems. In this report, we proposed a modified version of TR-UWB, which can achieve 3 dB system performance improvement in SISO UWB scenarios.

For SISO UWB system, the transmitted signal has the form:

$$s(t) = \sqrt{E_p} \sum_{i=-\infty}^{\infty} b_i \sum_{n=0}^{N_x-1} w(t - nT_w - iT_f) \tag{2.4-5}$$

where $b_i = \pm 1$ are the data bits, $w(t)$ is the unit-energy transmit pulse with a length of T_w, N_x is the length of signal sequence, and T_f is the symbol length which is large enough to avoid ISI.

Using an L-path channel tap-delay model, the UWB channel is represented as:

$$h(t) = \sum_{l=1}^{L} \alpha_l \delta(t - \tau_l) \tag{2.4-6}$$

where α_l and τ_l are the amplitude (including polarity) and delay of the l^{th} multipath component, respectively.

The received signal, in the time interval $\lfloor kT_f \quad (k+1)T_f \rfloor$, can be written as:

$$r(t) = \sqrt{E_p} b_k \sum_{l=1}^{L} \alpha_l \sum_{n=0}^{N_x-1} w(t - nT_w - \tau_l) + n(t) \tag{2.4-7}$$

where k is a positive integer, and $n(t)$ is an zero-mean additive white Gaussian noise with power spectral density $\frac{N_0}{2}$.

Using *h(t)* as a prefilter and assuming the channel is slow varying, the received signal at the transmitter can be represented as:

$$r = b * h^*(-t) * h(t) + n(t) \tag{2.4-8}$$

Rewriting the autocorrelation term using channel convolution matrix, it can be shown that the maximum term in the vector R is $\sum_{i=1}^{L} h_i h_i^*$

$$R = \begin{bmatrix} h_1 & & & \\ h_2 & h_1 & & \\ & h_2 & & \\ & & & \\ h_L & h_{L-1} & h_1 & \\ & h_L & h_2 & \\ & & & \\ & & & \\ & & h_L & \end{bmatrix} \begin{bmatrix} h_L^* \\ h_{L-1}^* \\ \\ \\ h_1^* \end{bmatrix} = \begin{bmatrix} h_1 h_L^* \\ h_2 h_L^* + h_1 h_{L-1}^* \\ \\ \sum_{i=1}^{L} h_i h_i^* \\ \\ h_L h_2^* + h_{L-1} h_1^* \\ h_L h_1^* \end{bmatrix} \quad (2.4\text{-}9)$$

Recently published work shows that traditional TR techniques are typically only sampled at the peak of the received signal, hence, only about 60% of total energy is captured at the receiver. To solve this issue, we propose the use of a matched filter at the receiver, which has the template $Y = R^*$ in order to fully capture the energy of received signal. Simulation results are shown in Figure 2.4-6.

Comparing to other UWB sequence optimization techniques, with good channel estimation, the modified TR method is simpler without the computation burden. However, with poor channel estimation, the performance of modified TR method degrades quickly, as shown in Figure 2.4-6. The modified TR method is about 2 dB worse than sequence optimization techniques at low SNR scenarios when the number of pilots is only 250. To summarize, the modified TR UWB method can greatly improve link performance, but it is more vulnerable to channel estimation.

Application to Distributed MIMO

A natural extension of the TR technique is to the Distributed MIMO concept. If multiple nodes which are in close proximity can co-ordinate transmissions to within a symbol (not necessarily pulse) interval, nodes can improve the link SNR. An example is given in Figure 2.4-7 where 2, 4, or 6 nodes co-operate to improve link performance. We can see that modest improvements are achieved as compared to a single node, perfect Rake receiver (AWGN). Two nodes provided a 5.5 dB improvement due to: (a) coherent multipath combining and (b) node collaboration. Increasing to four nodes provides approximately 3 dB additional gain.

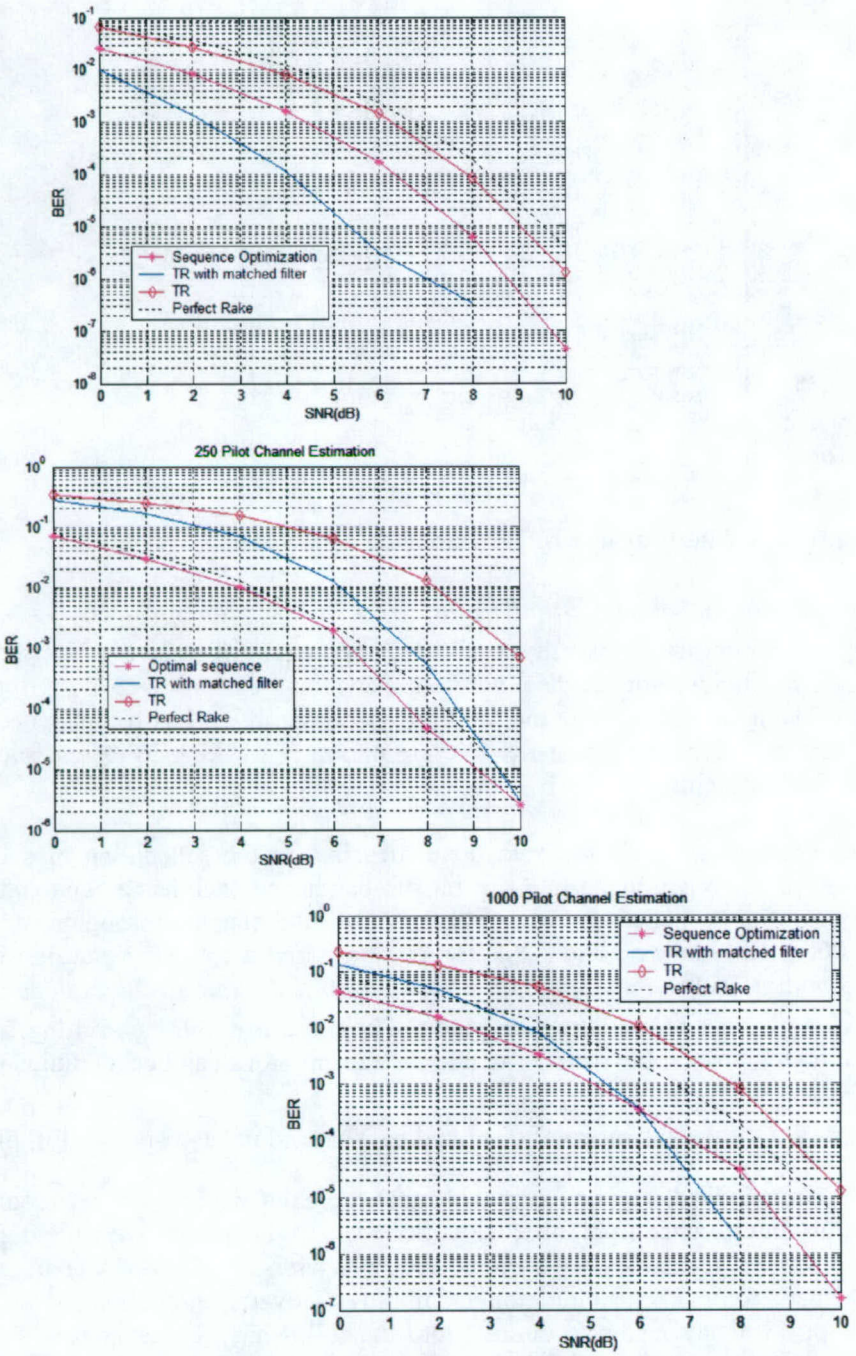

Figure 2.4-6 Modified TR-UWB. Top plot: Perfect Channel Estimation. Center plot: 250 pilots are used for channel estimation. Bottom plot: Pilot number is increased from 250 to 1000.

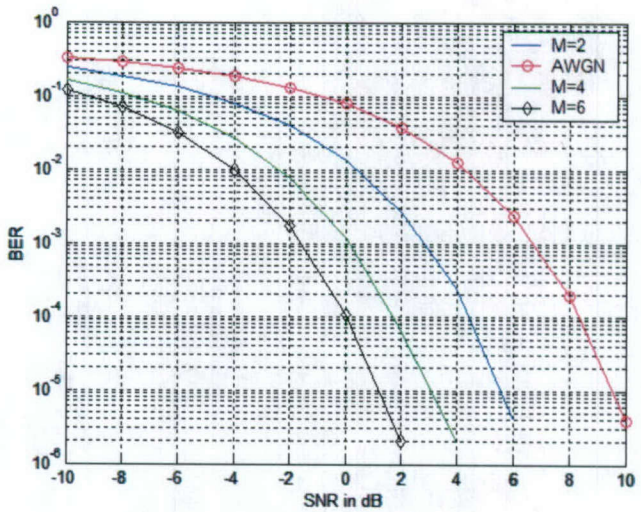

Figure 2.4-7 Performance of TR with node collaboration.

UWB Cross-Layer Design with Sequence Optimization

Recently published papers demonstrate that the traditional approach of layering network functions is not necessarily efficient for ad hoc wireless networks. Cross-Layer design to maximize total network throughput or minimize the total power consumption has recently been investigated for narrowband communication systems. We are currently working to extend such concepts to the design of UWB systems.

For UWB systems, some cross-layer work has been done focusing on the scheduling of sub-bands, in which the whole spectrum is divided into several sub-bands and each has a bandwidth larger than 500 MHz. By carefully scheduling these sub-bands, the total channel throughput can be greatly enhanced. In 2004, B.Radunovic and J-Y L.Boudec proposed a cross layer design to MAC design and routing with a goal to maximize $\sum \log f_i$ (where f_i is the rate of the i^{th} node in the ad hoc network) without constraining the sub-bands. They claimed that by setting an exclusion region (i.e., the region around the receiver where no transmissions can occur) radius to $r = \left(\frac{(\gamma - 2) P_{\max}}{2\eta} \right)^{\frac{1}{\gamma}}$, (where γ, η are the fading coefficient and background noise respectively), the total utility of the network maximized. Here, it is notable that the exclusion region is the key factor to control the arbitrary interference from other network nodes. In this report, we will adopt a UWB sequence optimization technique to combat the interference caused by parallel transmission, avoiding the need for an exclusion region and improving overall throughput.

The design of the UWB physical layer can be divided into the following two categories. For parallel transmission at the n^{th} time slot, one UWB link is randomly picked to maximize its SINR using sequence optimization technique, or each link will be assign their own optimal sequence to maximize its SNR only. As for the routing protocol, we assume the network size is one by one, and nodes are uniformly random distributed in this area. Two routing protocol will be considered, first, directly routing (DIR) which is a single hop routing protocol; second, minimum energy routing protocol (MER) which choose dynamic multi-hop protocol to minimize the energy cost function. Furthermore, two scheduling strategies are proposed; one is to send as many nodes as possible at one time (algorithm I), and another one is to remain a exclusion region to control the arbitrary interference level while a node is receiving data (algorithm II).

Now, the optimization problem can be written as:

$$\begin{aligned} \text{Max} \quad & \sum_{i=1}^{I} \log(f^i) \\ & Bf^n \le \sum_{n=1}^{L+1} w_n r^n \\ & r_l^n = K * SINR_l^n \\ & \sum_{n=1}^{L+1} w_n = 1 \\ & \sum_{l:l.src=0} 1_{\{p_l^n>0\}} + \sum_{l:l.des=0} 1_{\{p_l^n>0\}} \le 1 \\ & P_l^n \le P_l^{MAX} \end{aligned} \tag{2.4-10}$$

where *n, l,B,f, r* represents the time slots , link, routing matrix, flow and data rate respectively, *w* is the duration of time slots, and P is the power of nodes.

Figure 2.4-8 shows an example of ten randomly distributed nodes. The source and destination pairs are assumed to be nodes 1→6, 2→7, 3→8, 4→9, and 5→10. Hence, for the DIR routing protocol, the routing path is straight forward. The solid line in Figure 2.4-8 indicates the routing path calculated by MER protocol, here, the fading coefficient is assumed to be four and all nodes have the same initial power which equals P^{MAX}.

By solving (2.4-10), the total utility under different routing, scheduling and physical layer designs were calculated and are listed in Table 2.4-1. From the results we can see the following.

1. With scheduling algorithm I, the DIR routing protocol always performs worse than MER. However, one thing should be noted is that since one link is randomly chosen to maximize the SINR, it might be possible to find another link such that the total rate under the same time slot is maximized.

2. With the help of the exclusion region, the interference level is controlled to be small and DIR routing and MER routing have similar performance when the link is chosen to maximize its SINR. Furthermore, under such a scheduling algorithm, since interference is low, to maximize SNR may be more meaningful, which we will investigate shortly.

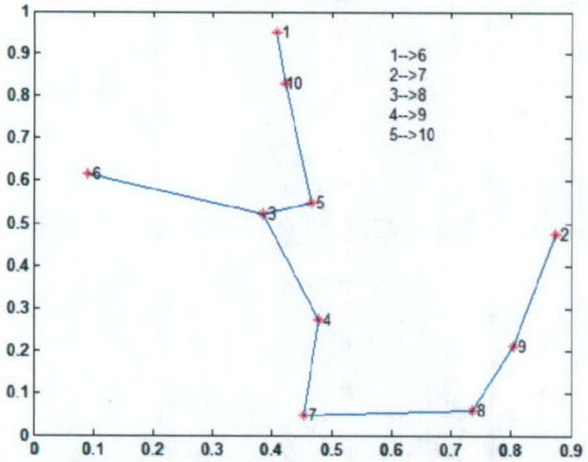

Figure 2.4-8 Randomly distributed ten nodes, where solid line represent routing path. For such ten nodes, the source and destination pairs assume to be node 1 to 6; 2 to 7, 3 to 8, 4 to 9 and 5 to 10, respectively.

Table 2.4-1 Total Utility Under Different Scheduling, Routing.

		Max (SINR)
All sending together-Scheduling I	MER	55.4636
	DIR	6.3708
Optimal exclusion region-Scheduling II	MER	41.1660
	DIR	47.5004

2.4.4 Productivity

Journal publications

1. J.Ibrahim and R.M. Buehrer, " Two-Stage Acquisition for UWB in Dense Multipath," submitted to *IEEE Journal on Selected Areas in Communications*, March 2005.
2. S. Venkatesh and R.M. Buehrer, " A New MAC Protocol for UWB-based Position-Location Networks: Framework and Analysis," submitted to *IEEE Journal on Selected Areas in Communications*, March 2005.

Conference publications

1. J.Ibrahim, R. Menon, and R.M. Buehrer, "UWB Sequence Optimization for Enhanced Energy Capture and Interference Mitigation," Accepted for Presentation at IEEE Military Communications Conference MILCOM2005, Atlantic City, NJ, October 2005.
2. J. Ibrahim and R.M. Buehrer, "Two-Stage Acquisition for UWB in Dense Multipath," Accepted for Presentation at IEEE Military Communications Conference MILCOM2005, Atlantic City, NJ, October 2005.
3. S. Ventkatesh, N. Kumar, and R.M. Buehrer, "A Spread-Spectrum MAC Protocol for Impulse-Radio Networks," accepted for presentation at the IEEE Vehicular Technology Conference, Fall 2005.

Students supported

Qiao Chen, January. 1, 2005 – present
Swaroop Venkatesh, January. 1, 2005 – present
Jihad Ibrahim, January. 1, 2005 – present

Faculty supported

R. Michael Buehrer, Jan. 1, 2005 – present
Scott Midkiff, Jan 1, 2005 - present

3. TASK 3 Visualization of Wireless Technology and Ad Hoc Networks

3.1 Overview

Task Objective: The objective of this task is to identify and investigate AWINN enabling technologies for the Close-in Sea basing.

Organization: The task is directed by Ali Nayfeh and Rick Habayeb. The personnel list follows.

Rick Habayeb, faculty
Ali Nayfeh, faculty
Ehab Abdul Rahman, faculty

Summary: The main activity during this period is integrating the crane controller into a fielded crane. This will provide the bridge to transition the UWB ranging technology into the Sea Basing environment.

3.2 Task Activities for the period

During this quarter we had a golden opportunity to establish a potential transition path for the AWINN technologies into the Sea Basing environment. Early in the quarter, the team was given approval to piggy-back on a fielded crane at the seaport of Jeddah, Saudi Arabia. The crane controller developed at VT was integrated into a fielded crane at the seaport. Experiments to evaluate the crane controller are still ongoing.

Also, we developed an integrated systems solution, which enables the transfer of cargo from one pitching, rolling, yawing, surging, heaving, and swaying ship to another pitching, rolling, yawing, surging, heaving, and swaying ship adjacent to it without damage to the ships or the material, personnel, or equipment. This particular proposed transfer process is a skin-to-skin replenishment in a more rigorous sea environment than sea state 3. The integrated system includes a process to ensure safe and expeditious ship approach, connection of ships, minimization of the absolute and relative motions between the ships, dynamic handling of the moored-ship assembly, separation of the ships in an open ocean environment and in sea states up to and including sea state 5, and safe cargo transfer.

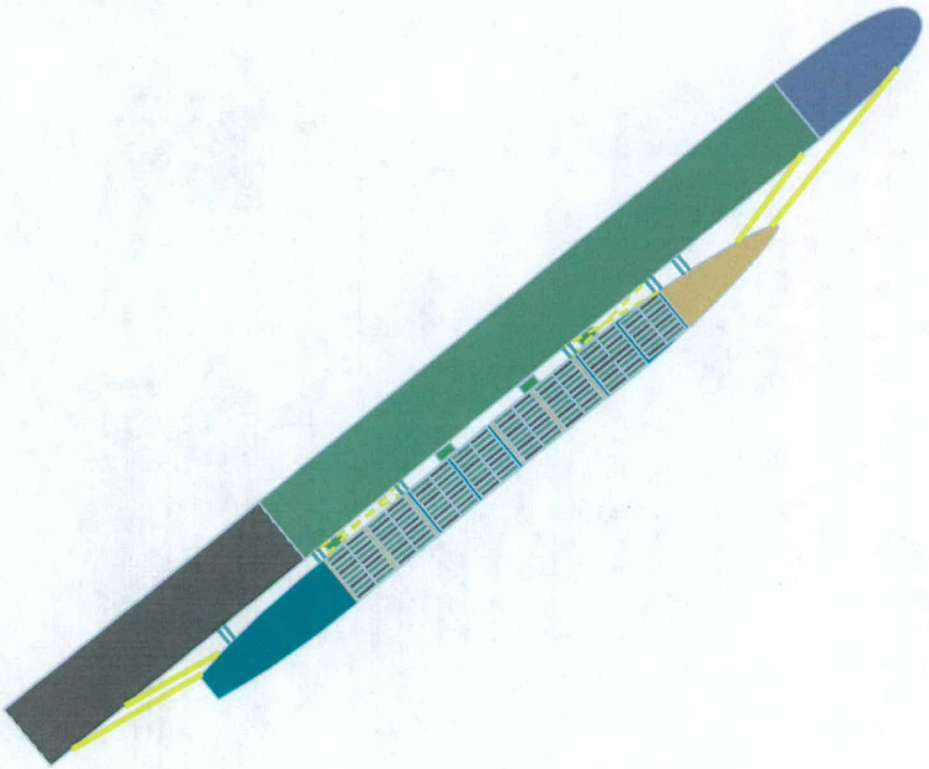

Figure 3 -1 Configuration of moored-ship assembly.

For the safe connection, the Navy ship (called MPF(F)) will deploy active anti-roll tanks and fenders and mooring lines to secure the two ships together, minimize their absolute and relative motions, and prevent damaging metal-on-metal contact. To accomplish this, we have developed an active anti-roll/mooring system as follows. The smaller containership is placed on the lee of the larger ship, the MPF(F), as shown in Figure 3-1. This shelters the smaller and livelier ship from incident wave. The heading of the MPF(F) is restricted to keep incident waves within a range of either off head seas on the bow or off following seas on the stern. The speeds of both ships are restricted to a range within 3-8 knots. We found that this configuration minimizes the roll motions of both ships and the relative yaw between them. Active anti-roll tanks are installed on the MPF(F) to control its heave, pitch, roll, and yaw, thereby allowing it to act as an absorber to the motions of the containership. The MPF(F) will deploy 4-8 inflatable fenders along the parallel sections (amidships) of the two ships. The fenders are placed fore and aft of the center of gravity of the MPF(F). The fenders are used as a passive shock absorber to provide a soft ride for the containership over the MPF(F) and prevent skin-to-skin contact between them. The modularity of the inflatable fenders allows for a balance between absorbing the energy of the relative ship motions and maintaining a minimum standoff distance between them. Active mooring winches and Lines are installed on and deployed by the MPF(F). Fifteen to twenty five winches are placed along one side of the MPF(F) and act on the containership through bow lines, stern lines, spring lines, and breast lines. At each breast location, multiple lines are deployed between two abreast locations on the MPF(F) and the containership. Some of the breast lines are attached above the deck of the containership and dubbed "High Breast Lines" and others are deployed at the level of the containership deck and dubbed "Low Breast Lines." The breast and spring lines are distributed fore and aft of the centers of gravity of the two ships.

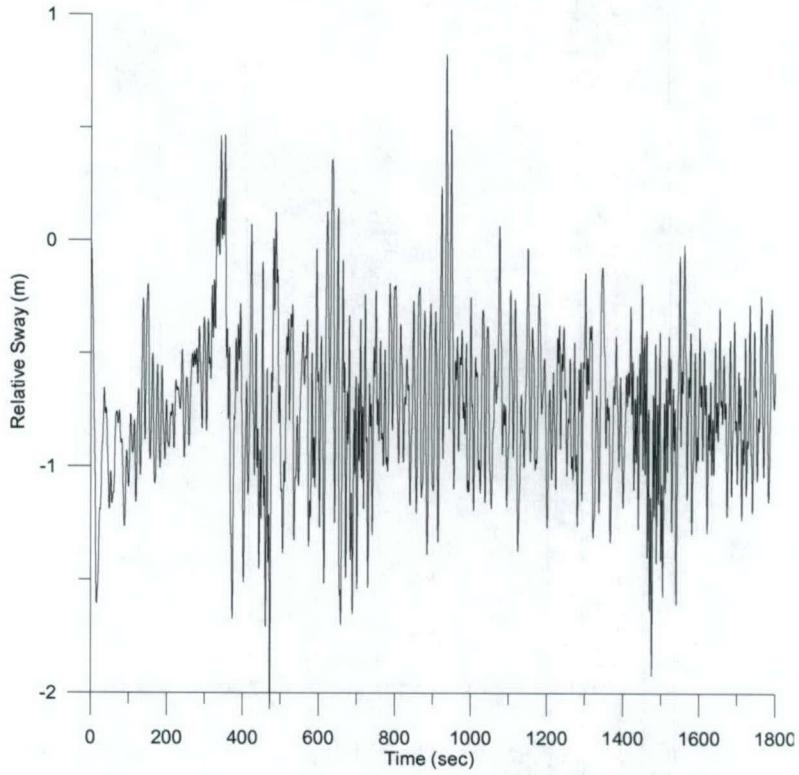

Figure 3-2 Simulation results for relative sway between the Bob Hope and the Argonaut in SS4. The incoming wave is incident on the Bob Hope stern at 20° off follower seas.

We simulated the motions of two notional ships (the Bob Hope and the Argonaut) connected and stabilized using a preliminary design of the active mooring system (4 fenders and 22 mooring lines). The simulations were performed using the Multiple-Body version of the Large Amplitude Motions Program (LAMP) of SAIC. All mooring lines were rated to carry a maximum load of 200 KN. The lines were designed to carry active, continuously varying loads defined by a closed-loop, feedback control strategy for each line. The control strategies use the line length and the states of each ship center of gravity to define the load for each winch. We used a conservative estimate of the damping effect of the anti-roll tanks on the Bob Hope motion. We succeeded in stabilizing the motions of the ships relative to each other in sea state 4 for all wave headings in a range of 15-25 off head and following seas and for ship speeds ranging from 3-8 knots. We show in Figures 3-2 to 3-5 the responses of the ships over a period of 30 minutes in sea state 4 with the incoming wave being incident on the Bob Hope stern at 20° off following seas.

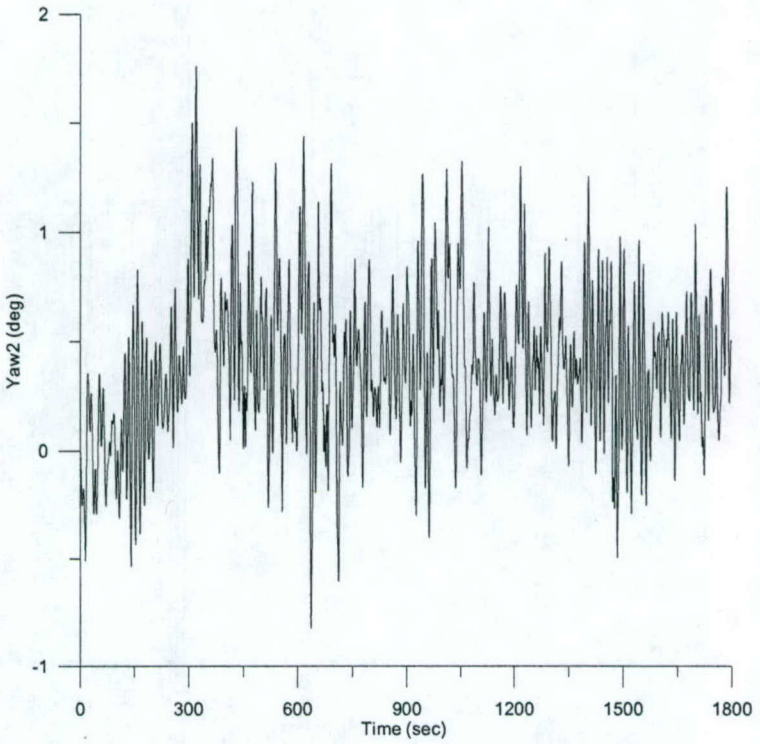

Figure 3-3 Simulation results for relative yaw between the Bob Hope and the Argonaut in SS4. The incoming wave is incident on the Bob Hope stern at 20° off follower seas.

These simulations and others show that the system maintains a skin-to-skin configuration with the relative sway being less than 1.5 m, the minimum ship separation being more than 5 m, and the relative yaw being less than 1 degree. Moreover, the system controls the heaves of the Bob Hope and Argonaut to less than 0.6 m and 1.0 m, their pitch angles to less than 0.25 degree and 1.5 degree, and their roll angles to less than 0.5 degree and 1.3 degree, respectively. Consequently, this system enables the crane-control system to transfer cargo softly and safely between these two ships in sea state 4.

These simulations are implemented in the one-wall CAVE and are being used to implement and evaluate the crane-control system with its four components: sensors, motion predictor, pendulation controller, and soft pick up and landing component.

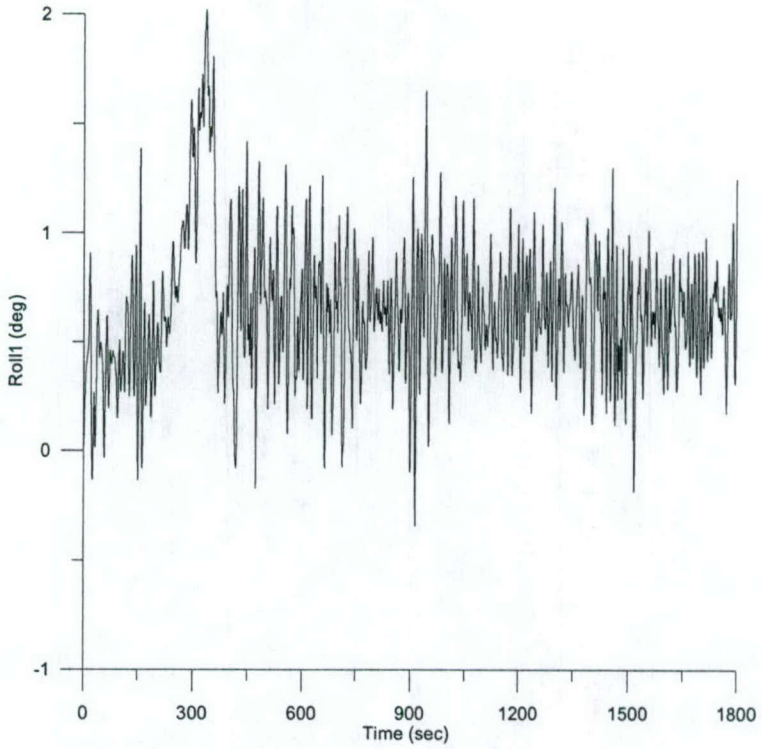

Figure 3- 4 Simulation results for Bob Hope roll in SS4. The incoming wave is incident on the Bob Hope stern at 20° off follower seas.

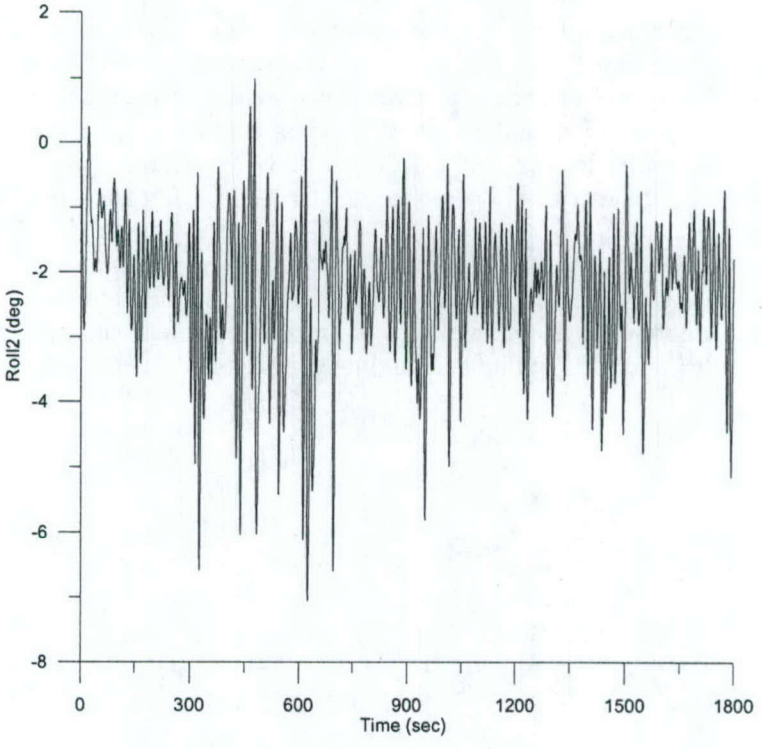

Figure 3-5 Simulation results for argonaut roll in SS4. The incoming wave is incident on the Bob Hope stern at 20° off follower seas.

3.3 Importance/Relevance

ForceNet is the Navy implementation plan for Network Centric transformation. There are three fundamental concepts in ForceNet: Sea Shield, Sea Strike, Sea Basing. Sea Basing is projecting joint operational independence. There several technological challenges associated with the Navy vision for Sea Basing. The first major challenge is the Close-in command, control, and communication (C3). Currently, ship-to-ship Close-in C3 during UNREP is tedious, time consuming, archaic, and labor intensive. This project will explore, develop, visualize, and integrate the high payoff enabling AWINN technologies for the Close-in sea basing environment.

3.4 Productivity

Students Supported

N. Nayfeh- January 25, 2005 to present
M.Daqaq – January 25, 2005 to present
O. Marzouk- January 25, 2005 to present

3.5 Summary Quad Chart

AWINN Task 3 - Visualization of Wireless Technology and Network

- Day Time Communication

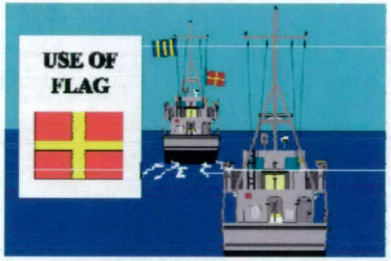

Technical Significance

To design and develop C3 using UWB sensors and Ad Hoc mesh networks

*Perform close-in ranging of cargo, ranging of ships during maneuver, and netting distributed sensors of a cluster of ships

•The close-in C3 will rely on the AWINN enabling technologies

Major Performers

Virginia Polytechnic Inst. and St. U.,
Dr. Rick Habayeb
Dr. Ali Nayfeh

Accomplishments and Approach

* Design and develop close-in C3
* Design and develop UWB cargo ranging sensors for soft pickup and landing of containers
*Design and develop UWB ship ranging Sensors and network
* Leverage and integrate AWINN wireless technologies and sensor networks to support the close-in Sea Basing missions

Impact

* Sea Basing missions require close-in C3 to transfer cargo and provide communication links. The AWINN provides the enabling technologies for the close-in sea basing missions.

3.6 Timeline Chart

Task 3 - Visualization of Wireless Technologies in Sea Basing Environment

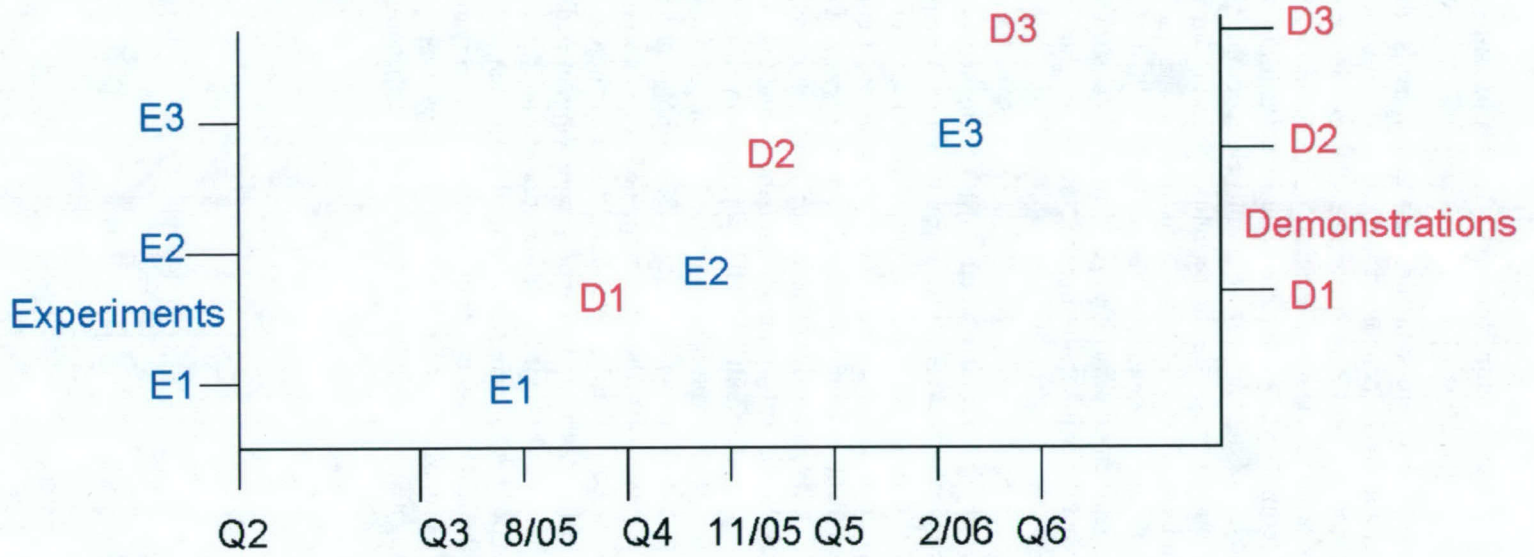

E1: Sensor fixed, Target moving

E2: Target and sensor moving

E3: 6 DOF Ranging

D1: Ranging technology

D2: Moving platform integration

D3: Crane integration

4. TASK 4 Testing and Demonstrations

4.1 TIP#1: Distributed MIMO UWB Sensor Networks Incorporating Software Radio

Task objective: The cost, weight, and poor aero-dynamics of antenna arrays greatly limit their practical use on both unmanned vehicles and dismounted tactical warfighters. However, recent developments in light-weight multi-mode/multi-band software radios can leverage a multi-band communication capability and network-wide position location information to achieve the same benefits offered by space-time coding (STC) and multiple-input-multiple-output (MIMO) communication systems without the use of antenna arrays. In this case, communication nodes in a tight cluster can coordinate both their transmissions and receptions to mimic an STC's operation as if they were part of a single antenna array platform. This novel technique, which we call *synthetic STC* (SSTC), can significantly extend the range of long-haul cluster-to-cluster communications. The objective of this research effort is to perform a design study and understand the benefits of SSTC for SDR radio networks in facilitating the Navy's 'toughest' communication needs.

Accomplishments during reporting period: In a distributed MIMO setup, sensor nodes/antennas are geographically distributed in a random manner within a transmit or receive cluster. Therefore, it is more likely that in a inter-cluster distributed MIMO communication each of the transmitter-receiver pairs will experience dissimilar average received SNRs and even fading with non-identical distributions unlike a collocated antenna MIMO array system. For example in distributed MIMO systems some Tx-Rx links may have LoS and others NLoS. We have developed a mathematical framework for analysis of outage probability and average symbol error rate which can be applied to evaluate such distributed MIMO systems with both identical and non identical fading distributions and average received SNRs per Tx-Rx pair [2]. Figure 4.1-1 shows the plot for outage probability using the above analysis for a 2x2 orthogonal space time block coding (OSTBC) system. Links with equally distributed average power (balanced) and dissimilar distribution (unbalanced) were analyzed for Rayleigh and Rice distributed channels. It is important to note that over identically distributed channels with similar path loss optimum performance is achieved when the links are balanced with the same transmit powers allocated to them. Hence, power allocation is important for achieving optimal performance when links have dissimilar path loss in a distributed MIMO system which is crucial for improving the energy efficiency of the sensor network. We propose to extend the framework developed in [2] to include effects of shadowing and also investigate power allocation strategies for optimum performance of distributed MIMO system.

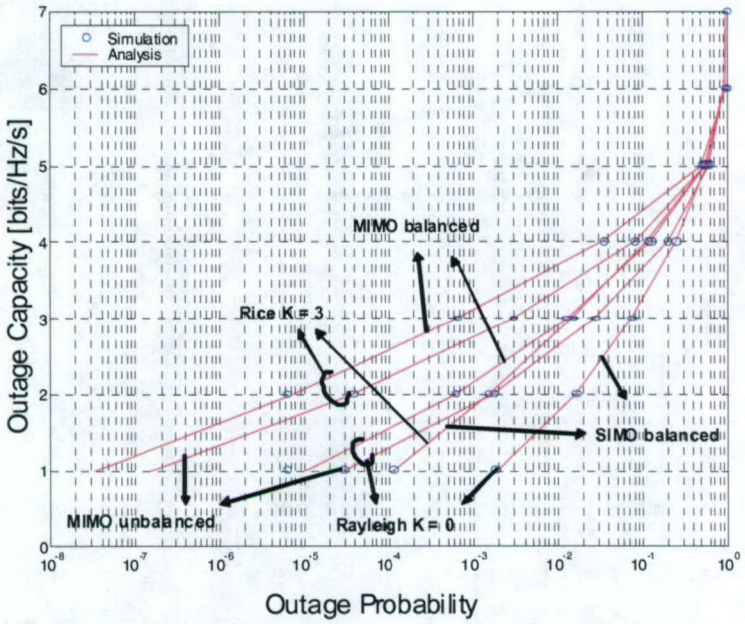

Figure 4.1-1 Computed outage capacity of distributed OSTBC versus outage probability for Rayleigh (K = 0) and Rice (K = 3) channels with distributed MRC in the receive cluster.

For cluster-to-cluster communication to be practical it is important that the clocks and oscillators of cooperating sensor nodes maintain reasonable precision. A credible investigation of distributed MIMO must also account for imperfections in timing synchronization. Figure 4.1-2 gives an illustration of this effect at the receiver when symbols with different delays are combined at the receiver.

Figure 4.1-3 shows the simulation results for intentional ISI due to the effect of differential delays at transmit nodes and jitter respectively with root raised cosine pulse shaping in a 2x1 distributed OSTBC system. The differential delay in transmission is a fraction of the total symbol duration relative to the reference antenna. Jitter on the other hand is modeled as uniformly distributed with a maximum deviation fixed at a fraction of the symbol duration. The performance degradation is small at low delays and jitters up to a fraction of 0.2T and then degrades severely. It can also be seen that the performance degradation is higher for the differential delay when compared to the same level of jitter. The exact analysis of the effect of the type of pulse shaping and ISI with non-identical fading channels is currently underway. This will be part of the investigation that will also help select the best pulse shape to minimize ISI in distributed MIMO set up. Novel space-time coding techniques like time reversed-STC (TR_STC) and space-time OFDM (ST-OFDM) schemes are effective in combating large synchronization errors in cooperative relaying without affecting the data rates. Their evaluation assumes Gaussian approximation with brick wall pulse shaping filters. We propose to extend this analysis to include effects of fading and shadowing along with pulse shaping to make a better selection of schemes for practical implementation.

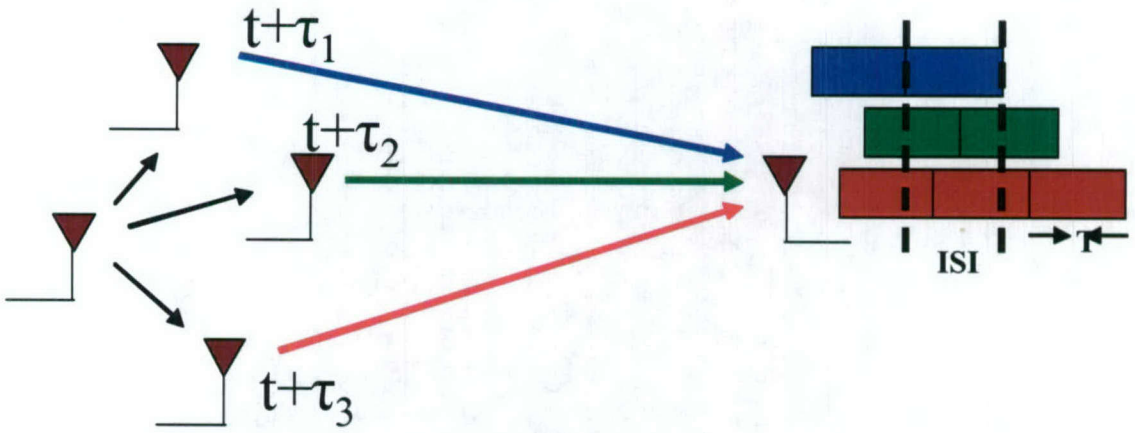

Figure 4.1-2 Illustration of intentional ISI in D-MIMO systems.

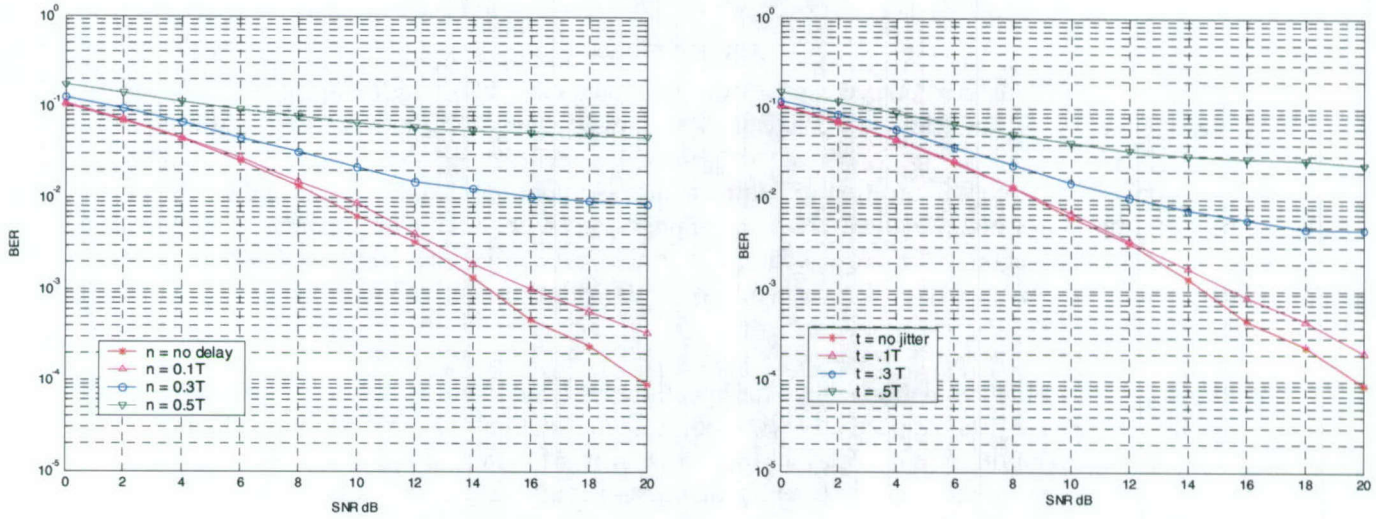

(a) (b)

Figure 4.1-3 Bit error rate (BER) computed from simulations for intentional intersymbol interference due to differential delays as illustrated in Fig. 4.1-2. (a) Effect of ISI due to differential delay. (b) Effect of jitter on the BER performance of 2x1 distributed OSTBC.

References

1. R. Chembil Palat, A. Annamalai, J. H. Reed, "Cooperative relaying for ad-hoc ground networks using swarm UAVs," submitted to MILCOM Nov, 2005
2. R. Chembil Palat, A. Annamalai, J. H. Reed, "Outage and ergodic capacities of STBC cooperative networks," submitted to IEEE Trans. Wireless Communications
3. R. Chembil Palat, A. Annamalai, J. H. Reed, "Outage and ergodic capacities of distributed STBC cooperative networks under generalized fading channels," submitted to MILCOM Nov, 2005
4. R. Chembil Palat, A. Annamalai, J.H. Reed, "Distributed MIMO for cooperative multi-hop wireless mesh networks," submitted, IEEE Wireless Communications Magazine

Schedule:

- January-Summer 2005
  - Develop UWB MIMO Algorithms
- Summer-Fall 2005
  - Simulate performance of UWB MIMO Algorithms
- Spring 2006
  - Begin Work on testing algorithms on Advanced SDR Reciver
  -

Personnel:

Dr. Jeff Reed, faculty
Dr. Michael Buehrer, faculty
Dr. William Tranter, faculty
Ramesh C. Palat

Summary Quad Chart

TIP #1: Distributed MIMO UWB Sensor Networks Incorporating Software Radio

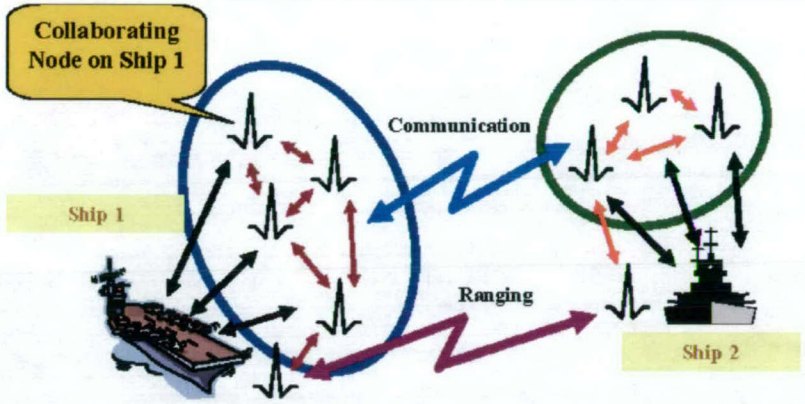

TIP Description

- Develop an Advanced Software Radio capable of supporting cross-layer optimization, ad-hoc networking, ranging/imaging and collaborative systems.
- Investigate novel algorithms for Ultra Wideband communications, with emphasis on ad-hoc networks, distributed MIMO, and ranging/position location.
- Integrate the use of the Software Radio and algorithms into Sea Basing

TIP Objectives

- Demonstrate range extension via collaborative networks using the Advanced Software Defined Radio.
- Demonstrate the ability of UWB signals to provide precision position location in an ad-hoc network environment.

Team

Dr. Jeffrey H. Reed, TIP Leader
Dr. R. Michael Buehrer
Dr. William H. Tranter

Experiments and Demonstrations

- Demonstrate UWB communication in a laboratory environment using prototype SDR receiver (Fall 2005).
- Demonstrate 3-D crane cargo container ranging using laboratory equipment (Fall 2005).
- Demonstrate integration of full UWB receiver with cargo ranging algorithm (Spring/Summer 2006).
- Demonstrate UWB communication in an office environment with full UWB receiver (Summer 2006).

Timeline Chart

TIP#1 Distributed MIMO UWB sensor networks incorporating software radio

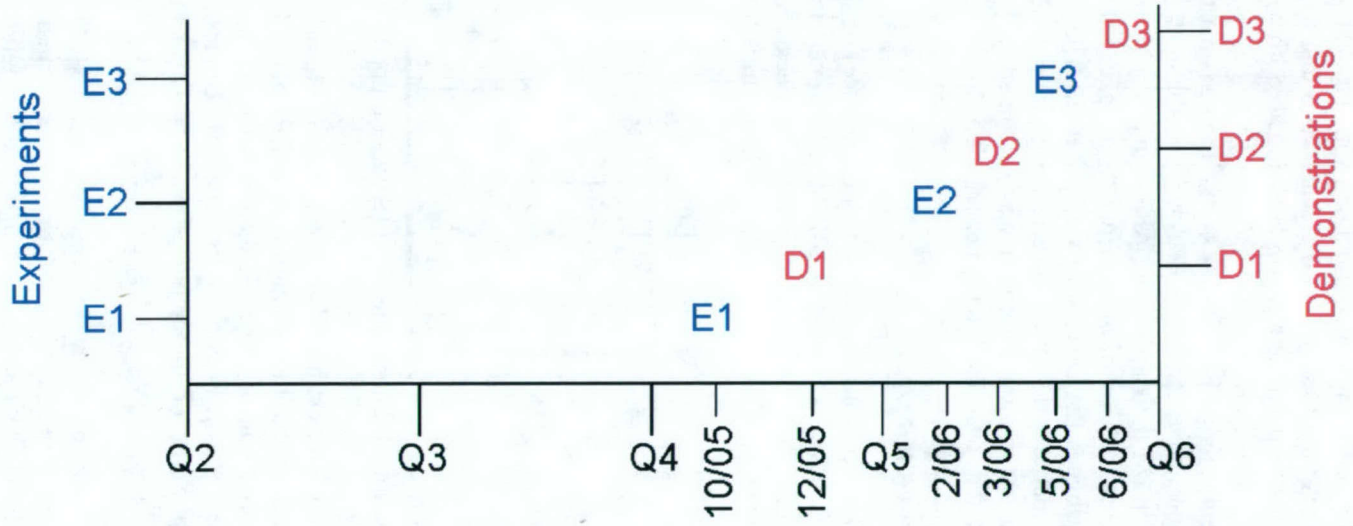

E1: Synchronization of 2 Prototype Receivers

E2: Synchronization of multiple Full Receivers

E3: Evaluate performance of algorithm for high data rate D-MIMO

D1: Low data rate 1x2 D-MIMO using Prototype Receivers

D2: Low data rate MxN D-MIMO using Full Receivers

D3: High data rate MxN D-MIMO using Full Receivers

4.2 TIP#2: Close-in UWB Wireless Application to Sea Basing

Task objective: The objective of this subtask is to develop algorithms for UWB technology to provide precision position location, precision ranging, and imaging. With a low duty cycle and wide bandwidth, UWB is naturally suited to radar and ranging applications. As the time duration of a pulse decreases, it provides finer resolution of reflected signals, such that the system can resolve distances with sub-centimeter accuracy using simple signal processing algorithms.

Accomplishments during reporting period: By the end of the last quarter the relationship between the traveled pulse and the height above the ship's deck was established. That relationship includes the traveled distance and the slope of the ship's deck. Although the ship's slope is unknown to each side, by iteratively combining four sets of measurements (from each side) we were able to write an algorithm that precisely estimates the exact ship's orientation. The algorithm was evaluated given artificial data assuming specific orientation and the algorithm was able to estimate the exact orientation. In addition, the estimation algorithm was evaluated under non-ideal conditions where error on the data was assumed as described in the next section.

Estimation Algorithm Evaluation

In this effort, we simulated the performance (estimation variance) of the estimation algorithm when the input data are assumed to have a variance of 1/SNR. The dimensions of the crate are assumed to be 5x5x5m and the maximum distance from the crate to the deck is 5 m; therefore, the maximum distance from the deck to the tx/rx is 10 m. Thus, the working range for the range estimator is 5 to 10 m (Figure 4.2-1).

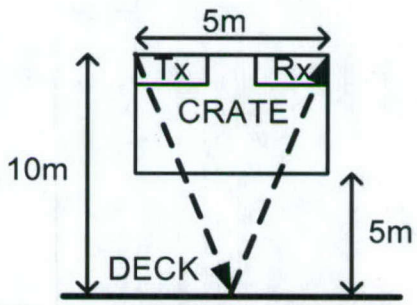

Figure 4.2-1 Nominal dimensions for a UWB-equipped crate above a ship deck.

Figures 4.2-2 and 4.2-3 show the estimated variance versus various SNR's and assumed heights. From Figure 4.2-2 it can be seen that the estimation variance does not vary significantly with height. In addition, it can be observed that as the SNR increases (input variance reduced) each line shifts down to lower variance levels; the shift seems to be equal between each SNR value, which suggests a linear relation between input SNR and the output estimation. This can be better proved from Figure 4.2-2.

Figure 4.2-3 shows the relation of estimation variance and SNR. It can be clearly seen that the relationship is linear. Furthermore, the same relationship is plotted for the two extreme cases of height, 5 m and 10 m, and shows that there is not a significant variation between each.

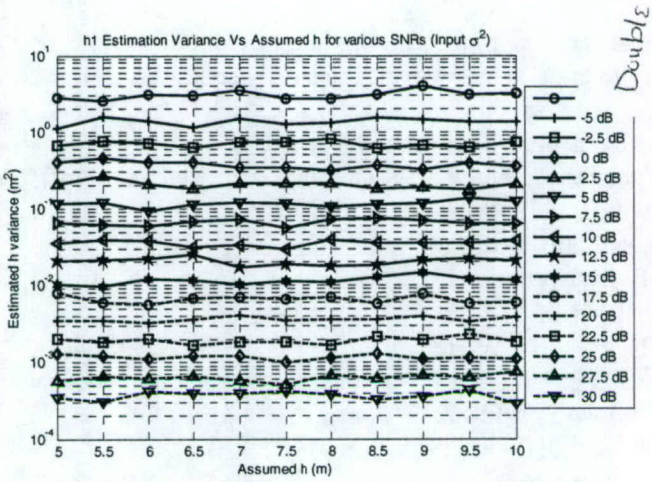

Figure 4.2-2 Simulation results for estimation variance vs. assumed height for various **SNRs.**

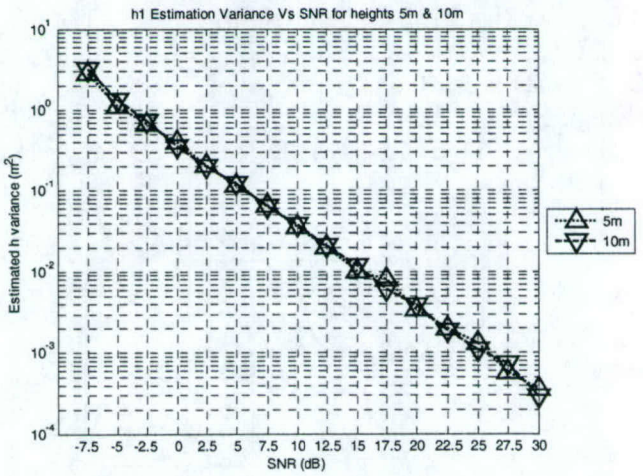

Figure 4.2-3 Simulation results for estimation variance vs SNR for various assumed heights.

From Figure 4.2-3, we can see that in order to achieve an estimation variance of 6.25×10^{-4} m^2 (σ=0.025 m=1 inch) is achieved with a SNR=29 dB; therefore, the input variance to the estimation algorithm must be < $1.25 \times 10^{-3} m^2$. In this case, the algorithm's output variance is half the input's variance.

Acquisition Parameters

Pulse Repetition: every 150 ns
Received Window: 150 ns
Pulse expected arrival time (max height): 70 ns
Latest reflection expected arrival time: <80 ns
Method: First arriving pulse detection
Acquisition Performance: Signal SNR for the required estimation variance equals 27 dB

Link Budget

At this point we have an estimate for the SNR needed for the required estimation accuracy (σ=0.025 m=1 inch.) The last part of the project is to calculate a link budget to determine the system parameters such as antenna gains, interleaving factor (how many pulses are needed for a complete waveform), and update rate that will archive the required SNR. The link budget is evaluated for two cases: Case 1

when the crate is at the maximum ranging height (5 m above the ship deck, 10 m for the tx/rx path), and Case 2 when the crate is half way to the ship's deck (2.5 m.)

Link Budget Parameters for Cases 1 and 2
Detection Algorithm required SNR (for an Est σ^2 <$1.25\text{x}10^{-3}m^2$): 27d B
Transmit Power (P_t): 1 mW
Tx,Rx Antenna Gain: 10 dBi
Floor Reflectivity(α)=0.5
Noise Figure (F)=1.25
Noise PSD (N_0)=$4\text{x}10^{-21}$ W/Hz
Pulse Width=300 ps
Detection Window(T_w): 150 ns
Interleaving factor: 250

Case 1
Max Traveled Distance (R): 21 m (Height=10 m)
Update Rate:2.2 Hz
Max Allowed Pulses (N_a)= $3\text{x}10^6$
Waveform Averaging (Nw):$12\text{x}10^3$
Evaluating equations (4.2-1) to (4.2-3): SNR_{Rx} =27.2 dB R_{max} =21.2 4m

$$P_r = \left(\frac{P_T G_T G_R \alpha \lambda^2}{(4\pi)^3 R^2} \right) \tag{4.2-1}$$

$$SNR_{Rx} = \frac{P_r N_a T_w}{N_0 F} \tag{4.2-2}$$

$$R_{\max} = \left(\frac{N_a P_T G_T G_R \alpha \lambda^2}{(4\pi)^3 N_0 SNR_{req}} \right)^{1/4} \tag{4.2-3}$$

The values calculated by the link budget suggest the received SNR is 27.2 dB and the maximum working range is 21.24 m; these values agree with the desired SNR and working range which are 27 dB and 21 m, respectively.

Case 2
Max Traveled Distance (R): 16 m (Height=7.5 m)
Update Rate:6.67 Hz
Max Allowed Pulses (N_a)= $1\text{x}10^6$
Waveform Averaging (Nw): $4\text{x}10^3$
SNR_{Rx} =27.15 dB R_{max} =16.14 m

From the above results we have an indication of the required antenna and receiver performance parameters. Furthermore, it can be seen that we can design an adaptive scheme that increases the update rate as the crate approaches the deck (SNR increases.) That is desirable because a higher update rate is required close to the deck.

Schedule:
- January-Summer 2005

- Begin algorithm development
- Test algorithms using the simple setups discussed above

– Summer-Fall 2005
  - Integrate ranging system into the crane hardware
  - Evaluate performance of position location algorithms in real-world environments

– January-Summer 2006
  - Finalize 3-D Ranging solution
  - Demonstrate passive and active position location system in laboratory environment.

Personnel:

Dr. Michael Buehrer, faculty and TIP Leader
Chris Anderson, GRA
Swaroop Venkatesh, GRA – Position Location Algorithm Development
Haris Volos, GRA – Ranging Algorithm Development

Summary Quad Chart

TIP #2: Close-in UWB Wireless for Sea Basing

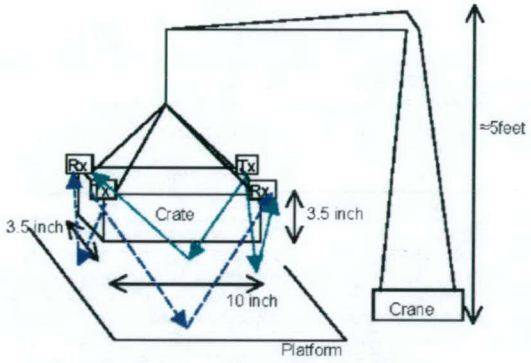

TIP Objectives

- To demonstrate the accuracy of a UWB-based ranging system in terms of
  - Distance from crate to deck
  - Orientation of crate relative to deck
- To demonstrate the ability of UWB to work in harsh environments

Team

Dr. R. Michael Buehrer, TIP Leader
Haris I. Volos
Chris Anderson
Swaroop Venkatesh

TIP Description

- Sea Basing requires the transfer of cargo between two ships that are potentially in rough waters
- Previously developed non-linear control algorithms address this, but require accurate information concerning the range and orientation of crate relative to deck
- We are using very narrow ultra wide band pulses which allow ranging resolutions of less than one centimeter.
- Demonstration uses a 1/24 scale system using antennas placed at four corners of the crate.

Milestones

- Receipt of antennas by end of August.
- Sept 05 – Initial ranging experiments with the antennas to determine exact mounting location on the crate.
- Oct 05 Build crate to 1/24 scale with mounted antennas mounted to it. Basic ranging demonstration in MPRG Lab.
- Nov 05 Demonstration using shakers in NL Dynamics Lab
- Dec 05. Final demonstration with the 1/24 scale crane.

Timeline Chart

Crane Ranging Demonstration Time Line

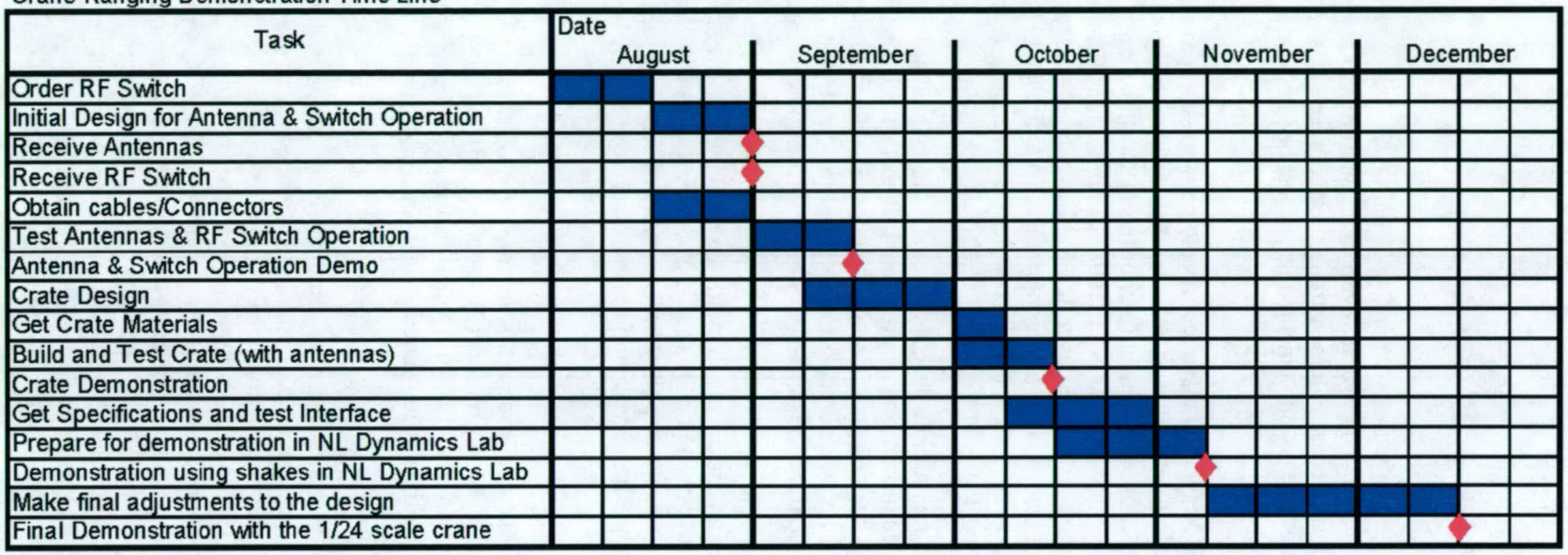

4.3 TIP #3: Secure Ad Hoc Networks

4.3.1 Project Description

The testing and demonstration of secure ad hoc networks involves integration and testing along three related tracks. Each of these will lead to a separate demonstration (or coupled set of demonstrations) using a common hardware and software base, as implemented in our test bed network (see discussion of Task 2.1).

1. Activities within Task 2.1 (Ad Hoc Networks) that support core network services will be integrated, tested, and demonstrated. Capabilities to be integrated include policy-based quality of service (QoS), security based on distributed certificate authorities (DCAs) for key management and trust grading, and mobile ad hoc network (MANET) routing support for QoS and security functionality and as a means to demonstrate cross-layer design. Cross-layer design techniques from Task 2.4 will be reviewed and incorporated as appropriate. Capabilities will be shown operating with Internet Protocol version 4 (IPv4) and, where feasible within the level of effort possible, Internet Protocol version 6 (IPv6).
2. A cross-layer approach to transporting multiple description (MD) video in ad hoc networks, also a part of Tasks 2.1, will be integrated, tested, and demonstrated. This task will utilize application-level routing to use application-specific optimal routes. It will integrate with the MANET routing effort of Task 2.1, e.g., with Open Shortest Path First-Multiple Connected Dominating Sets (OSPF-MCDS), to utilize the topology information efficiently obtained by the MANET routing protocol.
3. We will integrate real-time middleware from Task 2.2 with the combined QoS, security, and routing as discussed above and as investigated in Task 2.3. Specifically, we will investigate and develop methods and mechanisms to integrate policy-based quality of service (QoS) capabilities at the network level, and perhaps at the link layer, with real-time services offered by middleware.

4.3.2 Demonstration Description

Table 4.3-1 lists the themes, components, and leaders for the three demonstrations. Demonstration (1) focuses on core network services. Demonstration (2) involves network support for a video application. Demonstration (3) relates directly to Task 2.3 and involves the integration of network services with an application based on the time-utility function real-time middleware. We will adjust plans based on results from related tasks.

The components of the different demonstrations listed in Table 4.4-1 are currently envisioned to be the same except for the application – or application plus middleware in the case of Demonstration (2) – being supported. The security, QoS, and routing components are discussed further in this report in association with Task 2.1. Note that OSPF-MCDS-MC or, more simply, OMM, is a multi-channel version of the Open Shortest Path First with Minimum Connected Dominating Sets (OSPF-MCDS) MANET routing protocol. OLSR-MC is a multi-channel version of the Optimized Link State Routing (OLSR) MANET routing protocol. The topology viewer (TopoView) and topology emulation tools are carried over from the previous NAVCIITI project but will need to be modified to support new functions in the network and to work in an IPv6 environment. It is envisioned that additional performance monitoring and configuration control tools will be developed as part of Subtask 2.1e and used in the demonstrations.

Table 4.3-1. Demonstration Components and Leaders for the Three Demonstrations

Demonstration	Key Components	Leaders
a) Core network services	Security and key management system Policy-based quality of service OSPF-MCDS-MC and/or OLSR-MC routing TopoView network monitoring Performance monitoring tools Topology emulation	Scott Midkiff Luiz DaSilva
b) Cross-layer approach to MD video routing	OSPF-MCDS and/or OLSR routing TopoView network monitoring Performance monitoring tools Topology emulation	Tom Hou Scott Midkiff
c) Real-time middleware in an ad hoc network	Real-time middleware Security and key management system Policy-based quality of service OSPF-MCDS-MC and/or OLSR-MC routing TopoView network monitoring Performance monitoring tools Topology emulation	Scott Midkiff Luiz DaSilva Binoy Ravindran

4.3.3 Cooperative AWINN Elements

This test and demonstration requires the inputs from AWINN tasks as specified in Table 4.4-2.

Table 4.3-2. Inputs from Cooperative AWINN Elements

Task (Subtask)	Inputs
2.1a	Prototype implementation of a policy-based QoS scheme
2.1b	Prototype implementation of MANET security and key management scheme
2.1c	Optimized prototype implementation of a MANET routing, specifically OSPF-MCDS-MC and/or OLSR-MC
2.1f	Performance monitoring tools; enhanced TopoView; enhanced topology emulation
2.1d	Video sensor application and test bed components
2.2	Real-time middleware
2.4	Cross-layer optimization elements that can be integrated into the test bed for testing and demonstration purposes.

4.3.4 Cooperative Non-AWINN Elements

At this time, no non-AWINN components are required (except for tools and equipment carried over from the NAVCIITI project).

4.3.5 Schedule of Activities

A general schedule listing major milestones is provided in Table 4.4-3. Note that the schedule is divided into four phases. During Phase I, the emphasis is on core network services of Demonstration (a) running with IPv4. During Phase II, the emphasis is on core network services of Demonstration (a) running with IPv6. During Phase III, the emphasis is on integration of the MD video and real-time applications of Demonstrations (b) and (c), respectively. In Phase IV, the emphasis is on final

demonstration of the MD video and real-time applications of Demonstrations (b) and (c), respectively.

Table 4.3-3. Schedule of Activities

Activity	Date
Phase I: Demonstrate core services using IPv4	3Q2005
Phase II: Demonstrate core services using IPv6	4Q2005
Phase III (b): Initial MD video integration	1Q2006
Phase III (c): Initial real-time middleware integration	1Q2005
Phase IV (b): Final demonstration of MD video	2Q2006
Phase IV (c): Final demonstration of real-time middleware	2Q2006

TIP #3: Secure Ad Hoc Networks

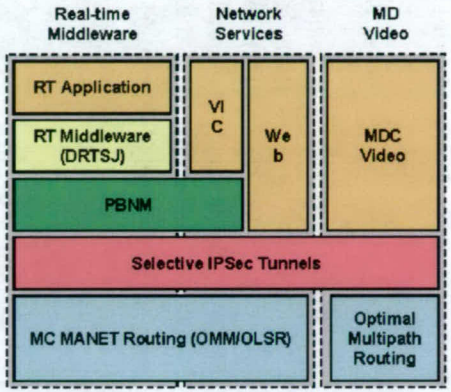

TIP Objectives

- To demonstrate adaptive, integrated core network services with multi-channel operation
- To demonstrate integrated application support for:
  - Multiple description (MD) video
  - Distributed real-time using Java

Team

Dr. S. F. Midkiff, Leader
Dr. L. A. DaSilva
Dr. Y. T. Hou
Dr. B. Ravindran
Dr. G. Hadjichristofi
Dr. S. Mao
U. Lee
W. M. de Sousa
X. Wang

TIP Description

- Network services
  - Demonstrate multi-channel routing, quality of service, and security in an integrated manner
- Multiple description video
  - Demonstrate resilience of MD video in the ad hoc network
  - Demonstrate importance of cross-layer design approach for multipath routing
- Real-time middleware
  - Distributed Real-Time Specification for Java
  - Use a futuristic, notional network-centric warfare application fragment
- Demonstrations will use a test bed of wired and wireless nodes

Milestones

- 9/05: Demonstrate network services with IPv4
- 12/05: Demonstrate network services with IPv6
- 3/06: Initial demonstrations of MD video and real-time middleware
- 6/06: Final demonstrations of MD video and real-time middleware

4.4 *TIP #4:* Integration of Close-in UWB wireless with ESM crane for Sea Basing applications

Task Objective: The goal of this task is to demonstrate the usefulness of UWB in close-in communications and ship-to-ship cargo transfer for sea-basing operations.

Organization: This task is managed by Dr. A. H. Nayfeh
Dr. A.H. Nayfeh, Faculty
Dr. E. Abdel-Rahman, Post Doc
N.A.Nayfeh, GRA

Accomplishment During Reporting Period: Extensive coordination activities with the TIP#2 team have positioned us to demonstrate the usefulness of UWB systems for ship-to-ship cargo transfer. The hardware for the demonstration will be 1/24 scale model of the Navy TASC crane. Scaling down of the antennas presents a major challenge, so we have included a $1/10^{th}$ scale model of the container crane as a back up. The planned testing and development of the UWB system include the following experiments.

- Measure an up and down moving object on a shaker. For this purpose, we identified two shakers in the Nonlinear Dynamics Laboratory: a shaker with a small stroke and another with a large stroke.
- Measure the orientation of a plate placed on top of a shaker whose head moves up and down.
- Measure the position of a point and the orientation of a plate on top of a shaker head that moves horizontally.
- Measure the position of a point and the orientation of a plate mounted on top of the Stuart platform in the Crane Control Laboratory. This platform has six degrees of freedom: heaving, pitching, rolling, surging, yawing, and swaying.
-

Once the hardware is developed, we will work with the TIP#2 team to perform the above identified experiments, culminating in demonstrating cargo transfer between two moving platforms.

4.4.1 Importance/Relevance

The proposed work has the potential of being very useful to the Navy's Transformational Sea-Basing System. The success of Sea Basing depends on the ability to sustain logistic operations with significantly reduced reliance on land bases. This requires the development of a high capacity, high reliability at-sea capability to transfer fuel, cargo, vehicle, and personnel in rough seas while underway from commercial container ships to large sea basing ships and then to smaller ships. The wave-induced motion of the crane ship can produce large pendulations of the cargo being hoisted and cause the operations to be suspended.

Personnel:
N.Nayfeh, January, 2005-present

5. FINANCIAL REPORT